FINAL TECHNICAL REPORT

STRUCTURAL CONSTRAINTS ON CRUSTAL SHORTENING IN THE BOLIVIAN ANDES

Barbara Moths Sheffels
Ph. D. Thesis, M.I.T.
September, 1988
(Research conducted under NASA Grant NAG5-300.)

Title of Grant	Seismicity and Active Tectonics of the Andes and the Origin of the Altiplano
Principal Investigators	P. Molnar B.C. Burchfiel
Period Covered	March 15, 1984-August, 1988
Grantee Institution	Dept. of Earth, Atmospheric, and Planetary Sciences Massachusetts Institute of Technology 77 Massachusetts Ave. Cambridge, MA 02139
Grant Number	NAG5-300

(NASA-CR-184599) STRUCTURAL CONSTRAINTS ON CRUSTAL SHORTENING IN THE BOLIVIAN ANDES Ph.D. Thesis Final Technical Report, 15 Mar. 1984 - Aug. 1988 (Massachusetts Inst. of Tech.) 326 p
N89-15471
Unclas
CSCL 08G 00/46 0179885

STRUCTURAL CONSTRAINTS ON CRUSTAL SHORTENING IN THE BOLIVIAN ANDES

by

Barbara Moths Sheffels

Submitted to the Department of Earth, Atmospheric, and Planetary Sciences on July 28, 1988 in partial fulfillment of the requirements for the degree of Doctor of Philosophy

ABSTRACT

The Bolivian Andes lie within an active, convergent plate margin in which oceanic lithosphere is subducted beneath continental. As such, they provide the opportunity to assess the relative importance of processes which contribute to mountain-building in that setting. Specifically, the roles of crustal shortening and of magmatic addition in the formation of the thickened crust and high elevations observed in the Bolivian Andes today have been the subject of much debate. Quantification of the amount of crustal shortening using balanced cross sections contributes to the resolution of this debate, and provides a key piece of data that can be used to test other hypotheses about mountain building.

Reconnaissance mapping and photogeologic analysis reveal that the back-arc orogenic belt is a substantially shortened fold and thrust belt. Decollement at depth is required by the geometry of deformation in the faulted structural packages, and is indicated by the parallel style of deformation observed, although few low angle thrust faults are observed. Decollement occurs within shales of three stratigraphic levels: the Devonian Icla Formation, the Silurian Kirusillas Formation, and the Ordovician Capinota Formation or lower Ordovician undifferentiated shale. The level of decollement ramps up toward the foreland, sometimes directly from the Ordovician shale to the Icla Formation. The percent shortening within different thrust sheets varies from 12 to 53%. Tear faults, lateral ramps and other features typical of fold and thrust belts are observed. Features unique to this mountain belt include large hangingwall cutoff angles (70°) and numerous backthrusts. The latter may be related to the presence of deeper, unexposed thrust faults, which exist throughout the mapped area. A triangle zone forms the thrust front south of the bend in the mountain belt, but emergent thrust faults mark the thrust front to the north. The bend in the mountain belt is, at least in part, the result of a wider depositional basin to the south.

The amount of crustal shortening that has occurred in the Bolivian Andes can be quantified using balanced cross sections. A minimum estimate of shortening of 210 kilometers is calculated from balanced cross sections that transect the Cordillera Oriental and Subandean Zone. The lack of penetrative interstratal strain and a relatively simple tectonic history in the mapped area ensure that the estimate of crustal shortening is well-constrained. Conservative interpretations of fault displacement, cutoff angles, and the structural packages comprising the concealed thrust sheets ensure that this estimate is a minimum.

The magnitude of crustal shortening, while a minimum, indicates that this process has been more important in forming the central Andes than the addition of mantle-derived magmas. Shortening of 210 kilometers accounts for at least 67% of the crustal cross sectional area observed today, assuming an average initial crustal thickness of 40 kilometers. Larger estimates of shortening and the extension of the thin-skinned style

of deformation into the Altiplano are plausible, and suggest that virtually the entire mountain range could have been built by crustal shortening.

Quantification of the amount of crustal shortening in the Bolivian Andes, the type locality of an Andean margin, also has implications for other hypotheses about mountain building. Substantially-shortened fold and thrust belts are postulated to be related uniquely to collision, and to form in an orientation synthetic to that of the subduction zone. The large amount of crustal shortening in the Bolivian Andes, however, has been a response to subduction of oceanic lithosphere only. It has not been driven either by collision, since there is no evidence of Tertiary collisions, or by compression generated by intrusion of magma, since magmatic material does not form a volumetrically important part of the mountain belt. Furthermore, although the sense of overthrusting in the Bolivian back-arc fold and thrust belt is antithetic to that of the subduction zone, it has accomodated substantial crustal shortening. These observations must be taken into account when using the Andean margin as an analogue for other orogenic belts.

Thesis supervisors: B.C. Burchfiel

Title: Schlumberger Professor of Geology

P. Molnar

Title: Senior Research Associate

©Barbara Moths Sheffels, 1988. All rights reserved
The author hereby grants to MIT permission to reproduce and to distribute copies of this thesis document in whole or in part.

TABLE OF CONTENTS

TITLE PAGE i

ABSTRACT ii

TABLE OF CONTENTS iv

ACKNOWLEDGEMENTS vi

DEDICATION vii

CHAPTER 1. INTRODUCTION 1

CHAPTER 2. METHODOLOGY 7

Table 16
Figure Captions 17
Figures 18

CHAPTER 3. STRATIGRAPHY 22

Figure Captions 36
Figures 37

CHAPTER 4. THE TIMING OF DEFORMATIONAL EVENTS IN THE BOLIVIAN ANDES 40

Figure Captions 47
Figures 48

CHAPTER 5. THE STYLE OF DEFORMATION IN THE BOLIVIAN ANDES 53

Tables 79
Figure Captions 83
Figures 86

CHAPTER 6. THE IMPORTANCE OF CRUSTAL SHORTENING IN THE FORMATION OF THE CENTRAL ANDES 112

Tables 134
Figure Captions 139
Figures 141

CHAPTER 7. BACK-ARC FOLD AND THRUST BELTS ALONG ANDEAN AND OTHER PLATE MARGINS 149

CHAPTER 8. CONCLUSIONS 153

REFERENCES 156

APPENDIX 166
LOCATION MAP OF EXAMPLE AIR PHOTOS 167
AIR PHOTO A 168
AIR PHOTO B 169
AIR PHOTO C 170

PREVIOUS PUBLICATIONS RELATED TO WORK SUPPORTED BY THIS GRANT 171

PLATES ..... Back pocket

PLATE 1. COCHABAMBA MAP SHEET
PLATE 2. PUNATA MAP SHEET
PLATE 3. SANTA CRUZ DE LA SIERRA MAP SHEET
PLATE 4. UNCIA MAP SHEET
PLATE 5. AIQUILE MAP SHEET
PLATE 6. VALLEGRANDE MAP SHEET
PLATE 7. ORURO-SANTA CRUZ TRANSECT
PLATE 8. ORURO-PUNATA-CHAPARE TRANSECTS

ACKNOWLEDGEMENTS

This work was completed with the financial, logistical, and emotional support of many others.

Financial support was provided by NASA Grant NAG 5-300, awarded to Peter Molnar and Clark Burchfiel, and a grant by Exxon Corporation.

In Bolivia, Father Ramon Cabré of the Observatorio San Calixto was instrumental both in obtaining air photos and in providing logistical help during my field work: he guided the air photos through a bureaucratic maze, generously made the observatory's jeep available during each of my trips to Bolivia, and helped me with many other things in La Paz. Salvador Gutierrez of the Observatorio San Calixto and Alejandrino Flores of GEOBOL drove many miles and patiently waited while we mapped, while also providing an introduction to Bolivian life. I thank Raul Carrasco of GEOBOL for providing a jeep, and for interesting discussions of the geology of the Bolivian Andes. Estela Minaya of the Observatorio San Calixto, Heberto Perez of GEOBOL, Oscar Aranibar and Jaime Oller (both from YPFB) accompanied me in the field, and provided me with a good foundation of knowledge about the seismicity, stratigraphy and structure of the Bolivian Andes. Discussions with other geologists, especially Ramiro Suarez, Miguel Cirbian, Marcimio Lopez and Eduardo Soria, were particularly helpful.

At MIT, I thank my advisors, Clark Burchfiel and Peter Molnar, for their advice and insights, and for giving me the opportunity to work on this project. Marcia McNutt advised me during my first year at MIT, and has been a source of good advice and a good friend since then. Dave Klepacki, Joann Stock and Jim Knapp took time from their own graduate studies to accompany me in the field.

Rick Allmendinger and the Cornell Andes Project shared their Thematic Mapper images of the Andes. I also benefitted from discussions with Kevin Biddle and others from the Andean Project of Exxon Company International, Inc. Jamie Rascoe, also of Exxon Company International, Inc., did an excellent job of drafting my maps.

Discussions and friendships with many other graduate students at MIT have been important to me. Dave Klepacki, Doug Walker, Paul Okubo and Joann Stock added greatly to my years at MIT. Mary Hubbard and Liz Schermer have been corrupting influences in ice cream consumption, but more importantly, good friends.

Outside of the geological community, it has been fun and inspiring to work and play with Erika, Nikki, Natascha, Tyrone, Francois, Nehemiah, Kenyatta, Charlene and all the other children at the Bird Street Youth Center, and to row with the Graduate Women's Crew Team. Finally, my family has been most important in preparing me for, and supporting me during, my years at MIT. Thank you, Mom, Susan, Lisa, Bruce, Doug, Yeti, and, of course, Eric.

I dedicate this thesis to the memory of my father. He would have liked to have read it, for he was a geologist as much as time and circumstances allowed him to be; he was, I suppose, my first teacher of geology. I would have liked him to have read it because, in all our discussions, whether about geology or other topics, he had the most perceptive insights of anyone I have ever met.

CHAPTER ONE

Introduction

Introduction

Continued debate on the relative importance of magmatism and crustal shortening in mountain building along Andean margins reflects the failure of simple correlations between mountain building processes and a given type of plate margin to explain the diversity of orogenic styles observed in mountain belts. Early thinking about mountain building in light of plate tectonics identified convergent plate boundaries as the loci of orogeny, and postulated that mountain belts along either collisional or non-collisional plate margins would also be of two distinct types (Dewey and Bird, 1970). Not only has further study revealed that there is not a deterministic relation between a given convergent tectonic setting and the style of orogenesis that results, but it has also shown that all mountain belts are not alike (Molnar and Lyon-Caen, 1988; Rodgers, 1987). The diversity of orogenic styles observed, regardless of the type of plate margin to which orogeny is related, raises fundamental questions about the relative importance of thin- versus thick-skinned deformation, about the role of basement involvement, and about the relative contributions of magmatism and of crustal shortening to thickening of the crust. Quantitative study of active orogens provides the only means of constraining the mechanism and evolution of mountain building in a given tectonic setting.

The Bolivian Andes provide a natural laboratory for quantitative study of orogeny in Andean margins. Quantification of the mountain building processes active in the Bolivian Andes contributes to our understanding of

those processes not only in the central Andes, where they remain incompletely understood, but also in other mountain belts, where the central Andes are used as an analogue for the development of these mountain belts.

Furthermore, within the central Andes, the tectonic history of the Bolivian Andes is relatively unknown. In the Peruvian, Argentine and Chilean portions of the central Andes, regions of distinct structural style along and across strike have developed contemporaneously with varying amounts and types of magmatic activity. The spatial coincidence of these regions with variations in the dip of the subducting slab is generally assumed to be causally related. In the well-exposed Bolivian Andes, however, neither the structural style nor its temporal evolution are well-defined. Specifically, thin-skinned thrusting is recognized in parts of the back-arc regions of the Peruvian and Argentinian Andes, but its role in the Bolivian Andes has not been assessed quantitatively.

The goal of this study is to determine the structural style of deformation within the Bolivian Andes, and to determine the amount of crustal shortening that has occurred in that deformation, through a combined field and photogeologic study of a transect across the mountains at 18°S. Although the Andes are commonly regarded as primarily the product of magmatic processes, it is difficult to quantify the contribution of mantle-derived magmatic additions. A minimum amount of crustal shortening across this mountain belt, however, can be quantified using balanced cross sections, and therefore the relative contributions of magmatism and crustal shortening to the thickened crust of the central Andes can be assessed. Because the Bolivian Andes are particularly well-

exposed, the amount of crustal shortening can be quantified in a well-constrained manner.

The magnitude of crustal shortening determined for this antithetic, back-arc fold and thrust belt provides a means with which to test various generalizations about mountain building. For example, the association of arc-continent and continent-continent collisions with large amounts of shortening in the Canadian Cordillera and the Alps, respectively, has led some to suggest that substantial crustal shortening can only occur in response to continental collision. Shortening in the Bolivian Andes has been contemporaneous with subduction of only oceanic lithosphere; if the Bolivian Andes have experienced a large magnitude of crustal shortening, then subduction of oceanic lithosphere alone must be sufficient to drive the formation of a substantially shortened back-arc fold and thrust belt.

Geologic Setting

The Bolivian Andes comprise the central part of the mountain belt that has formed along the western margin of South America in response to a lengthy history of subduction. Although morphologically continuous along their 7500 kilometer length, the Andes display marked differences in structural style and tectonic history along strike. A brief review of the salient characteristics follows, drawn primarily from Zeil (1979), Martinez (1980), Jordan et al. (1983), Mégard (1987a and references within), Jordan and Alonso (1987 and references within), and Jordan and Allmendinger (1986 and references within).

The Andes of South America are divided into three regions, northern, central and southern, on the basis of distinct deformational histories from Cretaceous time to the present (Zeil, 1979; Mégard, 1987). The central Andes extend from approximately 10°S to 35°S. In the northern and southern Andes, there is evidence for Cretaceous and younger accretion of exotic terrains, but along the margin of the central Andes, eastward subduction of only oceanic lithosphere beneath South America is inferred to have been continuous during this time period. Initiation of subduction in lower Jurassic time is indicated by calc-alkaline magmatism of that age; the persistence of calc-alkaline magmatism since then, and the intrusion of the Coastal Batholith of Peru and the smaller batholiths of northern Bolivia, indicate the continuity of the subduction process.

A primary feature of subduction beneath the Andes is the segmentation of the downgoing oceanic plate (Stauder, 1973, 1975; Barazangi and Isacks, 1976, 1979). Seismicity associated with the downgoing plate defines two relatively flat-lying (5-10° dip) portions of the slab flanking a central

portion that dips approximately 30°. The slab is warped to accomodate the change in dip at 15°S and between 24 and 27°S (Hasegawa and Sacks, 1981; Grange et al., 1984).

The southernmost change in the dip of the slab lies within the central Andes, and correlates with an along-strike change in the tectonic provinces of the central Andes. To the south, the Brazilian shield lies adjacent to the Sierras Pampeanas, a region of basement-involved block uplifts. West of the Sierras Pampeanas, a fold and thrust belt, the Precordillera, developed. Its western boundary flanks the longitudinal intermontane valley system, to the west of which lie the high Andes.

In the northern central Andes, however, these tectonic provinces are replaced by, from east to west, the Subandean Zone, the Cordillera Oriental, the Altiplano, and the Cordillera Occidental. The Subandean Zone is an arcuate region of relatively continuous folds and faults, involving primarily Devonian and younger rocks, and abutting the Brazilian shield. Holocene deposits are involved in the thrusting at the easternmost margin, and seismic reflection lines show that topographic highs east of the Subandean Zone correlate with thrust faults that propagated in that direction. The Cordillera Oriental, a region characterized by relatively steep faults within the thick Paleozoic sequence, lies west of the Subandean Zone. These tectonic provinces change markedly in width and trend at approximately 18°S, around the bend in the mountain belt known as the "elbow". The Altiplano, a high plateau covered by a thick sequence of Tertiary and Quaternary sedimentary rocks, lies west of the Cordillera Oriental. Where Paleozoic rock is exposed within the Altiplano, it is folded and faulted, along with some of the Tertiary cover, by both normal and thrust faults. The Cordillera Occidental is the locus of active and recently

active volcanoes. The magmatic arc is active above the steeply-dipping segment of the subducting slab; inactive arcs are present to the north and south above the shallowly-dipping segments of the slab. Mesozoic and Tertiary volcanic rocks are all arc type. Eastward migration of the Cretaceous and Tertiary magmatic arc is inferred in Peru and Chile.

Determination of the structural style of deformation and the amount of crustal shortening across the Bolivian Andes improves our understanding of the central Andes in particular, and of Andean margins in general. Furthermore, determination of the amount of shortening allows the testing of hypotheses about mountain building, and provides an improved analogue for application to other inactive mountain belts.

CHAPTER TWO

Methodology

Introduction

The goal of this study is to determine the style of deformation and the amount of shortening that has occurred in the Bolivian Andes. The area chosen for study crosses the entire width of the Cordillera Oriental and Subandean Zone of the Bolivian Andes. A geologic map across this zone has been compiled from field work and interpretation of air photos and Thematic Mapper imagery. Balanced cross sections have been constructed based on these maps and on a set of restrictive assumptions that would provide the most conservative interpretation in the sense of giving a minimum amount of crustal shortening.

Mapping

The mapped area (Figure 2.1) constitutes a zone approximately 100 kilometers wide between 17.5°S and 19°S, extending 370 kilometers from the thrust front at 63°15'W to the Altiplano at 67°W. The tectonic provinces of the Cordillera Oriental and Subandean Zone occupy the western and eastern halves of the mapped area south of the bend in the mountain belt, where the mountain belt is particularly wide and well-exposed. North of the mapped area, in the vicinity of the bend, the Subandean Zone narrows substantially. The mapped area lies within parts of the following 1:250,000 topographic map sheets: the Vallegrande, Aiquile, Punata, Uncía, and Cochabamba map sheets. Mapping by Plafker (1962) allowed me to extend the area of study north and east across the Santa Cruz de la Sierra map sheet.

The area is the most accessible area within the Bolivian Andes, because it is crossed by the only major east-west road in the mountain belt, that connecting the cities of Oruro, Cochabamba, and Santa Cruz. Subsidiary roads, while not numerous, are most prevalent near this road. Nevertheless, access to much of the region is difficult.

Roads are few, unpaved and in poor condition, and road maps were unreliable.

The elevation initially increases toward the east, rising from approximately three kilometers in the Altiplano to four to five kilometer peaks in the western part of the Cordillera Oriental. Elevations then decrease to the east to half a kilometer at the thrust front.

Five months of field work were carried out during three trips. Field work consisted primarily of mapping along all possible roads, supplemented by transects on foot and detailed mapping in some areas. The need to field check air photo interpretation across such a large region precluded much work away from roads. Maps of the southern and northern portions of the Aiquile and Punata map sheets, respectively, could not be finalized because access to those areas by road is poor. Field work was carried out during the dry season between May and November, which spans the South American winter.

Approximately 2000 vertical air photos at a scale of 1:50,000 to 1: 62,500 were examined on a Zeiss-Aerotopograph München Oblique Viewing Mirror Stereoscope. Almost complete coverage of Bolivia by air photos of excellent quality is available. The region northeast of the Oruro-Santa Cruz road, consisting of the eastern portion of the Punata map sheet and extending across the Santa Cruz map sheet, however, is frequently cloud-covered. The photos were generally examined without magnification, although 4x magnification was used to evaluate complex structural relationships in some areas. The following paragraphs describe how dips, structures, and stratigraphy were identified on the air photos.

Stratigraphic units were identified by their outcrop characteristics. Adjacent formations with similar outcrop styles were mapped together. Relatively heavy vegetation made these identifications more difficult in the Subandean Zone than in the Cordillera Oriental, where the climate is arid and the rocks are well-exposed. Despite poor exposures in the Subandean Zone, varying degrees of resistance clearly define

unit boundaries and could be correlated with formational divisions after field work. In the Subandean Zone north of the mapped area, the vegetation obscures the rock units on the Thematic Mapper imagery as well.

Thematic Mapper images of the western half of the study area are available. Although the resolution of the satellite images does not allow detailed mapping, significant variations in color between formations in the region of the Cochabamba map sheet helped to identify the boundaries of the Llallagua, Uncía, Catavi, and Cretaceous formations. Without these identifications, air photo interpretation in this area would have been difficult because the Silurian formations do not crop out well.

The clarity of structural geometries depends on the outcrop characteristics of the formations involved and the structural complexity of the area. Formations that crop out poorly, such as the Silurian Uncía Formation, and structures that cross strike, were the most difficult to map. Where the location of a structure is uncertain, the fold axis or fault is dashed; where its existence is uncertain, it is questioned.

The construction of balanced cross sections requires accurate dip measurements. Dips were estimated visually, with vertical exaggeration accounted for in the following way. Before mapping on the photos was begun, photos of the same scale and a map from a known but different area with considerable relief were studied in order to correlate accurate dips with the exaggerated topography in the photos. Dips estimated in this manner for the study area were checked thoroughly during the first month of field work (as well as in all succeeding field trips), and found to be in error by less than 5°.

Field data were integrated with the photogeologic interpretations through additional iterations of air photo analysis. The final maps (Plates 1 through 6) were compiled on overlays to 1:250,000 topographic map bases. The compilations were done almost entirely by eye; initial compilation using a zoom transfer scope was not significantly more accurate. Initial compilations of the mapping for the southern part of the mapped area (Uncía, Aiquile, and Vallegrande map sheets) and for the photogeologic

interpretations were checked in the field.

Construction of Cross Sections

Balanced cross sections are geometrically admissible cross sections that incorporate geometric constraints on fold and fault geometries and on the angles between stratigraphic layering and faults where the layering is truncated (hanging wall and footwall cutoff angles). As first defined explicitly in the literature by Dahlstrom (1969), a cross section is balanced if bed lengths or cross sectional areas within a deformed section are consistent, and if the section can be restored. Elliott (1983), Woodward et al. (1985), and Cooper and Trayner (1986) emphasized the importance of constructing the restored section to check for geometric compatibility and to check the orientation of the initial fault trajectories. Assuming conservation of volume, bed lengths or cross sectional areas within cross sections should be constant if there has been no movement of material out of the plane of the cross section. These conditions of plane strain require that cross sections be drawn parallel to the direction of transport. The direction of convergence (or extension) is usually assumed to be perpendicular to the strikes of folds and faults and parallel to lateral ramp orientations (Elliott and Johnson, 1980).

Fourteen cross sections within the mapped area were constructed (Figure 2.2), and are shown at 1:250,000, the same scale as the maps, on Plates 7 and 8. They are named for the map areas they transect, and are grouped into two transects across the mapped area: in the south, the Oruro-Santa Cruz transect (Plate 7) and, in the north, the Oruro-Punata-Chapare transects (Plate 8). These cross sections are preferentially located so that they maintain an orientation perpendicular to structural trends and so that they lie along transects made during field work. Percent shortening along each cross section is calculated between the pin lines indicated (Plates 7 and 8).

These cross sections have been drawn using a set of restrictive assumptions that would provide the most conservative interpretation in the sense of giving a minimum

amount of crustal shortening. Cross sections across the Cordillera Oriental and Subandean Zone are constrained primarily by the surface geology compiled from photointerpretation and field work. These data define only the shallowest surface of detachment in a given region, and its depth. The inferred depth of the shallowest detachment level is consistent with the observed structural thicknesses of the stratigraphic sequence and not with regional stratigraphic levels. Neither the level nor the number of deeper, blind thrust systems are constrained by the surface geology or by the seismic reflection or well data available to me. Well data, although abundant in the Subandean Zone, does not penetrate below the shallowest surface of detachment, and I did not have access to any seismic lines that imaged below this level of detachment.

Balanced cross sections are drawn in accord with rules governing the geometry of folds and the magnitude of cutoff angles, which are either determined observationally or are assumed. The only constraints available on subsurface fold and fault geometries in my analyses are the principles of parallel deformation and the general characteristics of fold and thrust belts, as summarized by Dahlstrom (1969, 1970), Bally et al. (1966), Boyer and Elliott (1982), and Butler (1982).

The observations made in the field and in air photo analysis, however, do not require the application of either the fault-bend or fault-propagation fold models, which are commonly used in analysis of fold and thrust belts. In order to ensure a minimum amount of shortening, therefore, the geometrical constraints of these models have been relaxed in one important respect. The cutoff angles of bedding along hanging wall and footwall fault ramps have deliberately been drawn steeper than is usually observed or presumed in foreland fold and thrust belts. Theoretical (Anderson, 1951) and experimental (Jaeger and Cook, 1979) results indicate that footwall cutoff angles should be less than 30°. In fact, faults are seldom observed to ramp up at angles greater than 20°, and therefore this angle is usually assumed as a constraint in

constructing cross sections. Balanced cross sections drawn with these small cutoff angles imply that a greater amount of shortening has occurred. Because I observe few footwall cutoff angles and some large hanging wall cutoff angles, and in order to ensure a minimum estimate of shortening, I allow high cutoff angles. The implication is that these folds are not interpreted as fault-bend or fault-propagation folds.

A second assumption relates to the amount of displacement along the thrust faults. Where hanging wall cutoffs are eroded, the amount of displacement along a thrust fault is unconstrained and must be assumed in order to calculate the shortening that has occurred. A minimum amount of shortening is determined by assuming that the displacement along a given fault is the minimum that can be proved. In general, this assumption does not yield a poor estimate because many thrust faults in the mapped area die out into folds along strike.

A third assumption is that all of the shortening that has occurred is represented in the deformation above the surfaces of decollement that are inferred from the surface geology, which are only the shallowest of the thrust fault system. Although slip on deeper fault surfaces is indicated throughout the mapped area by the exposure of stratigraphically low formations in structurally high positions and by the deformation of the inferred surfaces of decollement, no additional shortening is estimated. The amount of additional shortening theoretically possible due to these deeper, concealed faults varies over a wide range of values (Figure 2.3). In the Bolivian Andes, duplexing of Silurian and older formations below the exposed Devonian Icla and younger formations can account for the observed excess area near the foreland. Towards the interior of the mountain belt, however, the regional westward dip of the basement, the increase in elevation, and the uplift of progressively older formations combine to greatly increase the excess cross sectional area between the shallowest level of detachment and the projection of the basement and probably require buried thrust faults and additional shortening. The amount of additional shortening that occurs along these fault systems,

however, is unconstrained because the deeper structural packages are never observed. Therefore, additional shortening due to a duplex structure formed by a deeper fault or faults is included in the calculations in only two cases, those of the Uncía and west Vallegrande cross sections (Figure 2.4). In these cases, for a portion of the length of these cross sections, uplift of the shallowest surface of detachment is sufficient to allow duplication of the entire structural package above the regional level of that detachment as defined within the cross section, and therefore this additional bed length is included in the calculation of percent shortening. Although concealed overthrusting is probably present at depth along the other cross sections, no additional shortening is calculated for the cross sections crossing the Cochabamba, Aiquile, east Vallegrande, and Punata map sheets.

Potentially large errors in the calculation of percent shortening may result if the assumption of non-plane strain is violated, for example, in areas of metamorphism, areas of strike-slip faulting, or if the cross sections are not drawn parallel to tectonic transport. None of these sources of error are deemed important in the mapped area. Within the area mapped by Plafker, however, structural trends vary and the direction of transport is difficult to determine. For this reason, in part, estimates of shortening from the Totora, Limbo, and South Santa Cruz cross sections are only approximate.

Volume changes due to metamorphism or pressure solution introduce non-plane strain that will affect the calculation of shortening from a cross section. In the mapped area, however, there is no evidence of regional metamorphism. No rocks with Carboniferous or younger ages of metamorphism are present, and I observed no veining or cleavage that would indicate pressure solution. Therefore, volume changes due to these processes are not significant.

Some of the cross sections intersect tear faults or other structures that may have been the locus of strike-slip movement. Tear faults are present throughout the mapped area (for example in the eastern portion of the Aiquile map sheet), but the amount of

displacement along them is minor and the sense of displacement is such that excluding the displacement reduces the cross sectional areas or bed lengths measured in the cross sections. In addition to the tear faults, the orientation of cross strike structures in the region of the bend in the mountain belt and oblique folds in the central portion of the Aiquile map sheet suggest that strike-slip displacement may have occurred in conjunction with thrusting. In the former case, cross sections across this complex area are not rigorously balanced, and, in the latter case, the possibility is neglected in the absence of any additional evidence for strike-slip motion and therefore of any means of quantifying it. Again, if these folds represented drag features between left-lateral faults, the effect of including slip in this sense would be to reduce the shortening calculated from the cross sections.

Deviations from the direction of transport are assumed to be negligible in the Bolivian Andes, although the only indicator of transport direction, the direction of structural trends, varies within the mapped area. The trends of individual cross sections vary from one to another by as much as 30°. At most, these variations correspond to a 15% error in percent shortening (Price, 1981). Because the cross sections remain perpendicular to the strike of the major structures that they cross, however, their orientations are assumed to reflect the transport direction as accurately as is possible. The only exceptions to this statement are the north, central, and south Totora cross sections and the South Santa Cruz cross section, that intersect the oblique transfer structures characteristic of the Elbow region. This orientation is one of the reasons these sections are not rigorously balanced.

Uncertainties in percent shortening due to measuring errors are small. Bed lengths were measured several times on 1:250,000 or enlarged cross sections with a curvimeter, and the average values were used to calculate percent shortening. Standard deviations in the measurement of bed lengths of 1.26 km and .7 km were determined from 25 measurements each of a long (65km) and a short (30km) cross

section, respectively. Standard error propagation indicates a standard deviation in percent shortening for the various cross sections as shown in Table 1. The standard deviations range from 2.1 to 6.5 km, averaging 3.6 km.

In summary, the amount of shortening represented in these cross sections is subject to only a small uncertainty in measurement, to a potentially larger but unquantifiable error due to variations in the direction of tectonic transport, and to insignificant errors due to metamorphism. The calculation is strongly biased towards underestimating the amount of shortening that has occurred.

Table 2.1.

Cross section (Decollement level)	l_o (km)	l (km)	s (km)	σ_{meas}	Percent Shortening	$\sigma_{\%short}$
East Vallegrande	53	42	11	1.26	20%	3.73
West Vallegrande	105	49	56	1.26	53%	2.20
East Aiquile (Icla Formation)	30	16	14	.7	47%	4.14
East Aiquile (Kirusillas Formation)	17	13	4	.7	24%	6.54
East Aiquile (Lower Ordovician)	24	19	5	.7	21%	4.58
West Aiquile	85	68	17	1.26	20%	2.32
Uncía	83	51	32	1.26	38%	2.59
Cochabamba	53	38	15	1.26	28%	3.87
North Punata	57	49	8	1.26	14%	3.35
Central Punata	67	56	11	1.26	16%	2.89
South Punata	45	38	7	1.26	16%	4.28
(Punata region) South Punata (Totora region)	33	29	4	.7	12%	3.19
Average						3.64

σ_{meas} = standard deviation in measurement of bed length

$\sigma_{\%short}$ = standard deviation in percent shortening

Figure Captions

Figure 2.1. Location map showing 1) the geographic location of Bolivia and 2) the three tectonic provinces, the Altiplano, the Cordillera Oriental and the Subandean Zone, that cross Bolivia. The study area is outlined.

Figure 2.2. Outline of the map sheets which contain the mapped area. The areas mapped by Sheffels (this study) and by Plafker (1962) are outlined. Cross section locations, end point labels and names are shown within the outlines of the six map sheets. The endpoints of the two regional profiles, the Oruro-Santa Cruz and the Oruro-Punata-Chapare profiles, are labelled with dark arrows.

Figure 2.3. The deformation of the shallowest surfaces of decollement indicate the existence of deeper faults, which may accomodate additional shortening. Examples of various interpretations of the East Vallegrande cross section are used to show possible alternatives. a) The upper restoration shows the way in which shortening has been calculated for this study: only the shortening above the shallowest level of decollement (in this case, decollement within the Icla Formation) has been included. b) This restoration indicates the amount of shortening calculated if the area below the shallowest level of decollement is included and is assumed to be composed of imbrications of the Icla Formation. In this case, the calculated shortening is 46 km rather than 11 km. c) Alternatively, if the excess area is assumed to be composed of stratigraphically lower units (Devonian Santa Rosa and Silurian Tarabuco, Kirusillas, and Cancaniri formations), restoration of these units according to bed lengths yields no additional shortening.

Figure 2.4. Areas of concealed thrusting were included in the calculation of shortening in the cases of the Uncía and West Vallegrande cross sections. The lined areas indicate plausible duplexes of the same structural package exposed at the surface.

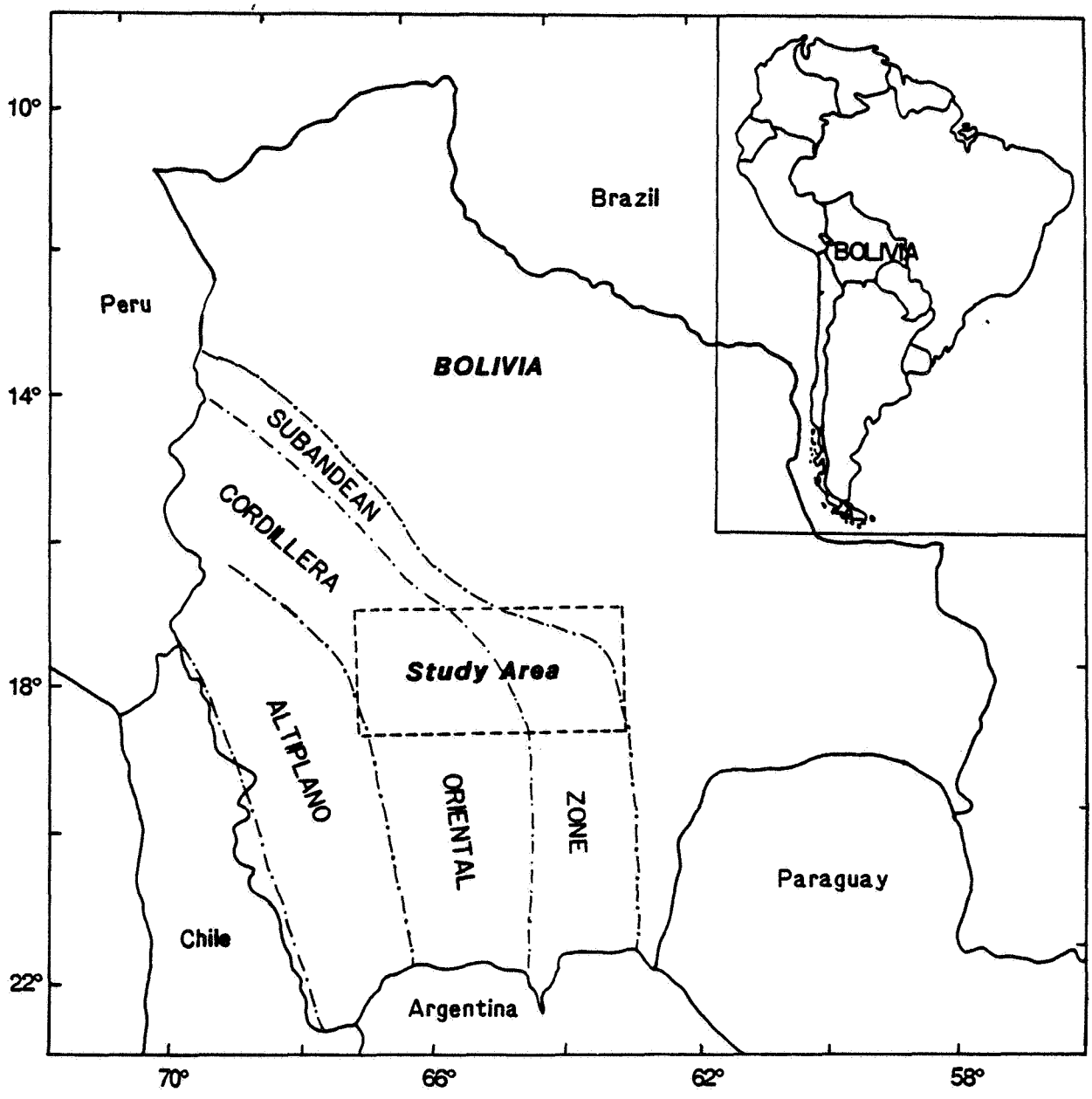
10°
14°
18°
22°
70°
66°
62°
58°
Brazil
Peru
BOLIVIA
Chile
Argentina
Paraguay
SUBANDEAN
CORDILLERA
ALTIPLANO
ORIENTAL
ZONE
Study Area
BOLIVIA

Figure 2.1

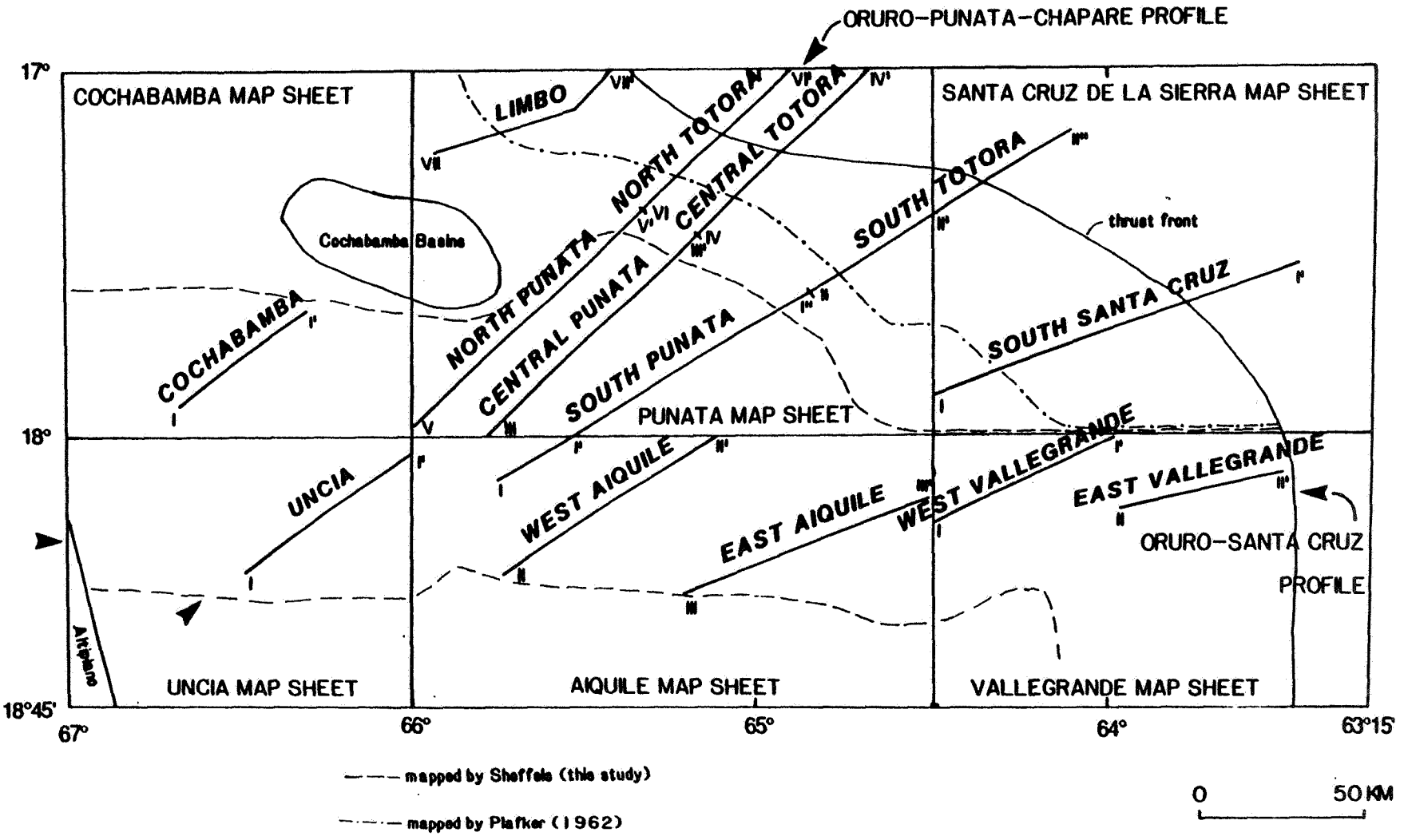
ORURO–PUNATA–CHAPARE PROFILE
17°
COCHABAMBA MAP SHEET
LIMBO
NORTH TOTORA
CENTRAL TOTORA
SOUTH TOTORA
SANTA CRUZ DE LA SIERRA MAP SHEET
thrust front
Cochabamba Basins
NORTH PUNATA
CENTRAL PUNATA
SOUTH PUNATA
SOUTH SANTA CRUZ
COCHABAMBA
PUNATA MAP SHEET
18°
UNCIA
WEST AIQUILE
EAST AIQUILE
WEST VALLEGRANDE
EAST VALLEGRANDE
ORURO–SANTA CRUZ
PROFILE
Altiplano
UNCIA MAP SHEET
AIQUILE MAP SHEET
VALLEGRANDE MAP SHEET
18°45'
67°
66°
65°
64°
63°15'
mapped by Sheffels (this study)
mapped by Plafker (1962)
0
50 KM

Figure 2.2

EAST VALLEGRANDE CROSS SECTION

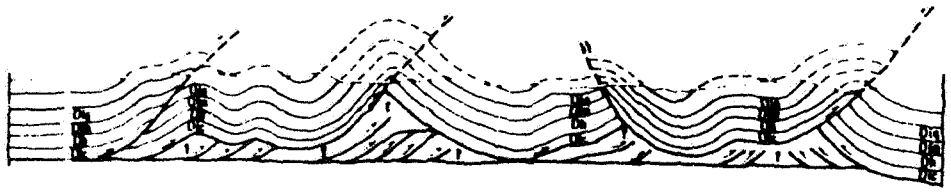

a) RESTORATION ABOVE **SHALLOWEST LEVEL** OF DECOLLEMENT--SHORTENING = **11 KM**

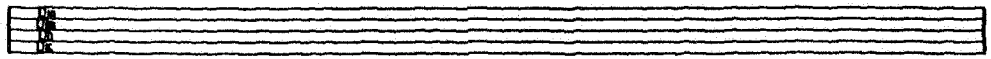

b) RESTORATION ABOVE "BASAL" DECOLLEMENT IN **ICLA** FORMATION--SHORTENING = **46 KM**

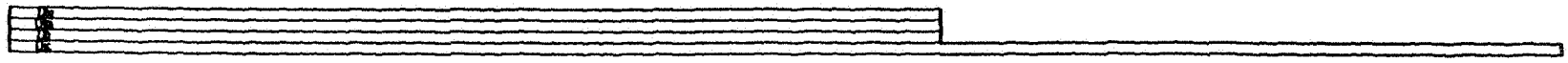

c) RESTORATION ABOVE "BASAL" DECOLLEMENT IN **KIRUSILLAS** FORMATION--SHORTENING = **11 KM**

Figure 2.3

WEST VALLEGRANDE CROSS SECTION
VALLEGRANDE MAP SHEET

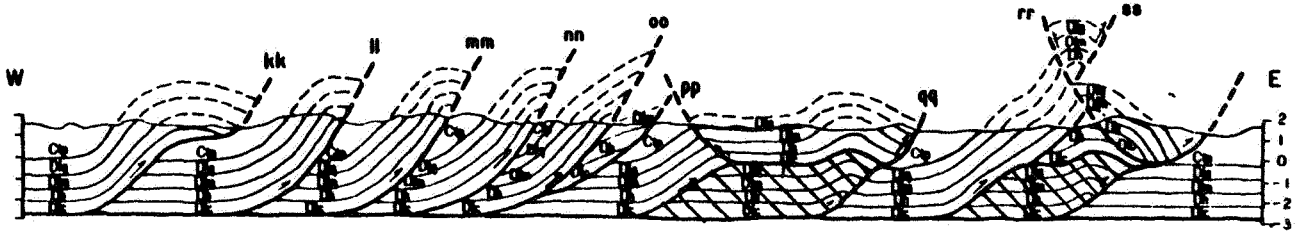

UNCIA CROSS SECTION
UNCIA MAP SHEET

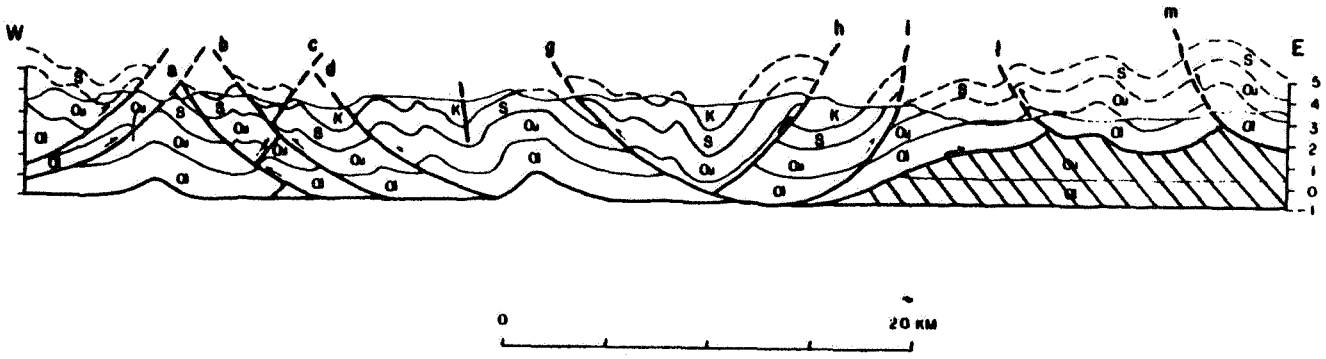

Area in which structural package is assumed to be duplicated; bed lengths included in calculation of percent shortening.

Figure 2.4

CHAPTER THREE

Stratigraphy

Introduction

Rock units exposed in the Cordillera Oriental and Subandean Zone of the mapped area range from Ordovician to Cenozoic in age. A monotonous and almost continuous marine sequence at least 8.5 km thick, dominated by alternating shale and sandstone units (Figure 3.1), makes up the majority of the Paleozoic sedimentary rocks. It is overlain by variable, Carboniferous to Recent lithologies, which are primarily continental in origin and have a cumulative thickness of from 0.5 to 2 km. Lithologies and thicknesses are summarized on stratigraphic columns (Figure 3.2a and b). The description of the units presented is not meant to be exhaustive but to highlight characteristics pertinent to this study. A more comprehensive discussion may be found in Rodrigo and Castaños (1978).

Ordovician rocks The oldest rocks exposed in the mapped area are Ordovician. Due to the monotonous lithologies exposed, the Ordovician sequence is only locally differentiated into formations. Near Cochabamba, in the southern and northwestern portions of the Punata and Aiquile map sheets, respectively, the following three units are recognized, from lower to upper: the Capinota, Cuchupunata, and San Benito formations.

The Capinota Formation consists of black to grey shale, with some silt-, sand- or mudstone layers. It is fossiliferous and bioturbation is present. Fossils are sometimes carbonatized, and *Lingula* is a common but not

diagnostic fossil. The Cuchupunata Formation comprises a thick sequence of green or brown mudstone that is usually thin- to medium-bedded but is more rarely massive. Interbedded shale with micaceous partings is present but is infrequent. The rocks are bioturbated and fossiliferous; *Lingula* is common as well as the trace fossil *Skolithos*. The San Benito Formation is composed of massive, pink, grey, or green quartzite that weathers into distinctive brown or grey cliffs. It is fossiliferous, and *Skolithos* tubes are common throughout the formation. All contacts between formations are conformable and gradational.

These formational divisions cannot be recognized beyond the Cochabamba region. Although the lower part of the Ordovician sequence elsewhere is lithologically similar to the Capinota Formation, the San Benito and Cuchupunata formations are replaced by a homogeneous grey-green siltstone with sandstone and quartzite interbeds. This sequence is micaceous and poorly-bedded; ripple marks and disruptions of bedding by bioturbation are common. In all areas beyond the Cochabamba region, therefore, I have informally divided the Ordovician sequence into lower and upper units, that correspond to a lithologic division between shale and sandstone, respectively.

The depositional environment of the Ordovician rocks was shallow marine, as indicated by abundant ripple marks, bioturbation, and the trace fossil *Cruziana* sp. Abundant fossils, including graptolites, trilobites, and brachiopods, date the rocks as Tremadocian to Ashgillian (Suarez S., 1976). The depositional basin had source areas to the east, south, and west. Facies variations and progressive younging of fossil stage ages to the east indicate a transgression from west to east.

Sections measured by other workers range from 3.5 kilometers to as much as 4.5 kilometers (Rodrigo and Castaños, 1978). Thicknesses inferred from maps of the study area, accounting for dip, range from 2.5 km in the east to 3.5-4.0 km in the west. The base of the Ordovician sequence is not exposed.

Silurian rocks Silurian rocks are represented by two sequences of formations. In the east, the Silurian rocks are divided into three formations, from lower to upper, the Cancaniri, Kirusillas, and Tarabuco formations, and in the west, they are divided into five formations, from lower to upper, the Cancaniri, Huanuni, Llallagua, Uncía, and Catavi formations.

The Cancaniri Formation is a grey diamictite, sometimes intercalated with small amounts of laminated dark shale, bedded sandstone, or conglomerate. The diamictite matrix varies in grain size, from mudstone to sandstone. Clasts of the underlying Ordovician units up to 0.5 cm in diameter as well as angular, striated clasts of unknown provenance and possible glacial origin are present. The Cancaniri Formation has been variously described as a tillite (Lohmann, 1970) or as a marine deposit with a reworked tillite component (Crowell et al, 1981). It is massive, and exhibits conchoidal weathering. Fresh surfaces are grey and weather purple or grey-green. This distinctive unit is present throughout the Bolivian Andes; within the mapped area, its average thickness is approximately 200 meters. The Cancaniri Formation paraconformably overlies the Ordovician sequence.

The Huanuni and Llallagua formations are only present in the western Cordillera Oriental near the towns for which they are named. The Huanuni

Formation consists of grey and green, micaceous, thin-bedded, unfossiliferous shale. It reaches a maxumum thickness of 600 meters near Llallagua, but thins rapidly away from that area. The Llallagua Formation is comprised of grey, clean quartzite and some well-indurated coarse-grained grey sandstone, which weather orange-green. It is locally 500 meters thick, but thins rapidly away from the type locality. Either of these two formations unconformably overlies the Cancaniri, and the Llallagua conformably overlies the Huanuni, where the Huanuni is present.

Throughout most of the mapped area, however, the Cancaniri is overlain directly by shale of the Kirusillas or Uncía formations. The Kirusillas and Uncía formations are lateral equivalents that are present in the eastern and western parts of the study area, respectively. The Kirusillas consists of fossiliferous black shale, with sandy concretions and some discontinuous sandstone layers. It is approximately 800 meters thick. It grades laterally to the west into the Uncía Formation, that consists of black, brown or grey, well-laminated, micaceous siltstone and shale, with rhythmic sandstone layers 1 to 5 centimeters thick, which occur 10 to 15 centimeters apart. The Uncía Formation is about 800 meters thick in the east and thins to approximately 600 meters to the west.

Above the Kirusillas and Uncía formations lie the Tarabuco and Catavi formations, respectively, which are lateral equivalents. Contacts between the Kirusillas and Tarabuco and the Uncía and Catavi formations are conformable and gradational. The Tarabuco Formation is comprised of approximately 600 meters of well-indurated, dirty, grey-green, fine-grained sandstone and grey quartzite, with minor red and grey shale. It is thin- to medium-bedded, fossiliferous, and commonly the bedding has been distrubed by bioturbation. Its lateral equivalent, the Catavi Formation is a

cross-stratified, dark red or grey sandstone, of variable bedding thickness. It is interbedded with black shale. The Catavi Formation is aproximately 400 meters thick.

A neritic depositional environment for all five formations is indicated by widespread bioturbation and fossil content. Source areas are presumed to have been located to the west, northeast, southeast, and south (Rodrigo and Castaños, 1978), but paleocurrent directions have not been studied. Facies variations suggest a predominantly western source.

Devonian rocks The Devonian sequence is differentiated into five formations (from lower to upper): the Santa Rosa, Icla, Huamampampa, Los Monos, and Iquiri formations. In the western Cordillera Oriental, the Santa Rosa Formation is replaced by its lateral equivalent, the Vila Vila Formation. These formations, particularly the Los Monos Formation, are sources of petroleum in the Subandean Zone.

The Santa Rosa Formation consists of approximately 400 meters of thin- to medium-bedded, pink and grey quartzite. The Vila Vila Formation consists of fine-grained, purple to light grey, medium-bedded quartzite and thin-bedded shale. It varies in thickness from 500 meters to more than 1900 meters, north of the mapped area. Its contact with the underlying Silurian Catavi Formation is conformable and gradational.

The Icla Formation forms the basal unit in an alternating sequence of shale and sandstone, which makes up the remainder of the Devonian formations. The Icla Formation consists of grey-green to black shale. Approximately 600 meters thick, it is thin-bedded, micaceous, and fossiliferous. The Huamampampa Formation is comprised of approximately 600 meters of fine-grained, dirty, yellow-green sandstone intercalated

with shale. Three thick sandstone subunits characterize the Huamampampa Formation in the Subandean zone, but to the west, the formation consists of a more homogeneous mixture of sandstone and shale layers. Well-bedded and laminated, it is micaceous and fossiliferous, and there is abundant evidence of bioturbation. The Los Monos Formation consists of primarily dirty, micaceous, fossiliferous, black shale, with minor intercalated, poorly-bedded, grey-green sandstone. It is 600 meters thick. The Iquiri Formation is composed of approximately 600 meters of sandstone, interbedded with shale and characteristically exposed in lenses rather than continuous planar beds. It is red-brown, green, or black on fresh surfaces and weathers yellow. Laminations are micaceous, and the formation is very fossiliferous. Sandstone grain size increases to the west.

All contacts within the Devonian sequence are conformable. Ripple marks, lithologies, and fossil content indicate that the depositional environment continued to be, as in Silurian time, shallow marine. The Devonian sequence thins and becomes finer-grained from north to south and from west to east. Isaacson (1975) suggested that these trends indicate a western source for the Devonian sediments.

Carboniferous rocks Carboniferous sedimentary rocks consist predominantly of terrestrial deposits, with some interbedded marine rocks. The Carboniferous rocks can be divided into the following formations (from lower to upper): Itacua, Tupambi, Tarija/Taiguati, Escarpment, Elvira, and San Telmo. These formations are sometimes combined into the Machareti (Itacua through Taiguati formations) and Mandiyuti (Escarpment Formation) groups, which are the divisions recognized on the air photos.

The Itacua Formation consists of grey-black diamictite, including some tillite, and multi-colored sandstone, mudstone and shale (IGCP, Rodrigo and Castanos, 1978; Helwig, 1972). Angular clasts in the diamictite include red granite. Soft sediment deformation is commonly present.

The Itacua unconformably overlies the Devonian rocks, but the angular discordance is never greater than 5° (Isaacson, 1975). The Itacua represents a mix of marine, as indicated by fossils, and glacial deposits. It varies in thickness from a maximum of 195 meters in the southern Subandean Zone (Helwig, 1972) to approximately 50 meters within the mapped area, where it is present irregularly.

The Tupambi Formation consists of coarse-grained, thick-bedded or massive, cross-bedded, red and yellow sandstone with some conglomeratic layers, that are particularly common near the base. The conglomerate contains clasts of red granites, whose source is to the southeast, and Devonian sedimentary rocks.

The Tupambi paraconformably overlies the Itacua. Its thickness is variable, but it is approximately 600 meters thick within the mapped area. The fluvioglacial sediments of the Carboniferous are the oldest continental deposits in the stratigraphic sequence.

Overlying the Tupambi is a complex sequence of sedimentary rocks that has been subdivided into the Tarija, Chorro, and Taiguati formations. The Tarija is comprised of multi-colored shale and diamictite, characterized by soft sediment deformation, with some sandstone layers. The Taiguati contains similar diamictite and shale, often red, as well as conglomeratic sandstone and mudstone. Diamictite in the Taiguati is thought to be primarily tillite whereas the diamictite of the Tarija is thought to be mostly marine sediment that has been reworked from tillite (tilloid)

(Helwig, 1972). Clasts in the diamictite consist of quartzite and volcanic fragments and acid plutonic rocks, including red granites from Argentina (Lohmann, 1970; Fernandez G., 1981). An interbedded, coarse-grained, yellow sandstone is locally extensive enough to the south of the study area to be mapped separately as the Chorro Formation.

The Tupambi Formation is unconformably overlain by either the Tarija, Taiguati, or Chorro formations. Depositional relations between the Tarija, Taiguati, and Chorro formations remain incompletely understood (J. Oller and O. Aranibar, 1985, pers. comm.). The Chorro Formation is described as a lateral equivalent of both the Tarija and the Taiguati formations (Helwig, 1972; Rodrigo and Castaños, 1978) and is in conformable contact at its base and top with either of these formations. The contact between the Tarija and Taiguati formations is also described as conformable. These formations are of variable and only locally significant thicknesses within the mapped area; they thicken to the south. The Tarija and Taiguati formations are typically less than 100 meters, although in one part of the mapped area, the Tarija reaches a thickness of 400 meters. The Tarija/Chorro formations are typically 300 meters thick (Helwig, 1972). Marine fossils in the Tarija and Taiguati formations indicate a return to a marine depositional environment from the terrestrial environment of the underlying Tupambi Formation. Source areas from the marine rocks are predominantly to the southeast.

The Escarpment Formation is made up of coarse- to medium-grained, very friable, cross-bedded, thick-bedded or massive, red and yellow sandstone that weathers into the distinctive red cliffs for which the unit is named. A basal conglomerate is commonly present. In the Cordillera Oriental, this formation is comprised of intercalated red silty shale and

sandstone with basaltic intrusions (Helwig, 1972). The source areas for the Escarpment were predominantly in the southeast and west (Helwig, 1972).

The Escarpment Formation lies disconformably on the Tarija/Taiguati formations or on older rocks. It varies in thickness from 100 to 500 meters; within the Subandean zone of the mapped area it is approximately 500 meters thick, whereas in the Cordillera Oriental it is approximately 300 meters thick. The fluvioglacial environment of the Escarpment Formation in the Subandean Zone is similar to that of the Tupambi. Correlative Carboniferous sedimentary rocks in the Cordillera Oriental are lacustrine (Helwig, 1972).

In the Subandean Zone, predominantly south of the mapped area, the Escarpment is comformably overlain by the Elvira and the San Telmo formations, which are made up of red-weathering, yellow sandstone. The Elvira Formation is variably present. The San Telmo Formation is fossiliferous. It was not observed in the mapped area.

Permian rocks The Permian Copacabana Formation consists of marine limestone, locally very fossiliferous, and calcareous sandstone. It is present in the mapped area only near the villages of Torotoro and Pasorapa (Aiquile sheet, Cordillera Oriental and Subandean zone, respectively).

The Copacabana Formation conformably overlies the Escarpment Formation. Within the mapped area, it is approximately 50 meters thick, and it thickens to the northwest towards Lake Titicaca (Helwig, 1972). Its lower Permian age is well-determined (Rodrigo and Castaños, 1978). Fossil content and lithology indicate that the Copacabana was deposited in a shallow, semi-isolated sea, with a source for the terrigenous sediments

primarily in the northeast, although transport of some material was also from the west and south (Rodrigo and Castaños, 1978).

Cretaceous rocks--Cordillera Oriental Although various formation and group divisions have been proposed by many workers, attempts to correlate the different units and define a general sequence for the Cretaceous rocks have been unsuccessful because of their lithological variability and the lack of age control. Sempéré's (1987) proposed stratigraphic column (Figure 3.2b) is used as a framework for discussing the Cretaceous rock present in the mapped area.

Sempéré recognized the following formations (from lower to upper, using traditional names except where noted): Sayari (proposed), Macha, Sicaya (proposed), Condo, La Puerta or Sucre, Tarapaya, Miraflores, Aroifilla, Chaunaca, El Molino, and Santa Lucia. Thicknesses of the different formations vary drastically between localities. In some places entire formations are missing. A complete sequence containing these formations is never exposed, and stratigraphic columns for specific locations should be consulted for information on the local rock sequences (see references in Sempéré, 1987). The depositional environments for the Cretaceous rocks alternated between continental and shallow marine to littoral settings, as indicated by variations in lithology and fossil content. None of the unconformities between the various units, however, are large angular unconformities.

The Sayari Formation consists of red conglomerate, conglomeratic sandstone, mudstone, and gypsiferous shale and white gypsum beds. It is present only in the Cochabamba region, where it unconformably overlies Paleozoic rocks. The Macha Formation comprises red and white cross-

bedded, coarse- to medium-grained sandstone with local basalt intrusions. It conformably overlies the Sayari Formation. The Sicaya Formation, present in the Cochabamba region, consists of oolitic limestone and calcareous sandstone, intercalated with green marl. It conformably overlies the Macha Formation. The Condo Formation consists primarily of red, coarse-grained, thick-bedded conglomerate, that becomes finer-grained upwards and grades into thin-bedded sandstone and siltstone and, locally, into well-developed red shale. It also contains basalt intrusions. It is bounded at both its base and top by unconformities. The La Puerta Formation comprises red, yellow or white, medium- to coarse-grained, well-indurated, massive, cross-bedded sandstone that is locally intruded by basalt. It is unconformably overlain by the Tarapaya Formation, a unit composed predominantly of mudstone and distinctive purple or red shale, with thin, interbedded sandstone. The Miraflores Formation, where present, unconformably overlies the Tarapaya Formation. It consists of marine limestone, that locally becomes sandy towards the base. The Miraflores Formation is unconformably overlain by red shale and shaly sandstone, with gypsum, of the Aroifilla Formation. The Chaunaca Formation rests conformably on the Aroifilla Formation, and consists of a basal limestone overlain by thin-bedded green and red mudstone and shale with gypsum and other evaporite beds. It is locally intruded by basalts. The El Molino Formation rests unconformably on the Chaunaca Formation and consists of marine limestone and, particularly towards its base, shaly limestone. The Santa Lucia Formation conformably overlies the El Molino. It consists of red shale and medium-bedded red sandstone, locally intruded by basalt. Deposition of the Santa Lucia extended from the Cretaceous into the Tertiary in some places, but elsewhere it is entirely Tertiary in age.

Within the mapped area, the Cretaceous rocks are characterized by red and white, massive, cross-bedded, well-indurated sandstone (Figure 3.2b). The position of these partial sequences within Sempéré's scheme or in absolute time is difficult to unambiguously identify without paleontological control. This study does not address this issue.

Cretaceous rocks--Subandean Zone Cretaceous sedimentary rocks in the Subandean Zone, primarily south of the mapped area, are divided into the following formations: the Ichoa, Yantata, and Cajones formations.

The Ichoa Formation is an unfossiliferous, friable, red sandstone with amber quartz. A conglomerate is sometimes present at the base of this cross-bedded sandstone.

The Yantata Formation is comprised of a massive yellow sandstone characterized by chert layers at its base. The contact between the Ichoa and Yantata formations is transitional.

The Cajones Formation is a grey or pink calcareous sandstone with shaly layers at its base. This red- or brown-weathering unit contains fish fossils that date it as Cenomanian to Maestrichtian in age. It conformably overlies the Yantata Formation.

Tertiary rocks--Cordillera Oriental Early Tertiary deposition occurred in a similar environment and was continuous with that of the Late Cretaceous, but middle and upper Tertiary to Recent sedimentary rocks were deposited only locally within the uplifted mountain belt. Paleocene through Eocene or Oligocene rocks are subdivided into the Santa Lucia, Tiwanaku, Coniri, and Kollu-Kollu formations, or Cayara, Potoco, and Mondragon formations (Soria, pers. comm., 10th Arg. Geol. Congress, 1987).

The younger Tertiary deposits are characterized by numerous angular unconformities and syntectonic deposition, as indicated by tectonic controls on sources and thicknesses (e.g. Herail et al;., 1987; Marocco et al., 1987).

Tertiary deposits in the mapped area consist primarily of red, poorly-indurated, often conglomeratic sandstone or white and red gypsiferous clays, typically preserved only in the cores of synclines.

Tertiary rocks--Subandean Zone The Tertiary sequence of sedimentary rocks within the Subandean Zone is divided into the following formations: Petaca, Yecua, and Chaco. These formations thicken considerably and are more widely exposed south of the mapped area.

The Petaca Formation is comprised of a red conglomerate, with calcareous cement and chert and limestone clasts derived from the Cretaceous sedimentary sequence. Its thickness is variable. It disconformably overlies Cretaceous and, to the south, progressively older rocks.

The Yecua Formation is predominantly multi-colored (violet, red, green) shale, with calcareous sandstone layers, gypsum layers, and pelecypod-bearing, green-grey, non-marine limestone layers. It conformably overlies the Petaca Formation.

The Chaco Formation is a poorly-sorted, poorly-consolidated, red-brown sandstone intercalated with shale, but is characterized by many facies changes. Generally, the proportion of sandstone increases and the sandstones become cleaner towards the top of the formation. Vertebrate fossils indicate that its age is Miocene, and it disconformably overlies the Yecua Formation.

Stratigraphic Units recognized on the air photos

The following units were mapped on the air photos (Figure 3.2a). In the Subandean Zone, Cretaceous and Tertiary sedimentary rock of the Subandean Zone sequence could not be differentiated into individual units; and the Carboniferous Tarija/Taiguati and the Itacua formations were mapped with the Tupambi Formation. Units within the upper and middle Devonian sequence could be differentiated easily because of the alternation of incompetent shale and resistant sandstone units. Throughout the map area, the Devonian Santa Rosa and Silurian Tarabuco formations were mapped together, and the Silurian Cancaniri and Kirusillas formations were mapped together. In the Cordillera Oriental, Tertiary and Cretaceous formations could not be differentiated based on photointerpretation alone, and the Devonian Vila Vila and Silurian Catavi, Uncía, Llallagua, and Cancaniri formations were variously mapped together or in subgroups. The contacts between the Vila Vila, Catavi, and Uncía formations are gradational. The Vila Vila and Catavi formations cannot be discerned from the photos because there is no change in resistance across the contact between these two units. The boundary between the Catavi and Uncía formations, while marked by a variation in resistance, is often difficult to identify because the formations have been disrupted by faulting. Similarly, the Cancaniri, Llallagua and Uncía formations show no significant changes in resistance associated with their contacts and they cannot be differentiated on the photos.

Figure Captions

Figure 3.1. Photo of the Paleozoic marine sedimentary sequence from the Cordillera Oriental (Punata map sheet). Ordovician through middle Devonian units dip gently in the direction of view. The hill in the foreground is made up of the Ordovician San Benito quartzite; the valley between it and the hill in the background, which is made up of the Devonian sequence, is underlain by the poorly-outcropping Silurian Kirusillas and Cancaniri formations. The alternation of sandstone and shale units in the Devonian sequence is apparent in the outcrop pattern observed going upsection up the hill.

Figure 3.2a. Stratigraphic column showing lithologies, formation divisions, and units mapped together on the photos.

Figure 3.2b. Stratigraphic column drawn from Sempéré's (1987) description of Cretaceous stratigraphy in the Bolivian Andes, and schematic sections observed in various localities during field work. Thicknesses are unknown; the scale is expanded to show the variation in lithologies observed. Ages based on dating of fossils and basalt flows. For locations of sections based on field work, see Figure 5.1.

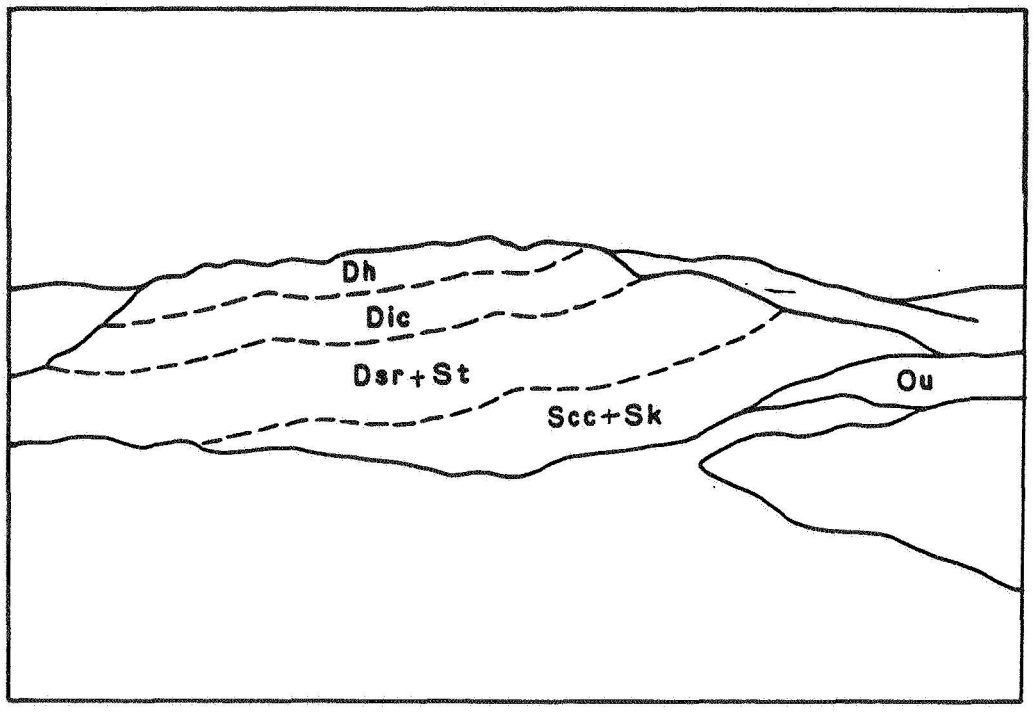

Figure 3.1

Stratigraphic column for the mapped area of the
Cordillera Oriental and Subandean Zone, Bolivia

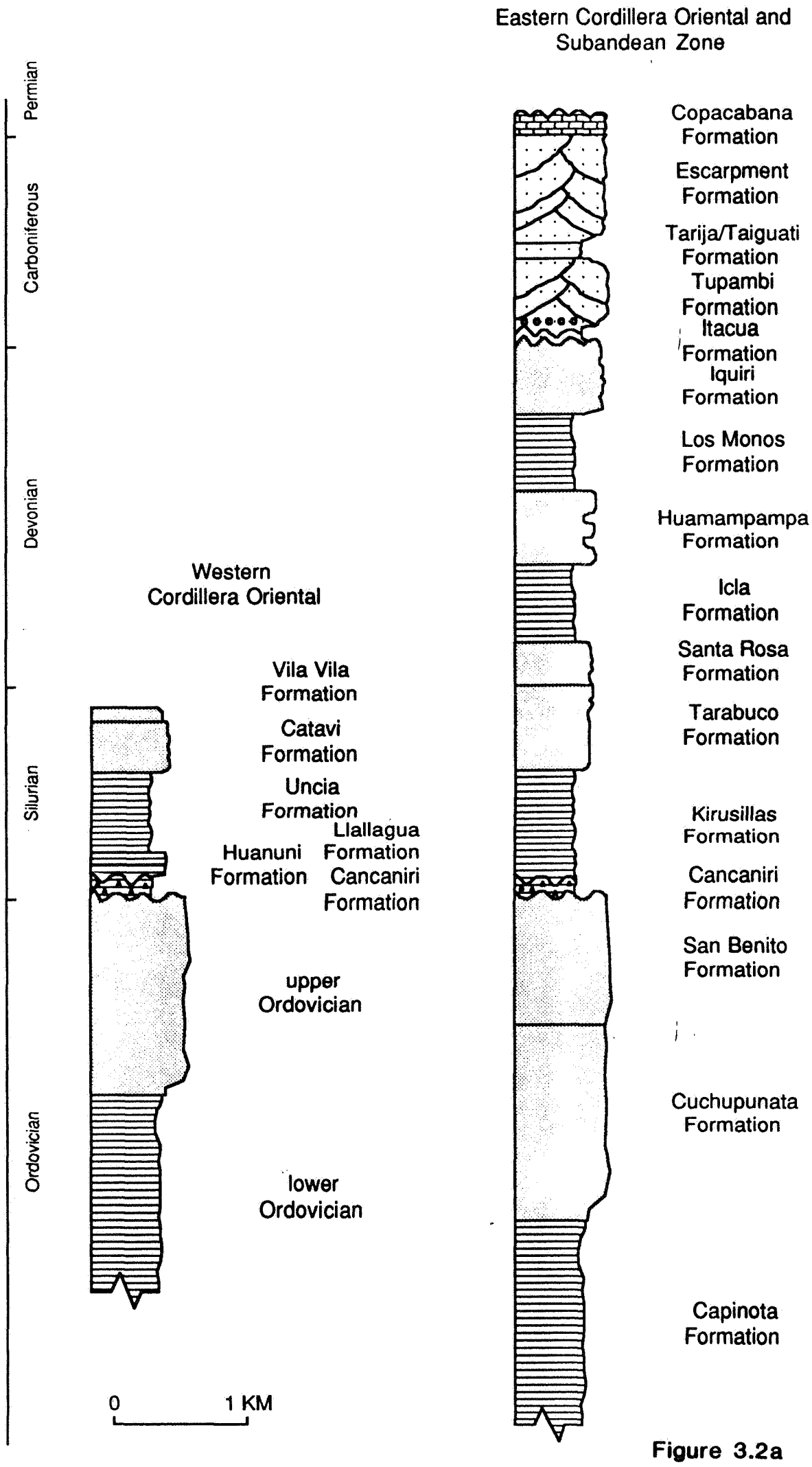

Figure 3.2a

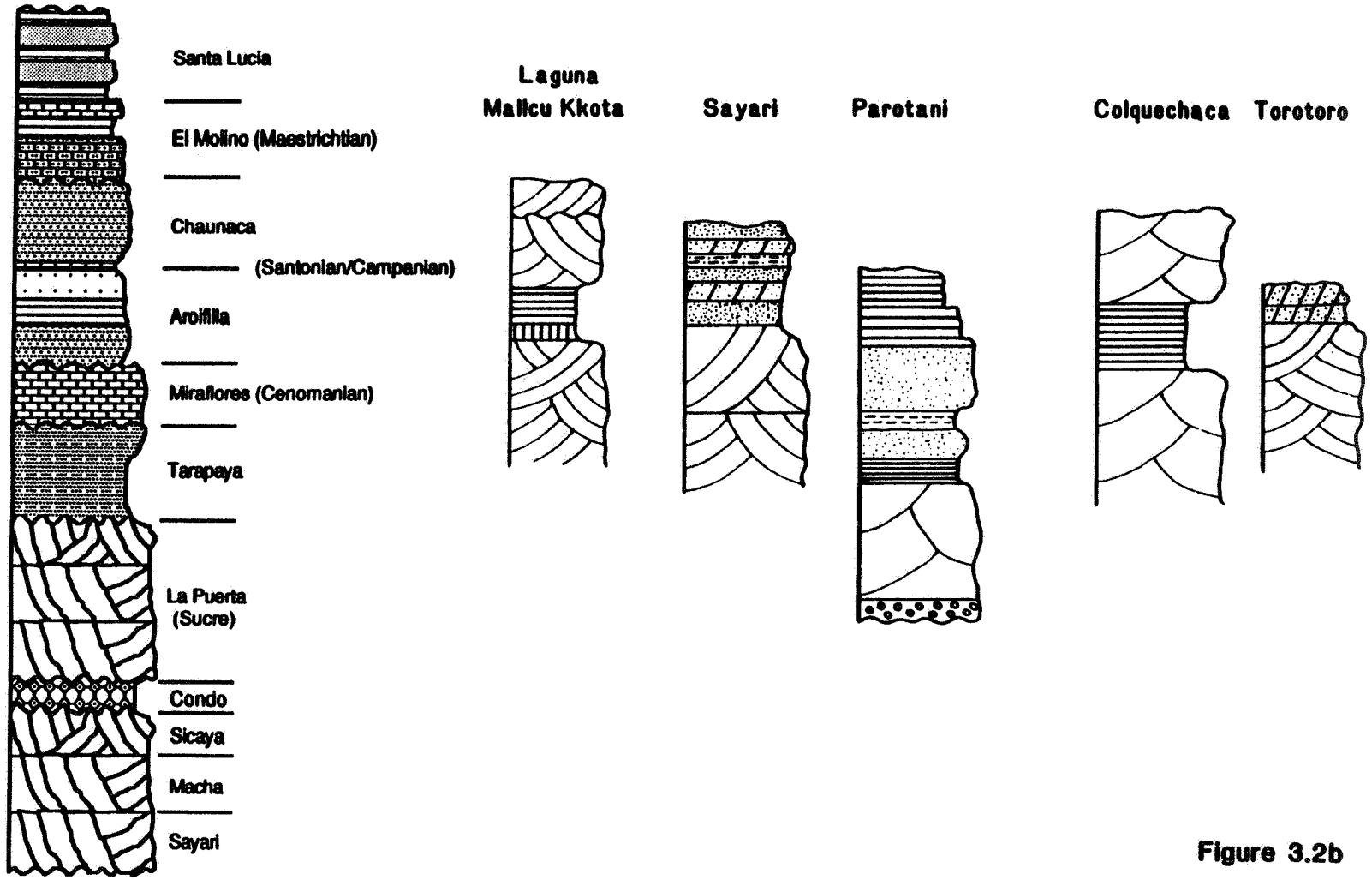
Santa Lucia
El Molino (Maestrichtian)
Chaunaca
(Santonian/Campanian)
Aroifilla
Miraflores (Cenomanian)
Tarapaya
La Puerta
(Sucre)
Condo
Sicaya
Macha
Sayari
Laguna
Mallcu Kkota
Sayari
Parotani
Colquechaca
Torotoro

Figure 3.2b

CHAPTER FOUR

The timing of deformational events in the Bolivian Andes

Introduction

Accurate determination of the style of deformation and of the amount of crustal shortening in a given deformational event requires an understanding of the history of prior deformational events in order to isolate their effects from those of interest. In the Bolivian Andes, a precise chronology of deformational events is not known: poor exposure in the Altiplano, combined with a lack of Tertiary deposits within the Cordillera Oriental and of age constraints on Tertiary deposits within the Cordillera Oriental and Subandean Zone, do not allow the definition of a detailed tectonic history. The recognized distribution and deformation of Tertiary sedimentary rocks and the lack of angular unconformities prior to Oligocene time over much of the mapped area suggest that "Andean" deformation in the Cordillera Oriental and Subandean Zone of the Bolivian Andes occurred primarily after the Oligocene Epoch and continued to the present; they do not rule out the onset of deformation prior to Oligocene time. The definition of the main phase of tectonic activity within the Bolivian Andes as post-Oligocene only is based on observations made during this study, as well as previous studies of the stratigraphic, structural and volcanic history. If correct, it is significantly different from the history of deformation defined for the central Andes based on observations in Peru and Argentina, and implies that, within the overall setting of oceanic

subduction that characterizes the central Andes, different tectonic regimes were present during at least the Mesozoic and Cenozoic Eras along the length of the central Andes.

Evidence for the age of deformation in the Bolivian Andes

Within the Subandean Zone, primarily south of the mapped area, extensive Tertiary sedimentary deposits, some dated by vertebrate fossils, and seismic reflection records (J. Lowell, 1988, pers. comm.) clearly show the onset of major deformation in Miocene time, and the overthrusting of Quaternary sedimentary rocks at the thrust front indicate that the thrust belt is still active (Plafker, 1962; Pareja L., 1978). Within the Cordillera Oriental, it is more difficult to define pre-Oligocene deformational events because fewer Tertiary sedimentary rocks crop out and their ages are poorly known. Tertiary deposits are observed, however, across the entire width of the Cordillera Oriental (Figure 4.1). Based on a correlation with a distinctive conglomerate exposed in the southern Subandean Zone, whose Eocene age is determined from vertebrate fossils (H. Perez, pers. comm.), similar conglomerate within the Cordillera Oriental is presumed to be Eocene in age. Because the Tertiary sedimentary sequence within the Cordillera Oriental constitutes the youngest deformed rock in this region, its deformation suggests that the deformation is at least post-Eocene (Figure 4.2).

These observations are consistent with the conclusions of previous, primarily stratigraphic, studies of the Bolivian Andes (Ahlfeld, 1972; Lohmann, 1970; Helwig, 1972; Isaacson, 1975). The stratigraphic record in the Bolivian Andes records the onset of major deformation in mid-Tertiary time. Continuous marine deposition occurred throughout the Silurian and the Devonian Periods. Its interruption and eventual termination in

Carboniferous time is documented by the parallel or low-angle unconformities that characterize the record of sedimentation from Carboniferous through mid-Tertiary time. These unconformities record a history of minor warping, epeirogenic uplift, and erosion, but the lack of large angular unconformities indicates that these interruptions in sedimentation were not due to major deformational events.

The first period of continental sedimentation occurs in the Carboniferous sequence where coarse-grained sandstone unconformably overlies the marine Devonian Iquiri Formation. The angular discordance of bedding at the unconformity is nowhere greater than 5° (Isaacson, 1975), ruling out any major pre-Carboniferous deformation. Unconformities associated with the alternation between marine and non-marine sedimentary rocks within the Carboniferous sequence are not angular, indicating that only mild local warping and erosion occurred during this period (Helwig, 1972; Lohmann, 1970). These relations are primarily observed within the Subandean Zone, but Carboniferous sedimentary rocks are also observed paraconformably overlying older Paleozoic rocks in the vicinity of Torotoro (Figure 4.3).

The Permian Copacabana limestone crops out only locally within the mapped area, where its basal contact may be a disconformity. Near Lake Titicaca to the north the basal contact is transitional (Helwig, 1972).

The Cretaceous sedimentary sequence was deposited after an interval of erosion. It lies unconformably on rocks of all ages between Ordovician and Carboniferous. Although the Cretaceous sedimentary rocks lie on such a diverse range of stratigraphic units, the observed angular discordance at the unconformities is generally small. Figures 4.3 and 4.4 show the angular relationships typically observed in the field. Cretaceous strata within the

central western Cordillera Oriental are never observed to lie on Paleozoic sedimentary rock with greater than 10° of angular discordance (Thormann, 1966); the classic example observed near Potosí of a basal Cretaceous conglomerate unconformably overlying Ordovician strata involves an angular discordance that is only "slight" (Lohmann, 1970).

The first major angular unconformities within the mapped area separate Miocene and younger sedimentary rocks from underlying formations (Lohmann, 1970), and mark the time from the Oligocene until the present as the main period of folding and faulting (Zeil, 1979; Lohmann, 1970; Jordan and Alonso, 1987). Abundant evidence for Miocene and younger deformation exists in the Subandean Zone north and south of the mapped area, where thick Tertiary sedimentary sequences are definitively involved in the deformation (e.g. Marocco et al., 1987). Recent detailed studies of distinct Tertiary deposits in the Cordillera Oriental (Ybert and Perez, 1986; Cirbian et al., 1986; Sempéré et al., 1986) document the unconformable relationship between middle and upper Tertiary formations and underlying Paleozoic formations, where deposition has followed, or may even be controlled by, mid-Tertiary thrust faulting. Furthermore, Oligocene sedimentary rocks in the eastern Altiplano (Cirbian, pers. comm., 1986) that are deformed with the underlying Paleozoic sequence indicate that the onset of deformation in that locality is post-Oligocene.

Two uncertainties remain in the above conclusion. First, angular unconformities between Paleozoic rocks and Eocene deposits in the eastern Altiplano (Hofstetter, 1968; Hayashida et al., 1984), and between Paleozoic and Cretaceous rocks in the southern Cordillera Oriental and Altiplano (R. Carrasco, pers. comm.) suggest that pre-Oligocene deformation occurred south and west of the mapped area. Second, the ages of the Tertiary

sedimentary rocks in Bolivia are too poorly known to allow correlations with the Miocene and younger phases of deformation recognized in Peru and Argentina.

A Neogene age of deformation is in accord with independent studies of denudation. Fission track ages from the Cordillera Real (Benjamin et al., 1987) indicate an increase in denudation rate beginning approximately 25 Ma, and geomorphologic evidence indicates that the central part of the central Andes, e.g. south-central Peru and northern Chile, low-lying areas in the Oligocene, experienced rapid denudation in Miocene time, probably in response to uplift (Tosdal et al., 1984). Jordan and Alonso (1987) similarly conclude, on the basis of stratigraphic relations, that the region as far south as 20°S was low-lying in Oligocene time. South of this latitude, angular unconformities due to pre-Cretaceous deformation are observed in the Altiplano and Cordillera Oriental near the Bolivia-Argentina border, indicating an approximate southern limit at 20°S of the region possibly unaffected by major pre-Oligocene deformation.

The involvement of Quaternary and Holocene rocks at the thrust front indicates that deformation continues, and suggests that deformation has migrated eastward with time. Along the thrust front, not only are Quaternary sedimentary rocks tilted and faulted, but seismic reflection data and topographic highs also indicate the propagation of surfaces of decollement into the foreland as blind thrusts. A decrease in the intensity of deformation to the east in the Subandean Zone south of the bend in the mountain belt may indicate an eastward progression of deformation. Although the thrust front is active, deformation in the westernmost part of the Cordillera Oriental appears to have ceased, at least in part. In the Cordillera Oriental, near the boundary between the Altiplano and the

Cordillera Oriental, Andean structure is overlain unconformably by Miocene ignimbrites. Within the mapped area, the Morococala Ignimbrites, dated as 5 to 7 Ma, are undeformed and rest on the thrust-faulted and folded sedimentary rocks, indicating that no deformation has occurred in this locality since late Miocene time.

Comparison with the history of deformation in Peru and Argentina

The correlation between the phases of deformation recognized in Peru and Argentina has been assumed to indicate that the same deformation history is applicable to Bolivia (Megard, 1987a, b; Martinez, 1980). The history of deformation outlined above, however, is distinct from that observed to the north, in Peru, and to the south, in Argentina (Figure 4.5). Beginning in Late Devonian time, numerous periods of deformation are recognized in Peru and Argentina. These include Late Devonian to Early Carboniferous deformations (the eo-Hercynian and tardi-Hercynian deformations), followed by at least six Albian to Mio-Pliocene phases of Andean deformation. Occurrences of metamorphism, schistosity, and cleavage are cited as evidence for these phases of deformation in the Bolivian Andes (Martinez, 1980; Megard, 1987a and b), and Ar^{40}/Ar^{39} data are suggestive of a "cryptic" deformational event around 40 Ma (Farrar et al., 1978). As discussed above, however, the stratigraphic and geochronologic record in Bolivia indicates that at least pre-Eocene, and possibly pre-Miocene, deformations did not affect this part of the Andes.

The above discrepancy may be resolved in the following ways. First, cleavage and metamorphism appear to be localized near intrusive contacts in the Cordillera Real, suggesting that these features may be associated with contact metamorphism, or they may have resulted from Tertiary deformation, rather than older regional deformational events.

Second, a non-uniform tectonic history along strike within the central Andes may be hypothesized. Variations along strike in the orientation of the plate margin with respect to the direction of convergence between the subducting and overriding plates, for example, could allow deposition of Devonian, Carboniferous, and Cretaceous sedimentary rocks in one area, adjacent to areas along strike or west of the mapped area, which were experiencing deformation during those time periods. Miocene and younger deformation within the mapped area may, in fact, have been facilitated by the thickness of sediments deposited during the quiescent periods. Whatever the explanation for the distinct histories of deformation may be, variations along strike in the style of deformation or in its lateral extent in the central Andes must play a role.

In summary, currently available data on the distribution and ages of Tertiary sedimentary rocks suggest that the major deformation within the mapped area may be post-Oligocene in age. Within the mapped area, therefore, the style of deformation and the amount of shortening that has occurred since the Oligocene is probably not superimposed on older events or complicated by metamorphism. The possibility of an earlier onset of deformation is not definitively ruled out, and older deformation is indicated in parts of the Altiplano, as well as to the north, in Peru, and to the south, in Argentina.

Figure Captions

Figure 4.1. Areas of outcrop of deformed Tertiary sedimentary rock mapped in the study area are shown within the outlines of the mapped area. The ruled areas are Tertiary outcrops identified in the field; since Tertiary rocks could not be differentiated on the air photos, it is likely that there are more Tertiary outcrops.

Figure 4.2. Photo from the Subandean Zone showing the involvement of Tertiary sedimentary rocks in the deformation. The light-colored rocks in the foreground are Tertiary (Eocene?) clays (T) that are vertical. The hill behind the Tertiary rocks is made up of the middle and upper Devonian Icla (Dic), Huamampampa (Dh), and Los Monos (Dlm) formations, which are overthrusting the Tertiary clays. The thrust fault is concealed from view; vertical to overturned bedding within the Tertiary is indicated by dashed lines.

Figure 4.3. Thematic Mapper image from the Cordillera Oriental. The syncline shown involves Ordovician through Tertiary rocks. No large angular unconformities can be seen between the various units. The Cretaceous-Paleozoic contact is marked by a light-colored band; Cretaceous bedding is parallel to that of the underlying Paleozoic units. O--Undifferentiated Ordovician sedimentary rocks; S--Cancaniri and Kirusillas formations; K--undifferentiated Cretaceous sedimentary rocks; T--undifferentiated Tertiary sedimentary rocks.

Figure 4.4. Photo from the Cordillera Oriental, West Aiquile region, Aiquile map sheet, showing another example of the lack of angular discordance between Cretaceous and underlying units. In this case, Cretaceous sandstone (K--center of photo, forming core of a gentle syncline) overlies the Silurian Kirusillas and Cancaniri formations (S) and the Ordovician San Benito Formation (Osb), which make up the cliffs and gently-dipping bedding surfaces in the foreground.

Figure 4.5. Correlation diagram of deformational events along the central Andes. Abbreviations: ftb--fold and thrust belt; K--Cretaceous.

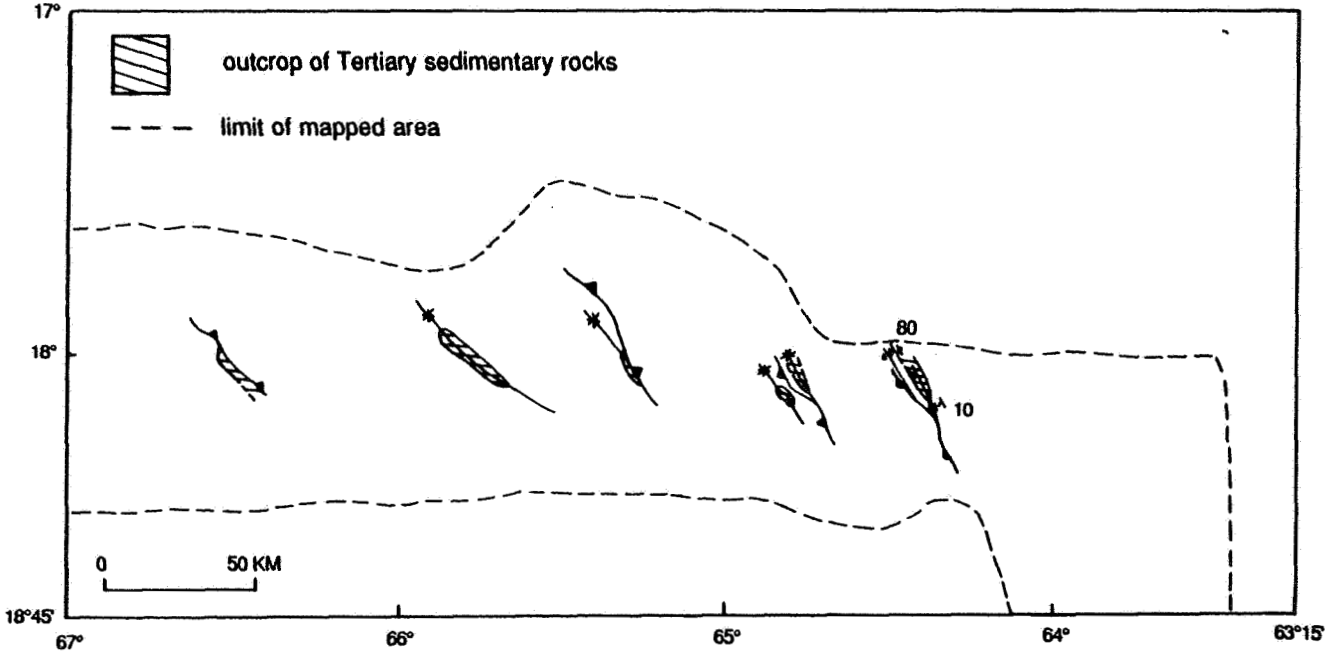
17°
18°
18°45'
67°
66°
65°
64°
63°15'
outcrop of Tertiary sedimentary rocks
limit of mapped area
80
10
0
50 KM

Figure 4.1

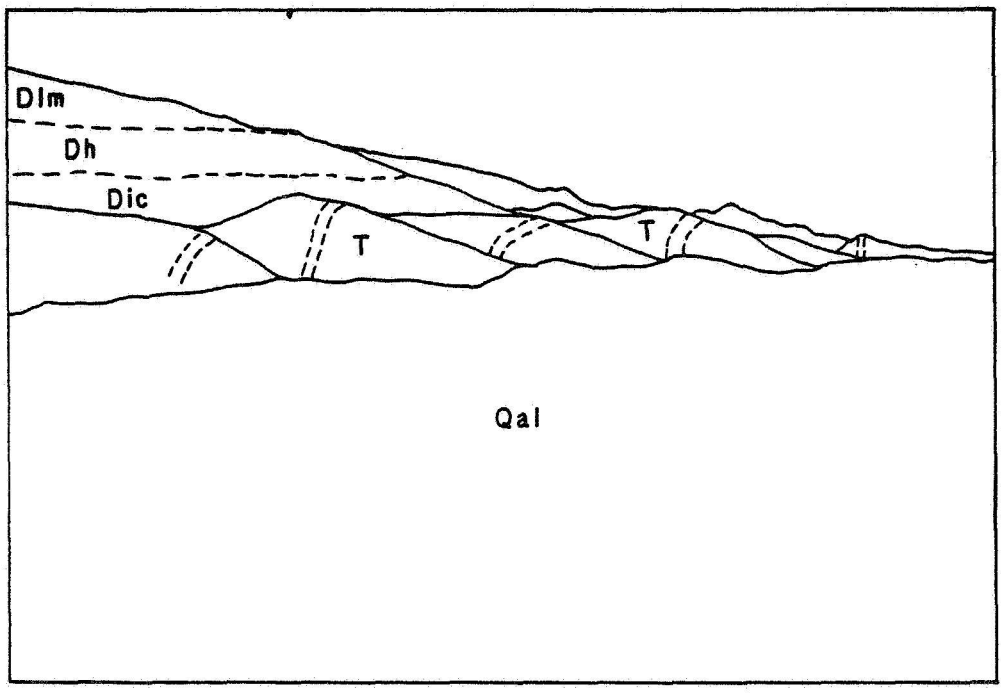

Figure 4.2

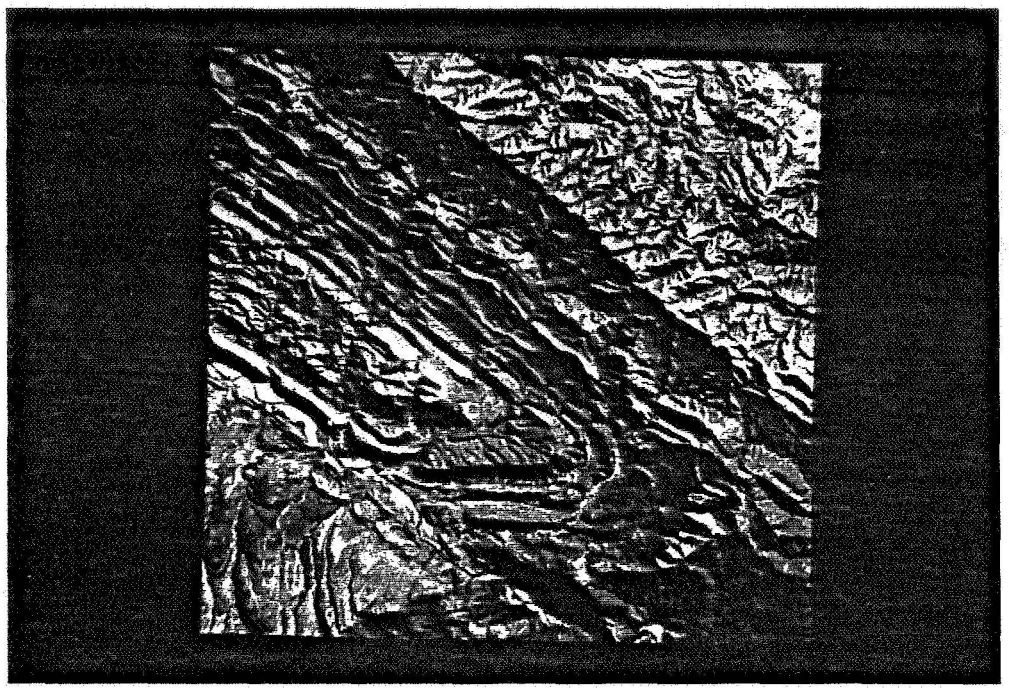

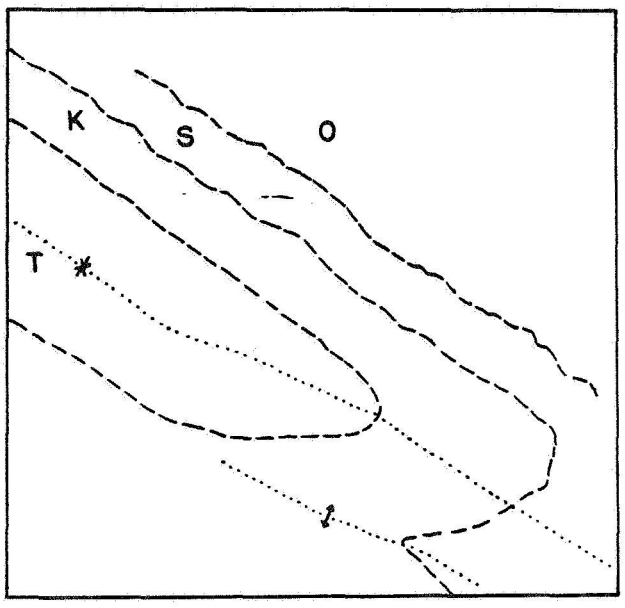

Figure 4.3

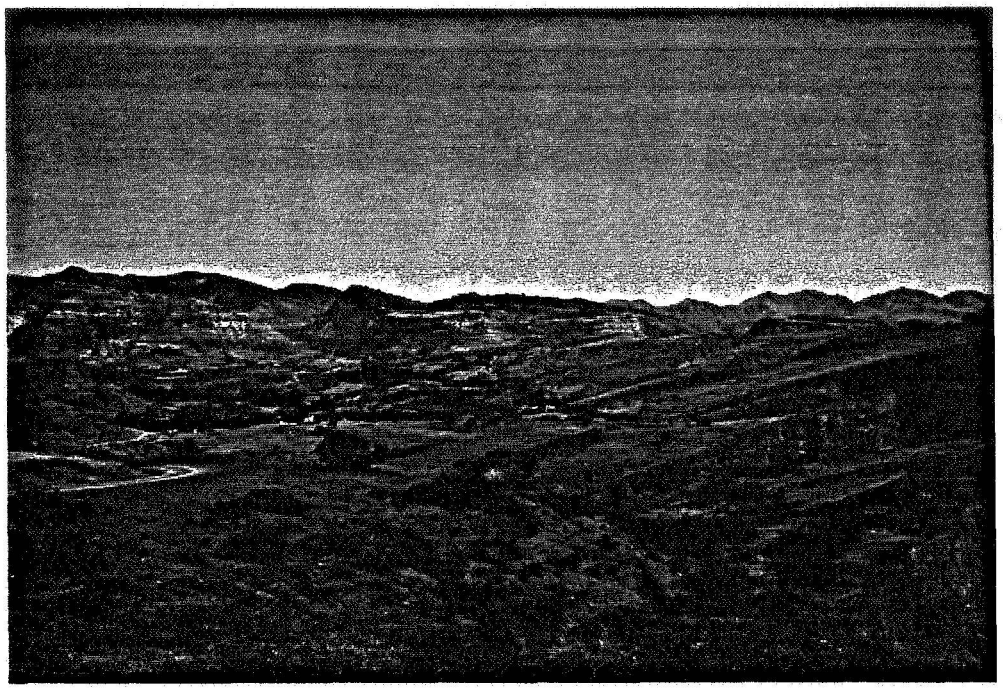

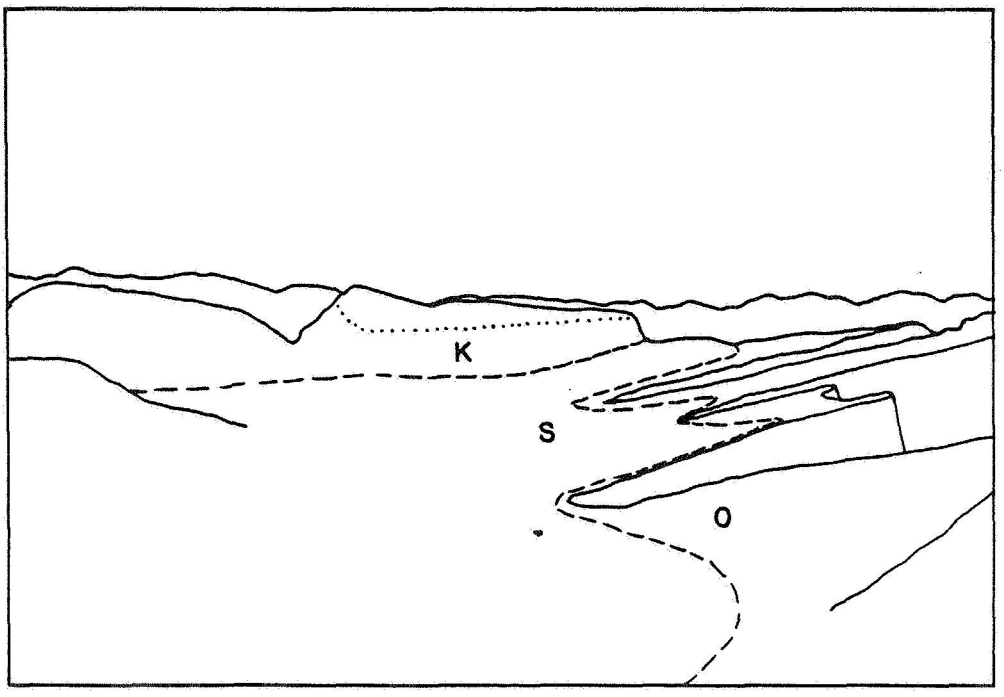

Figure 4.4

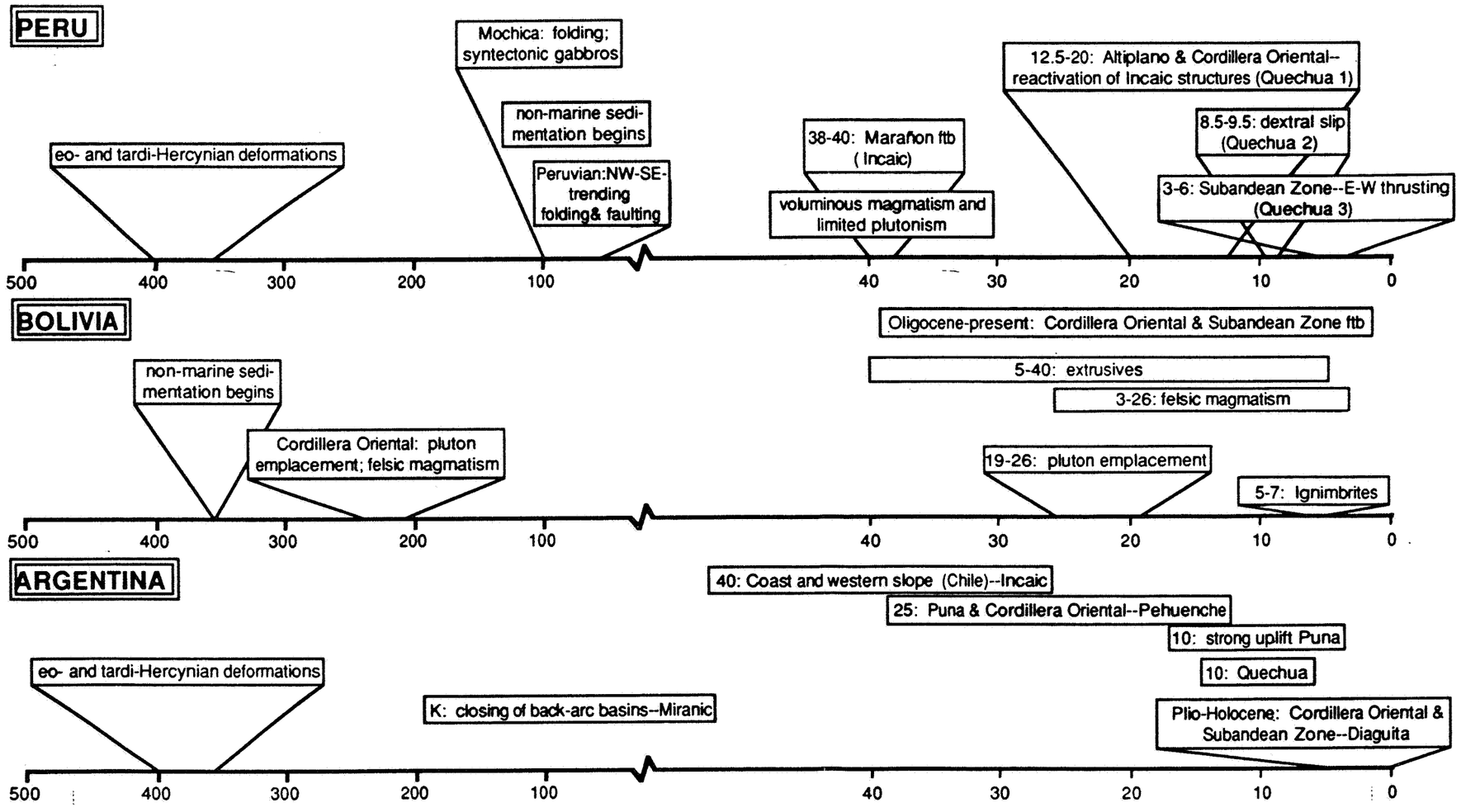
PERU
Mochica: folding; syntectonic gabbros
non-marine sedi-mentation begins
eo- and tardi-Hercynian deformations
Peruvian:NW-SE-trending folding& faulting
38-40: Marañon ftb (Incaic)
voluminous magmatism and limited plutonism
12.5-20: Altiplano & Cordillera Oriental--reactivation of Incaic structures (Quechua 1)
8.5-9.5: dextral slip (Quechua 2)
3-6: Subandean Zone--E-W thrusting (Quechua 3)
500 400 300 200 100 40 30 20 10 0
BOLIVIA
Oligocene-present: Cordillera Oriental & Subandean Zone ftb
5-40: extrusives
3-26: felsic magmatism
non-marine sedi-mentation begins
Cordillera Oriental: pluton emplacement; felsic magmatism
19-26: pluton emplacement
5-7: Ignimbrites
500 400 300 200 100 40 30 20 10 0
ARGENTINA
40: Coast and western slope (Chile)--Incaic
25: Puna & Cordillera Oriental--Pehuenche
10: strong uplift Puna
10: Quechua
eo- and tardi-Hercynian deformations
K: closing of back-arc basins--Miranic
Plio-Holocene: Cordillera Oriental & Subandean Zone--Diaguita
500 400 300 200 100 40 30 20 10 0

Figure 4.5

CHAPTER FIVE

The Style of Deformation in the Bolivian Andes

Introduction

New interpretations of the structure of the Bolivian Andes, based on mapping and photogeologic interpretation, indicate that the Cordillera Oriental and Subandean Zone of the Bolivian Andes have been deformed in the thin-skinned style typical for foreland fold and thrust belts. Although it has been hypothesized, based on work done in Argentina, that the Bolivian Andes are structurally similar to the detached tectonic provinces of the Precordillera and Subandean Zone in Argentina (Jordan et al., 1983), previous work in Bolivia concluded that thick-skinned deformation characterized the Bolivian Andes (Martínez, 1980; Zeil, 1979). On the basis of the observation that faults at the surface dip steeply both east and west throughout the Bolivian Andes, Martínez concluded that block uplift of crustal extent occurred along these reverse faults of mixed vergence. New mapping in Bolivia (Plates 1 through 6, Figure 5.1), however, reveals structures that require that the deformation be thin-skinned. Although many of the features of this fold and thrust belt are typical of other foreland belts, some are unique to the Bolivian Andes.

Evidence for a thin-skinned style of deformation

Two field observations are crucial to the interpretation that the Bolivian Andes are comprised of a thin-skinned fold and thrust belt. One is that the oldest formation exposed in a given area is typically adjacent to

the thrust faults. The other is that neither the stratigraphic level nor the elevation of the cores of synclines varies greatly within a given area. These observations require that the steep to moderate dips of the faults observed at the surface become gentle to horizontal at depth and merge into a decollement, even though this style of deformation is not observed directly at the surface (Buxtorf, 1916). Many of the features of the style of deformation, such as the parallel folding, bedding-parallel shear, and transfer structures that characterize the mapped area (discussed below in detail), corroborate the thin-skinned interpretation. These features are characteristic of thin-skinned deformation of sedimentary sequences that are composed of an alternation of competent and incompetent units (Rich, 1934; Bally et al., 1966; Dahlstrom, 1970).

Levels of Decollement

As discussed in Chapter 2, the lack of subsurface information means that both the stratigraphic level and the depth to the surfaces of decollement must be inferred from the surface geology, and that the surfaces of decollement depicted are only the shallowest ones of the thin-skinned thrust system.

Using the criteria that the surface of decollement lies within the oldest formation that is adjacent to the thrust faults at the surface, three levels of decollement are identified in the mapped area. All of the decollements are located within shale units: 1) the Lower Ordovician Capinota Formation or undifferentiated shale of Lower Ordovician age, 2) the Silurian Kirusillas Formation, and 3) the Devonian Icla Formation. The level of decollement varies within the mapped area in a way typical of fold and thrust belts. In the northern part of the mapped area, where the mountain belt becomes narrower, the level of decollement remains localized within

the Lower Ordovician shales, until quite close to the thrust front where it ramps up into Devonian rocks or even into Tertiary rocks. In the southern part of the mapped area, the level of decollement ramps up to the east approximately halfway across the present-day width of the mountain belt. From the Lower Ordovician shales, it may either ramp up directly into the Devonian Icla Formation or it may follow an intermediate flat in the Silurian Kirusillas Formation. Folding and relative uplift of the observed surfaces of detachment indicate that there are deeper, unexposed levels of decollement. In the Subandean Zone south of approximately 18°S, these deeper faults comprise a blind fault system that extends to the thrust front (Figure 5.3).

The depth to the various surfaces of decollement must also be defined by the surface geology. The limited subsurface information that was available to me did not define the deep geometry of the fault system because it did not extend to a great enough depth. Furthermore, the regional uplift caused by the deeper, blind decollements precluded using conventional depth to detachment calculations: calculations yielded depths in excess of the entire stratigraphic column due to the excess area introduced by deformation on the deeper faults. In the outer part of the mountain belt, the shallowest surface of decollement, within the Icla shale, lies at approximately three kilometers below sea level, as defined by observed stratigraphic thicknesses. This level is approximately 4 km higher than the regional stratigraphic level defined by well and seismic reflection data in the foreland (Figure 5.4). The implications of this difference in structural level will be discussed later. The depths of the surfaces of decollement within the Kirusillas and Capinota (or Lower Ordovician) formations, which are inferred from the surface geology, are

variable, reflecting the unconstrained geometry of the deeper faults. Throughout much of the eastern part of the mapped area, displacement of the older formations onto the footwall flat within the Devonian Icla Formation is either consistent with observed structural thicknesses (east Aiquile cross section), or is assumed (Punata cross section extensions and south Santa Cruz cross section). Therefore, these surfaces of decollement and their overlying structural packages are uplifted, like the structural package above the decollement localized in the Icla Formation, to approximately three kilometers below sea level. In the interior of the mountain belt, the depths to surfaces of decollement within the Silurian and Ordovician units vary, and are generally even shallower than three kilometers below sea level.

Regions of distinct deformational style

Each of the structural packages carried above a certain decollement surface exhibits a structural style distinct from that of the other thrust packages, and may exhibit more than one style of deformation depending on its position in the mountain belt and competence contrasts between rock units within the structural package. These variations in the stratigraphic level of decollement and the overlying fold and fault geometry define eight regions within the mapped area (Figure 5.5). Recall that the thrust sheets exposed at the surface lie above the shallowest surfaces of detachment inferred from the surface exposures, and that the geometry of deeper structures is unconstrained. These are (named according to map sheet or for a local town or feature) the Bolivar, west Aiquile, Punata, Totora, Elbow, Peña Colorada, San Isidro, and east Vallegrande regions. The differences in percent shortening calculated from balanced cross sections across these regions are a reflection of the variations in structural style

within the mapped area (Table 1). The maps and cross sections are reproduced at a scale of 1:250,000 on Plates 1 through 6, and Plates 7 and 8, respectively. Cross sections at a reduced scale are included in the text. The deformational styles observed are discussed below, region by region.

Bolivar Region

The Bolivar region comprises the westernmost part of the mapped area and is adjacent to the Altiplano. The Cochabamba and Uncía cross sections, from the map sheets of the same names, cross this region in the north and south, respectively (Figures 5.6, 5.7 and 5.8). To the west of the Bolivar region, the undeformed Miocene Morococala Ignimbrites overlie the deformed Paleozoic sedimentary rocks, and conceal the deformational style of the western Cordillera Oriental, except for a narrow region exposed at the boundary between the Altiplano and Cordillera Oriental. The structural style beneath the ignimbrites is presumed to be the same as that observed in the Bolivar region.

The style of deformation in the Bolivar region varies slightly along strike above a level of decollement that is localized within either the Capinota Formation or within undifferentiated Lower Ordovician shale. This region is marked by a "pop-up" feature that can be traced continuously for the length of the region. The pop-up is bounded by the Sayari fault (fault h) on the east and a major backthrust (Fault g) on the west (Figures 5.1,5.7, and 5.8). To the east of the pop-up, west-vergent faults predominate in the southern portion of this region, but in the northern portion, east-vergent faults are present. West of the pop-up in the south, faults dipping both northeast and southwest separate folds of various styles. Fault displacements, which are unconstrained because hanging wall cutoffs are generally eroded, range from a minimum of 2 to a minimum of 5

kilometers. To the north (on the Cochabamba map sheet), consistently west-dipping (east-vergent) thrusts carry hanging wall anticlines that are sometimes overturned. Minimum fault displacements are typically less than 1 kilometer. This decrease in fault displacement reflects the distribution of shortening over a larger number of structures in the northern part of the region. The change in the number of structures coincides with a change in structural trends, from N30-40°W in the south to N40-50°W in the north.

Crosscutting relationships indicate that the west-vergent backthrusts post-date the west-dipping (east-vergent) thrusts in some locations, and therefore they are assumed to be younger where age relationships are not clear. The calculation of percent shortening is not significantly affected by this assumption. Backthrusting is apparently prevalent beneath the ignimbrites as well: Thematic Mapper imagery shows that, at the westernmost extent of the region, the boundary between the Cordillera Oriental and Altiplano, is defined by a backthrust (Figure 5.9).

Secondary faults include east-west-trending tear faults and steep, local faults that accomodate folding in massive Cretaceous sandstone. The tear faults are more prevalent in the southern part of the region.

Geometric constraints in both cross sections require the Upper and Lower Ordovician formations to be thinner than observed to the east, by one and two kilometers on the Uncía and Cochabamba map sheets, respectively. This variation in thickness may correspond to a facies change in the Ordovician sedimentary rock. It is spatially coincident with a change in the style of deformation in the adjacent region to the east, where the exposed, thicker thrust sheets have not been as severely shortened.

The magnitude of the minimum percent shortening is dependent on the

inclusion of buried overthrusting. The thrust faults in this region flatten into decollement horizons at or above sea level, clearly indicating regional uplift that at elevations ranging from 2.5 to as high as 4.5 km must involve duplication of the structural package beneath the surface of decollement. A high percent shortening, 41 percent, reflects the inclusion of a minimum amount of overthrusting at the eastern end of the Uncía cross section, where the shallowest level of detachment has been uplifted enough to allow duplication of the exposed structural package. Along the Cochabamba cross section, such buried overthrusting or duplication is not included, even though it may be present, and percent shortening is correspondingly lower: 28 percent.

West Aiquile Region

The west Aiquile region makes up the northwestern portion of the Aiquile map sheet and extends, to the north, to the southern limit of the Cochabamba and surrounding basins, on the Punata and Cochabamba map sheets. It lies adjacent to the Bolivar region on the west, and its eastern extent varies from north to south. In the northern part of this region (Punata map sheet), the region terminates at a frontal ramp marked by the Chahuarani fault system, an east-verging thrust and splays from it that have imbricated the hanging wall. To the south, the region extends to the east of this fault system, across the western half of the Aiquile map sheet. Portions of the Punata cross sections (Figures 5.10, 5.11 and 5.12) and the west and east Aiquile cross sections (Figures 5.13 and 5.14) detail the structural style within this region.

The style of deformation varies from west to east across the region. Throughout the region, thrust faults sole into a surface of detachment within the Lower Ordovician. In the western part of this region, bounded on

the east by the Chahuarani fault system, there is a broad region of unfaulted folds in the north. A broad anticlinal structure, with large parasitic folds and structures that are overturned to the west, lies west of a large, Tertiary-cored syncline. These folds are doubly-plunging inward, and as structural level rises to the south, east- and west-dipping thrust faults are exposed that separate folds that have become upright, broad, gentle folds with wavelengths of 10-15 km. Structural trends are N45-55°W in the northern part of this region, and become almost westerly (N60-70°W) in a narrow zone on the Aiquile map sheet before returning to N45-55°W trends in the south. Farther to the east, structures with these trends are crosscut by structures with north-south trends, and the structural style becomes more complex. A network of mutually crosscutting north-south-trending, east-vergent thrust faults and northwest-southeast-trending, west-vergent thrust faults merge together to the south and east. This convergence results in a change to north-south trends, and a decrease in the number of structures to the south within this zone. Complexities within the zone include rotated broad folds and west-northwest trending tear faults. Minimum displacements on the thrust faults throughout the west Aiquile region are small, and range from 1 to 2 km.

The change in structural style and trend is associated with a change in the thickness of the Ordovician formations. These units are approximately 2.5 kilometers thick on the east Aiquile cross section, as opposed to 4 kilometers thick on the West Aiquile and Punata cross sections to the west.

The depth of the decollement undergoes both frontal and lateral changes within this region. From west to east across the Cochabamba, Punata and

northwest Aiquile map sheets, the depth of the decollement increases from approximately sea level to 1 kilometer below sea level to as much as 6 kilometers below sea level, and across the west Aiquile cross section from approximately sea level to two kilometers below sea level. Therefore, laterally, the depth of the decollement decreases from as much as six kilometers below sea level in the north to approximately two kilometers below sea level in the south.

Two estimates of percent shortening were calculated from the east and west Aiquile cross sections: 21 and 20 percent, respectively. No buried overthrusting is included in this estimate, even though the shallow depth to decollement in the west requires an additional but unconstrained amount of shortening. The Punata cross sections were not used to calculate percent shortening within the west Aiquile region.

Punata Region

The Punata region lies north and east of the west Aiquile region and extends to the northern boundary of the mapped area. Its western boundary lies approximately along the center of the Punata map sheet. The north, central and south Punata cross sections (Figures 5.10, 5.11, 5.12) cross this region.

The surface of decollement is still localized within Lower Ordovician shale, but the style of deformation is distinct from that of the surrounding regions. Deformation is characterized by broad, very gentle folds with a wavelength of approximately 20 km and a gentle southward plunge, that are displaced by consistently west-vergent (east-dipping) thrust faults. Structures trend N40-50°W, curving to become more westerly (N60-70°W) in the northernmost part of the mapped area. Because hanging wall anticlines generally are not eroded, displacements on thrust faults are

constrained to range from 0.5 to 1 km.

The thrust faults sole into a level of decollement that is very shallow. Slip along a surface of detachment only one to two kilometers above sea level has placed the lowest stratigraphic levels in the mapped area, the Lower Ordovician sequence, in the structurally highest position, over the entire area.

Minimum estimates of percent shortening calculated from the north, central and the western half of the south Punata cross sections are 14, 16 and 16 percent.

The south Punata cross section (Figure 5.12) shows a variation in the thickness of the Ordovician formations. The variations observed in the Ordovician formations within the anticline-syncline pair on the south Punata cross section (western end) reflect the pinchout of the Upper Ordovician and younger units in the Tintin area along an angular unconformity. The angular unconformity consists of, at most, 10° of angular discordance between formations and is the result of a pre-Cretaceous normal faulting event. Normal faults offset the Devonian Icla and Huamampampa Formations by 50 meters where exposed in the hills south of Tintin. Cretaceous sedimentary rock overlaps either formation with a small (less than 5°) angular unconformity. This deformational event is observed only within this small area, and is unusual for the mapped area (as discussed in the preceding chapter).

Totora Region

The Totora region is adjacent to the Punata region on the west and extends across the Punata map sheet to the east, at least to the limit of the mapped area and possibly into the area mapped by Plafker (1962). Its southern boundary is poorly defined by the mapping, and is assumed to lie

just north of the Aiquile map sheet. The north, central and south Punata and north, central, and south Totora cross sections cross this region (Figures 5.15, 5.16, 5.17). The extent of the region is defined by the increase in the depth of the decollement to 2.8 kilometers below sea level that occurs east of the Punata region, and by the eastern limit of decollement localized in the Lower Ordovician rocks.

Within this region, the style of deformation is variable. In the northwest, it is characterized by regularly-spaced (10 km) thrust slices of a structural package containing Ordovician and, locally, Silurian formations, displaced by east-dipping thrust faults. Hanging wall anticlines are not eroded, constraining the slip on the thrust faults to be small, .5 to 2 km. An east-west tear fault separates these east-dipping faults on the north from a folded but unfaulted region on the south. The tear fault dies out to the east within the mapped area. East of the gap in map coverage, a style similar to that of the faulted structural packages is observed, but the vergence of the faults has changed, as indicated on the north, central and south Totora cross sections. The structures that accomodate this change in vergence are unknown due to the gap in map coverage between Plafker's and my mapped areas.

Geometric constraints imposed by the spacing of the thrust sheets suggest that the Ordovician formations are one-half to one kilometer thinner in this region than in the region to the west.

Minimum estimates of percent shortening from the central and south Punata cross sections are 14 and 12 percent.

Peña Colorada Region

The Peña Colorada region comprises a narrow north-south strip on the eastern half of the Aiquile map sheet, adjacent to the west Aiquile region

and south of the Totora region. It extends to the east for approximately 25 kilometers. It is crossed by the east Aiquile cross section (Figure 5.14).

The style of deformation in this region, which is underlain by decollement within the Silurian Kirusillas Formation at 2.8 kilometers below sea level, is quite distinct from that to the west and north. Thrust faults verge both west and east, and override gently- to steeply-dipping, eastern or western limbs of synclines. The structural trend becomes more westerly from east to west across the region, changing from N30°W to N50°W. The primary folds and thrust faults are broken by oblique tear faults that trend N60-70W. Hanging wall cutoffs have been removed by erosion, allowing only a minimum estimate of displacement along each fault of 1 to 2 kilometers.

An atypical geometric relationship between folds and faults is observed within this structural package. As drawn, the hanging wall cutoff of the structural package comprised of Silurian and Lower Devonian formations implies that folding preceded faulting, and that faults propagated out of a syncline, cutting across the eastern fold flank until becoming bed-parallel with the Devonian Icla Formation. A similar relationship between synclinal folding and faulting is inferred from the surface geology to the west in the same region.

The minimum percent shortening calculated from the east Aiquile cross section is 20 percent.

San Isidro Region

The San Isidro region, crossed by part of the east Aiquile and the west Vallegrande cross sections (Figure 5.18), is adjacent to the Peña Colorada region on the east. Its northern boundary is poorly defined but is presumed to extend in an east-west orientation just north of 18°S. The western

boundary lies along the center of the Vallegrande map sheet.

A consistent style of deformation results from slip along a surface of detachment localized in the Devonian Icla Formation throughout this region. East-verging (west-dipping) major thrust faults imbricate the relatively thin, gently folded sedimentary sequence overlying the Icla shale. These thrust faults either break through to the surface or form duplex structures at depth. Minor backthrusts accomodate shortening in the cores of anticlines and above frontal ramps. The trends of the structures change from N10°W to N30°W, gradually becoming more northwesterly towards the west. Oblique tear faults are common, and trend N50°W to N70°W. Some hanging wall anticlines are preserved, sometimes faulted by upward imbrication of the hanging wall. Synclines are generally symmetric, narrow, and sometimes cut by tear faults, with a very gentle plunge either to the south or to the north. The spacing of thrust faults ranges from 4 to 10 km, with displacement on these faults decreasing correspondingly from a range of 9 to 11 km to a range of 4 to 6 km.

This style of deformation defines the highest percent shortening observed in the mapped area, 47 and 53 percent, along the east Aiquile and west Vallegrande cross sections, respectively. The latter estimate includes displacement along the overthrusts bounding the duplex structures that are required by the surface geology along the west Vallegrande cross section.

East Vallegrande Region

The east Vallegrande region lies between the San Isidro region on the west and the thrust front on the east. Its northern boundary is a continuation of that of the San Isidro region, at approximately 18°S. It is crossed by the east Vallegrande cross section (Figure 5.19)

Although the surface of detachment remains in the Icla Formation in the east Vallegrande area, the intensity of deformation decreases markedly in comparison with that observed in the San Isidro region. Thrust faults that dip both east and west cut narrow anticlines and override broad synclines. Along strike, faults of opposing vergence crosscut one another. The spacing of thrust faults and the wavelengths of folds are both approximately 12 km. Folds plunge very gently to the south and are infrequently broken by tear faults. The trend of structures is north-south close to the thrust front, but changes to a northwest orientation both to the north and to the west of the Vallegrande map sheet. Minimum displacements on the thrust faults range from 1.5 to 6.5 kilometers.

The thickness of the Devonian formations apparently varies across this region. Because these variations are not associated with the geometry of folds, they are attributed to variations in original stratigraphic thicknesses rather than to a style of folding that is not parallel.

A minimum estimate of percent shortening across this region is 20 percent.

Elbow Region

The Elbow region extends from a southern boundary adjacent to the San Isidro and east Vallegrande regions, north to 17°S, the northern extent of the Punata map sheet. It is bounded on the east by the Tertiary anticlines observed east of the thrust front, and on the west by the Totora region. It is crossed by the north, central and south Totora, the south Santa Cruz, and Limbo cross sections (Figures 5.20 and 5.21).

Mapping by Plafker (1962) and Brockman et al. (1972) in the area allows only a general assessment of the structural style in the region of the bend in the mountain belt, due to poor exposure, rugged terrain, structural

complexity, different base maps, and different stratigraphic nomenclature and divisions. Their maps, however, do provide the basis for schematic interpretations that extend out to the thrust front, and allow the calculation of crude estimates of percent shortening.

Plafker's maps are based on photogeologic interpretation and field work along rivers and by helicopter in the Subandean Zone north of 18°S (Figure 5.2). I have constructed new cross sections, using recompilations of Plafker's maps on the Punata and Santa Cruz map sheets, and I have reinterpreted Brockman's cross section.

The style of deformation is quite complex and variable in this region. I interpret the level of decollement in this region to rise from the Lower Ordovician shales in the west into the Devonian Icla Formation in the east. I have assumed that both these stratigraphic levels of decollement lie at a depth of 2.8 kilometers below sea level, as observed further to the south, but this depth is dependent on variations in formational thicknesses as shown on the cross sections. In fact, formation thicknesses vary markedly across this region, and I have used the thicknesses measured by Plafker as guides for constructing the cross sections. In the northwestern part of the Elbow region, the style of deformation is similar to that observed in the Totora region; this part of the Elbow region is probably a continuation of the Totora region, but a gap in the mapping leaves this relationship unclear. Farther to the east, west-dipping thrust faults and uneroded ramp anticlines, that are generally tighter than elsewhere in the mapped area and sometimes overturned, characterize the deformation. The trends of structures go through two major bends within the region. First, a north-south orientation in the south is broadly curved, to the north, to an east-west orientation at approximately 17°15'S. To the north, this trend is then

sharply curved back to N45°W, the trend of the mountain belt farther to the north. The east-west trending faults are associated with zones of intense shearing. Although there is probably a component of strike-slip motion along them, they do not form a simple, through-going tear fault system.

Uncertainties in the mapping due to poor exposure and different base maps, rapid changes in the level of decollement, and the likelihood of non-plane strain preclude rigorous balancing of the cross sections. I have calculated, however, an approximate percent shortening by restoring to its original length one unit that appears in all the thrust sheets, or a combination of units if necessary, on a given cross section (Figures 5.15, 5.16 and 5.17). Calculations of minimum percent shortening for the south Santa Cruz cross section and the north and south Totora cross sections yield 35, 24 and 27 percent, respectively.

The northernmost part of the Elbow region is marked by the exposure of Cambrian rocks, not exposed elsewhere in the mapped area nor for several hundreds of kilometers along strike. The Limbo cross section (Figure 5.21) crosses this area and is based on field work by Brockman et al. (1972), rather than the map by Plafker, which is primarily based on photogeologic interpretation and did not focus on this region. The Cambrian Limbo Group consists, in its basal part, of anhydrite that provides another stratigraphic level of decollement. The rocks are uplifted and exposed due to overthrusts that stack the structural packages. To the west, the Cambrian detachment surface ramps down and is no longer exposed while the Lower Ordovician surface of detachment accomodates shortening through gentle folds between imbricate thrust faults. To the east, deformation dies out rapidly as the level of decollement ramps up, apparently into the Tertiary section. The schematic representation in Figure 5.21 results in 37 percent

shortening, not including the overlap between the two restored structural packages.

General features of the deformational style

Cutoff angles

The models of fault-bend and fault-propagation folding have proven useful in drawing balanced cross sections because of their predictive capability. Neither of these two models have been used to draw the cross sections for this study, and therefore these cross sections may look unusual compared to the cross sections typically drawn for fold and thrust belts, particularly with respect to the interpretation of hanging wall and footwall cutoff angles. The purpose of this section is to show that the cutoff angles shown in the cross sections are, however, both consistent with the field data and reasonable, given the uncertainties in deeper fault structures and given the constraint that the amount of shortening implied in the cross sections should be a minimum.

It is necessary to discuss hanging wall and footwall cutoff angles separately because they are distinct theoretically and because there is field evidence in this study primarily for the hanging wall cutoff angles. The fold geometry and the angles β, the hanging wall cutoff angle, ϕ, the angle through which the trajectory of the surface of decollement is rotated, and θ, the initial ramp angle or footwall cutoff angle are shown in Figure 5.22.

As discussed in Chapter 2, footwall cutoff angles have deliberately been drawn steeper than typically shown on cross section interpretations of other mountain belts because 1) footwall cutoff angles are not observed, 2) an accurate geometry of bedding in the footwall can not be drawn without subsurface information, and 3) because larger cutoff angles imply

less shortening.

Hanging wall cutoff angles are determined by field observations of fault dips and interlimb angles, measured where variations in erosion along strike expose the thrust faults beneath the anticlines (Table 2). The dip of the backlimb of the fold was assumed to equal the dip of the fault. For thrusts within the Icla Formation and the Lower Ordovician, respectively, the average interlimb angles of the anticlines are 129° and 102°, and the average fault dips are 36° and 40°. Large hanging wall cutoff angles are required in a balanced cross section interpretation that is consistent with these angles and that implies a minimum amount of shortening.

The observed data could be fit by the fault-bend and, in some cases, fault-propagation models. In both cases, bed thickness is assumed to remain constant. In the fault-bend case, equations from Suppe (1983) can be used to determine the dependence of the hanging wall and footwall cutoff angles (ϕ and θ) on the interlimb angle (γ). Two cases were considered: 1) θ equal to 30° (assumed), and ϕ and β were calculated, and 2) θ equal to ϕ, and β was calculated. In the former case, the average footwall cutoff angle would be 31° and the average hanging wall cutoff angle would be 80°; in the latter case, the corresponding average values would be 27° and 72°, respectively (Figure 5.23). (The data for decollements within the Icla Formation and the Lower Ordovician have been averaged together.) In other words, small footwall cutoff angles but large hanging wall cutoff angles (Mode II folds) would be required for this interpretation. The fault propagation model would be applicable only to strata above decollements within the Lower Ordovician. In this case, again assuming constant bed thickness, an average ramp angle of approximately 45° and an average hanging wall cutoff angle of approximately 80° is indicated (Figure 5.23).

For the interlimb angles observed in anticlines above decollements in the Icla Formation, there is no possible geometry consistent with the fault-propagation model (Figure 5.23).

Interpretations of cross sections that are consistent with these models could therefore be drawn. Like the cross sections constructed for this study, however, these interpretations would invoke numerous large hanging wall cutoff angles because the data from the Bolivian Andes require them.

Deep structure of the fold and thrust belt

The balanced cross sections and maps discussed above define the structural style above the shallowest surface of decollement, but leave undefined the deep structure below this level and above undeformed crust. Without subsurface information, neither the geometry of faulting nor the lithologies involved can be determined, and therefore no attempt at representing this deeper deformation is made. Thrust sheets involving either sedimentary cover, as observed at the surface, or basement may fill this area, the extent of which will vary depending on the depth to undeformed crust. Duplexes of either sedimentary cover or of basement, made up of either thick or thin thrust sheets, could account for the cross sectional area below the shallowest surface of decollement, and for the locally higher structural relief in the West Aiquile and Punata regions. Whether the geometry at depth is analogous to the thin slices of sedimentary cover deformed in an antiformal stack inferred in the Canadian Cordillera (Price, 1981), to the thick basement duplexes of the Romanzof Mountains (Vann et al., 1986), to the thin basement slivers observed in the Scandinavian Caledonides (Bjorklund, 1985; Tilke, 1986; Burchfiel and Royden, 1988), or to the large overthrust sheets of sedimentary cover, as defined in the Appalachians (Mitra, 1988) remains to be determined. Thin

thrust sheets imply large amounts of shortening in addition to that calculated from the surface geology, but little additional shortening would result from deformation involving thick thrust sheets.

The presence of additional, concealed deformation provides an explanation for the atypical number of backthrusts (Figure 5.24) and the unusually steep dips of the thrust faults observed in the Bolivian Andes.

Where backthrusting is observed in other fold and thrust belts, it is attributed either to an extremely weak decollement surface or to folding of a thrust sheet as it moves over a footwall ramp or responds to deformation of an underlying thrust sheet. In the latter case, various geometries of accomodation are observed within an overlying thrust sheet in response to displacement along a blind thrust system (Serra, 1977). For example, Dunne and Ferrill (1988) identify forethrusting, backthrusting, and decoupling as possible end member types of accomodation. The most frequently observed of these is a combination of fore- and backthrusting. In the former case, in which backthrusting is the result of slip along a weak surface of decollement, the low critical taper required for the slip of thrust sheets above a basal decollement that lies in evaporitic layers allows the development of both back- and forethrusts. The orientation of principal stresses that results from a low critical taper defines failure planes that dip at approximately equal angles towards the foreland and hinterland, and, therefore, are equally likely to be the loci of slip (Davis and Engelder, 1985).

Backthrusting in the Bolivian Andes is plausibly due to either of these mechanisms. It may be due to accomodation within the observed, upper thrust sheets to slip along an unexposed, west-dipping thrust fault system. In this case, if deeper levels of the Bolivian Andes were exposed, a fault

system that consistently dipped west would be observed. Backthrusting may also reflect weak coupling along the basal decollement. The overthrusting of a relatively thick (7-8 kilometers) and competent (low percent shortening--12-28 percent) structural package suggests the presence of an extremely weak basal detachment layer (Davis et al., 1983; Dahlen et al., 1984). The exposure of Cambrian anhydrite (the Limbo Group) at approximately 17°S raises the possibility that this basal layer may be localized in these evaporites. However, this distinctive unit is not exposed elsewhere within the fold and thrust belt, and therefore its lateral extent is unknown.

The presence of buried faults also accords with the unusual prevalence of steeply-dipping faults. Although low-angle thrust faults are observed locally in the mapped area, the major structures dip 40 to 60°. The formation of multiple imbrications at depth will fold and rotate overlying thrust sheets into steeply-dipping orientations, with the final dip depending on the number of imbrications and the initial ramp angle. Rather than being primary, the dips of the observed thrust faults are probably due to rotation by imbrication at depth. Dips of approximately 40° can be obtained from two or three imbrications of thrust sheets with initial ramp angles of 24 or 15°, respectively. Because the deeper fault structures are unconstrained, an interpretation of this type is not shown.

The thrust front of the Bolivian Andes

Frontal thrusts within fold and thrust belts may be either emergent or buried (Vann et al., 1986; Morley, 1986). One type of buried thrust front is a triangle zone (Price, 1981; Jones, 1982) or passive roof duplex (Banks and Warburton, 1986), which is now recognized as a common structure along mountain fronts. The presence of foreland-dipping strata at a

mountain front has been shown to be caused by uplift and backthrusting above a foreland-directed duplex. The backthrust is often eroded or difficult to identify.

Two reasons are postulated as causes of triangle zones. First, a stronger decollement zone along or across strike is hypothesized to cause backthrusting. If there is a change along strike in the type of thrust front, it is inferred that the decollement is stronger where the triangle zone develops. Alternatively, a thrust front may change from emergent to buried if, as it progresses to the exterior of a mountain belt, the strength of the level of decollement increases. Second, it is postulated that decreasing stress levels as an orogeny ends may initiate backthrusting.

The thrust front of the Bolivian Andes changes from a buried triangle zone in the south to an emergent thrust front in the northern part of the mapped area. Two lines of evidence require a triangle zone at the thrust front south of the bend in the Bolivian Andes. One is that east-dipping foreland sediments are observed at the thrust front within the mapped area (Figure 5.19) and extending to the south along the length of the Bolivian Andes (Mather, 1922). The other is that the regional offset between stratigraphic levels within the Subandean Zone and the foreland requires a blind thrust system at depth. The level of decollement within this blind thrust system may lie in the Silurian shales. Seismic reflection data suggest that thrusts that have advanced out into the foreland sole into either the Silurian or the Devonian sedimentary rocks; the more conservative interpretation of the thrust fault geometry assumes that the thrusts flatten in the Silurian Kirusillas Formation.

The change to an emergent thrust front in the northern part of the mapped area is apparent on the North and Central Totora cross sections

(Figures 5.15 and 5.16). On these cross sections, the level of decollement climbs from the Lower Ordovician shales into the Devonian Icla Formation and probably into Tertiary units, and these faults ramp up to the surface. This emergent thrust front is presumed to extend to the Peru-Bolivia border. Roeder (1988) indicates no offset between stratigraphic levels within the Subandean Zone and the undeformed foreland on cross sections in northern Bolivia, and consistently shows the thrust front to consist of emergent, west-dipping thrust faults. Furthermore, Thematic Mapper imagery shows west-dipping sedimentary rocks and emergent thrust faults, offset by tear faults in a manner similar to that observed in the Pine Mountain block of the Appalachians (Mitra, 1988), in the Subandean Zone just north of the mapped area. The change in the thrust front is apparently due to the termination along strike of the Silurian shale unit as a surface of decollement (Figure 5.25). This termination correlates with northward-plunging folds and east-west trending faults that accomodate the change in vertical relief due to the stacking of duplexes, whose sole thrust lies in the Silurian Kirusillas Formation, south of the bend.

Contrary to the proposed hypotheses on the occurrence of triangle zones, however, the triangle zone in the Bolivian Andes is not associated with the portion of the thrust belt that has advanced least. In the Jura, the McKenzie Mountains, and the Appalachians, for example, triangle zones are associated with the narrower, less advanced parts of the mountain belts, where the surfaces of decollement are not localized in salt (Vann et al., 1986; Morley, 1986). In Bolivia, the triangle zone is associated with the widest part of the thrust belt, and there is no obvious difference in the strength of the decollement zone north or south of the change in the thrust front. Neither is there an obvious change in the strength of the

decollement zone to the east: the thicknesses of the Icla and Kirusillas formations do not change along the seismic reflection line east of Santa Cruz. The differential advance of the thrust front appears to be controlled by the pre-orogenic basin geometry, rather than the strength of the decollement zone. This interpretation suggests that, at least in part, the bend in the mountain belt is due to the propagation of thrust faults into a wider basin.

The nature and origin of the bend in the fold and thrust belt

The prominent bend in the Bolivian Andes at approximately 18°S is characterized by a left-lateral offset of the thrust front, a change in the trend of structures, a reduction in the width of the mountain belt to the north, and the presence of the extensional basins in the vicinity of Cochabamba. Its origin has variously been attributed to oroclinal bending (Carey, 1958; Heki et al., 1985), to left-lateral faulting (Rod, 1960), or to differential shortening in the adjacent portions of the thrust belt (Isacks, 1988; Sheffels and Klepacki, 1985). All of these processes may have played a partial role in the development of the bend; existing data do not allow definitive conclusions to be drawn.

Beck (1988) analyzed the orocline hypothesis by examining the available paleomagnetic data from the central Andes. He found that the well-constrained paleomagnetic data do indicate rotations north and south of the bend, but these rotations are too small to explain the trend of the mountain belt today.

Isacks (1988) hypothesized that shortening, estimated from variations in crustal thickness, diminishes north and south of the region of the bend. He attributed the observed bend to the enhancement of a pre-orogenic bend by this differential shortening and the differential shortening to variations

in the amount of heating to which the crust has been subjected. based on the inferred paleodip of the subduction zone. While this interpretation is plausible and appealing, it is difficult to assess quantitatively the thermal history of the plate margin.

Surficial structural constraints, however, allow determination of the amount of shortening and of the style of deformation. These features of the Bolivian Andes at 18°S reveal observable structural and paleogeographic factors that have probably contributed to the formation of the bend. First, evidence for a through-going left-lateral fault system is lacking. Although a major, left-lateral fault, the Tapacarí fault, does exist in the Cordillera Oriental, no continuation of it to the thrust front could be found by the author, Plafker (1962), or Pareja L. et al. (1978). The orientation and strike-slip nature of the fault system indicate that it comprises a tear fault system, the Cochabamba fault system (Sheffels and Klepacki, 1985), which is limited to interior thrust sheets. Across a left step in this fault system, the basins of the Cochabamba valleys have opened as thin-skinned, pull-apart basins. The role that displacement along this tear fault system may have played in the development of the bend is undetermined.

A factor for which the surficial structure indicates a more important role is the paleogeography of the Paleozoic basin. The change in the thrust front shown on the cross sections indicates that the northern limit of decollement in the Silurian shale followed the bend of the mountain belt. Seismic reflection profiles verify that the depocenter for the Silurian, Devonian and Carboniferous sedimentary rocks extended further to the east along and south of an east-west-trending feature that lies at the bend in the thrust belt (Figure 5.26) (Paulsen, 1988; M. Lopez and M. Cirbian, 1986,

YPFB, pers. comm.; Zeil, 1979). Compression across a basin that varies in width would produce a thrust belt that also varied in width. Therefore, the bend is, at least in part, caused by the paleogeography of the Paleozoic basin.

Table 5.1. Summary of percent shortening calculations

Region (Map sheets)	Cross section	Level of detachment	l (km)	l_o(km)	s(km)	Percent shortening
Bolivar (Cochabamba and Uncía)	Uncía	Ol	51	86	35	41
	Cochabamba	Ol	38	53	15	28
West Aiquile (Aiquile)	West Aiquile	Ol	68	85	17	20
	East Aiquile	Ol	19	24	5	21
Punata (Punata)	North Punata*	Ol	49	57	8	14
	Central Punata*	Ol	56	67	11	16
	South Punata (W half)	Ol	38	45	7	16
Totora (Punata)	Central Totora**	Ol	25	29	4	14
	South Punata (E half)	Ol	29	33	4	12
Elbow (Punata and Santa Cruz)	North Totora**	Ol, Dic	31	41	10	24
	South Totora**	Ol, Dic	35	48	13	27
	South Santa Cruz**	Ol, Dic	64	99	35	35
	Limbo**	C, Ol	55	87	32	37
Peña Colorada (Aiquile)	East Aiquile	Sk	13	17	4	24
San Isidro (Aiquile and Vallegrande)	East Aiquile	Dic	16	30	14	47
	West Vallegrande	Dic	49	105	56	53
East Vallegrande (Vallegrande)	East Vallegrande	Dic	42	53	11	20

* The easternmost portion of this cross section should probably be included in the Totora region, but the length is too short to calculate percent shortening separately.

**The percent shortening calculated is approximate because the estimate is based on a reinterpretation of others' mapping, and because stratigraphic thicknesses and structural trends vary within this region.

Table 5.2 Hanging wall cutoff angles (β) for the fault-bend fold model

Location	level of dec	γ	fore-limb	back-limb	verg-ence	β*	ϕ = θ*	fault dip	ϕ**	β**
Angostura	Dic	125	10	45	E	55	29.87	45	29.64	55.36
Samaipata	Dic	130	10	40	E	50	29.44	40	28.64	51.36
Samaipata	Dic	120	10	50	E	60	30.00	50	30.00	60.00
S of Vallegrande	Dic	140	10	30	E	40	27.52	30	30.00	40.00
W of Vallegrande	Dic	95	45	40	W	85	27.51	–	19.25	95.75
Pampa Grande	Dic	110	40	30	W	70	29.54	–	28.35	71.65
SE of San Isidro	Dic	160	0	20	E	20	17.88	–	14.06	35.94
Pulquina	Dic	150	10	20	E	30	23.79	–	20.10	39.90
Perez	Dic	120	10	50	E	60	30.00	50	30.00	60.00
W of Pasorapa	Dic	135	15	30	W	45	28.68	30	27.10	47.90
W of Estanzuelas	Sk	110	30	40	E	70	29.54	40	28.35	71.65
S of Aiquile	Ol	100	40	40	E	80	28.33	–	23.08	86.92
E of Tintin	Ol	90	50	40	W	90	26.57	–	15.00	105.00
"	Ol	115	25	40	W	65	29.88	–	29.60	65.40
"	Ol	135	20	25	W	45	28.68	15	27.10	47.90
Chaharuani N	Ol	95	40	45	E	85	27.51	45	19.25	95.75
Chaharuani S	Ol	125	10	45	E	55	29.87	45	29.64	55.36
Rio Caine	Ol	140	10	30	W	40	27.52	30	30.00	40.00

Table 5.2. (continued)

Location	level of dec	γ	fore-limb	back-limb	verg-ence	β*	$\phi = \theta$*	fault dip	ϕ**	β**
Torotoro	Ol	125	0	55	E	55	29.87	–	29.64	55.36
Sivingani	Ol	150	0	30	E	30	23.79	–	20.10	39.90
Jatun Mayu-1S	Ol	85	50	45	W	95	25.52	45	10.75	114.25
Jatun Mayu-1N	Ol	90	50	40	W	90	26.57	40	15.00	105.00
Jatun Mayu-2	Ol	120	40	20	W	60	30.00	–	30.00	60.00
"	Ol	90	45	45	W	90	26.57	–	15.00	105.00
E of Monte Puncu	Ol	75	60	45	W	105	23.15	45	3.83	131.17
Pojo	Ol	120	30	30	E	60	30.00	–	30.00	60.00
Colluma S	Ol	100	40	40	W	80	28.33	40	23.08	86.92
Colluma N	Ol	90	50	40	W	90	26.57	40	15.00	105.00
Kayastia	Ol	110	30	40	W	70	29.54	40	28.35	71.65
Sayari F.	Ol	105	20	55	E	75	29.02	55	26.17	78.83
S of Sacaca	Ol	105	45	30	W	75	29.02	30	26.17	78.83

Table 5.2. (continued)

Location	level of dec	γ	fore-limb	back-limb	verg-ence	β*	$\phi = \theta$*	fault dip	ϕ**	β**
S of Capinota	Ol	110	40	30	W	70	29.54	–	28.35	71.65
"	Ol	80	50	50	W	100	24.37	–	6.92	123.08
"	Ol	75	70	35	W	105	23.15	–	3.83	131.17
SE of Arque	Ol	120	10?	50	W	60	30.00	50	30.00	60.00
S of Arque	Ol	95	40	45	W	85	27.51	45	19.25	95.75
E of Sayari	Ol	110	10	60	W	70	29.54	60	28.35	71.65
Sayari backthrust	Ol	130	10	40	W	50	29.44	40	28.64	51.36
N of Bolivar	Ol	90	45	45	W	90	26.57	45	15.00	105.00
W of Confital	Ol	90	70	20	W	90	26.57	–	15.00	105.00
Leque--1	Ol	10	-50	40	W	170	3.33	40	22.71	177.29
Leque--2	Ol	85	45	40	W	85	25.52	40	10.75	114.25
S of Confital	Ol	90	45?	45	W	90	26.57	45	15.00	105.00

* $\beta = \theta - \phi + (180 - \gamma)$ and

$$\phi = \tan^{-1} \frac{-\sin(\gamma/2 - \theta)\,(\sin(\gamma - \theta) - \sin\theta)}{\cos(\gamma/2 - \theta)\,(\sin(\gamma - \theta) - \sin\theta) - \sin\gamma}$$

$\theta = 30°$ (assumed)

** $\beta = \theta - \phi + (180 - \gamma)$ and

$$\phi = \theta = \tan^{-1} \frac{\sin\gamma}{1 + 2\cos^2\gamma/2}$$

Figure Captions

Figure 5.1. Simplified geologic map of the study area, extending from the thrust front in the east to the outcrop of the Miocene Morococala ignimbrites in the west. Mapping by Plafker (1962) is also compiled. Abbreviations: LMK--Laguna Mallcu Kkota; SY--Sayari; PT--Parotani; CQ--Colquechaca; TR--Torotoro; TN--Tintin; SF--Sayari fault; CFS--Chahuarani fault system.

Figure 5.2. Photo from the western Cordillera Oriental, West Aiquile region, Cochabamba map sheet, showing typical parallel fold style. The syncline is cored by the Lower Devonian Tarabuco Formation.

Figure 5.3. Surfaces of decollement are observed at three levels: Lower Ordovician shale, the Silurian Kirusillas shale, and the Devonian Icla shale. The level of decollement ramps up to the east, toward the foreland, but the deeper levels of decollement remain active as far east as the thrust front. The geometry of faulting depicted below the Icla Formation is schematic only.

Figure 5.4. Sketch of the data from the thrust belt and the foreland, south of the bend in the mountain belt, that show the regional uplift observed in the cross sections. An approximately four-kilometer offset is observed.

Figure 5.5. Outline of the study area showing regions of distinct deformational style, their names and the percent shortening calculated from the cross sections that cross these regions. The cross section locations are shown.

Figure 5.6. Legend for the cross sections.

Figure 5.7. Uncía cross section, Uncía map sheet, Bolivar region.

Figure 5.8. Cochabamba cross section, Cochabamba map sheet, Bolivar region.

Figure 5.9. Thematic Mapper image of the boundary between the Cordillera Oriental and the Altiplano at approximately 18°30'S. Fault scarps indicating an east-dipping fault are marked with arrows.

Figure 5.10. North Punata cross section, Punata map sheet, Punata and Totora regions.

Figure 5.11. Central Punata cross section, Aiquile and Punata map sheets, Punata and Totora regions.

Figure 5.12. South Punata cross section, Aiquile and Punata map sheets, Punata and Totora regions. Note the variation in bed thickness of the Upper Ordovician and the Silurian units between faults q and r.

Figure 5.13. West Aiquile cross section, Aiquile map sheet, West Aiquile region.

Figure 5.14. East Aiquile cross section, Aiquile map sheet, West Aiquile, Peña Colorada, and San Isidro regions. Note the propagation of thrusts gg and ii out of the adjacent synclines.

Figure 5.15. North Totora cross section, Punata map sheet, Elbow region.

Figure 5.16. Central Totora cross section, Punata map sheet, Elbow region.

Figure 5.17. South Totora cross section, Punata and Santa Cruz de la Sierra map sheets, Elbow region.

Figure 5.18. West Vallegrande cross section, Vallegrande map sheet, San Isidro region.

Figure 5.19. East Vallegrande cross section, Vallegrande map sheet, East Vallegrande region.

Figure 5.20. South Santa Cruz cross section, Santa Cruz de la Sierra map sheet, Elbow region.

Figure 5.21. Limbo cross section, Punata map sheet, Elbow region.

Figure 5.22. Geometry of folding, showing the angles used to calculate cutoff angles (from Suppe, 1983).

Figure 5.23. Theoretical ramp and hanging wall cutoff angles for the application of the fault-bend and fault-propagation fold models to the structures of the mapped area. Given the interlimb angle (γ) and assuming constant bed thickness, theoretical ramp angles (θ) and hanging wall cutoff angles (β) are determined from diagrams in Suppe (1983) and Jamison (1987). Data points are circled. a) A ramp angle of approximately 42° is determined for strata above decollements localized within Lower Ordovician rocks for the fault-propagation model. No solution is obtained for strata above decollements localized within the Icla Formation. b) Ramp angles of

Lower Ordovician shale and the Icla Formation, respectively, correspond to average observed interlimb angles for the fault-bend fold model. c) Theoretical hanging wall cutoff angles for the fault-bend fold model.

Figure 5.24. Summary of fault dip (vergence) across the mapped area. Cross section locations are labelled according to the level of decollement, and the dip of each observed fault is marked. The region is characterized by an unusually high number of backthrusts (east-dipping thrust faults).

Figure 5.25. Schematic cross sections interpreted below the shallowest level of decollement in order to show the change in the thrust front from a triangle zone (Oruro-Santa Cruz profile) to an emergent thrust front (Oruro-Punata-Chapare profile). Associated with the triangle zone is the presence of a surface of decollement in the Silurian Kirusillas Formation (Unit labels identify the location of the surface of detachment: Ol--Lower Ordovician shale, Sk--Silurian Kirusillas Formation, Dic--Devonian Icla Formation). Duplexes that sole into the Silurian Kirusillas Formation are present where the triangle zone is present, but not to the north, where the level of decollement ramps up directly from Ordovician shale to Devonian shale.

Figure 5.26. The approximate northern limit of the Silurian, Devonian and Carboniferous depositional basins relative to the bend in the thrust front.

SIMPLIFIED GEOLOGIC MAP OF THE BOLIVIAN ANDES
17°S to 18°45'S

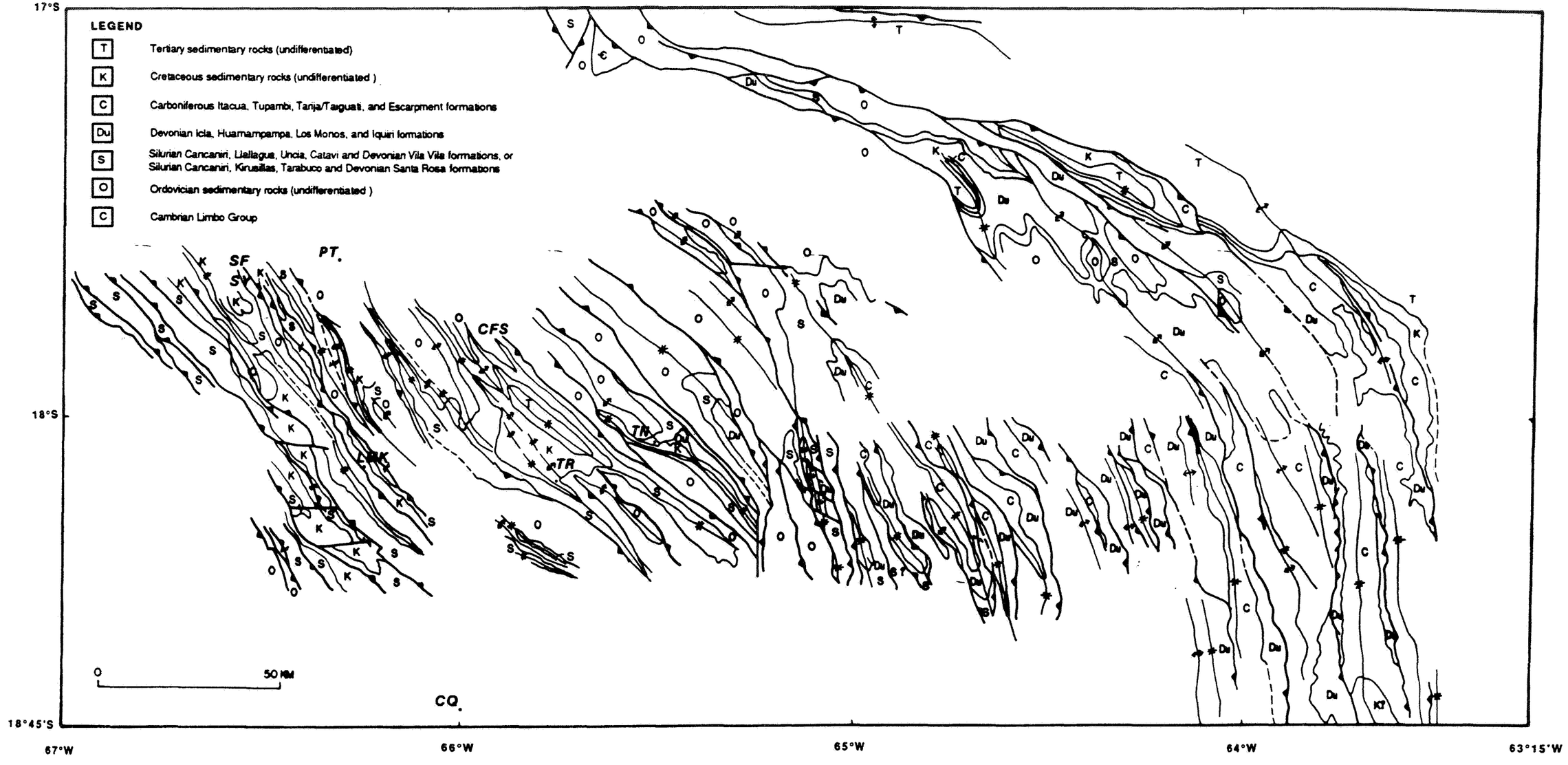

Figure 5.1

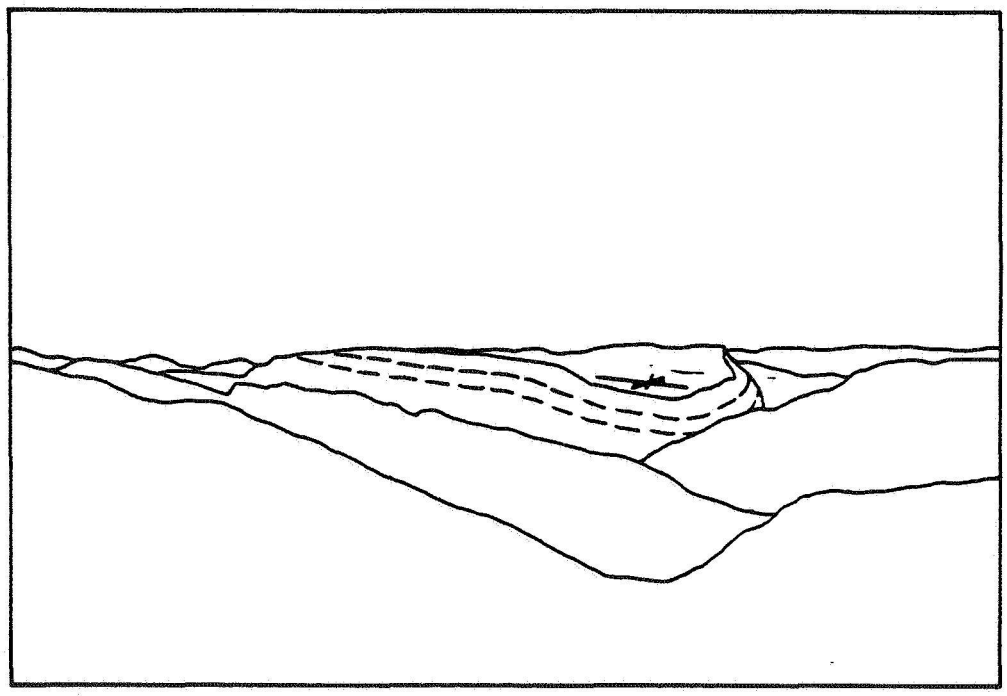

Figure 5.2

Levels of Decollement

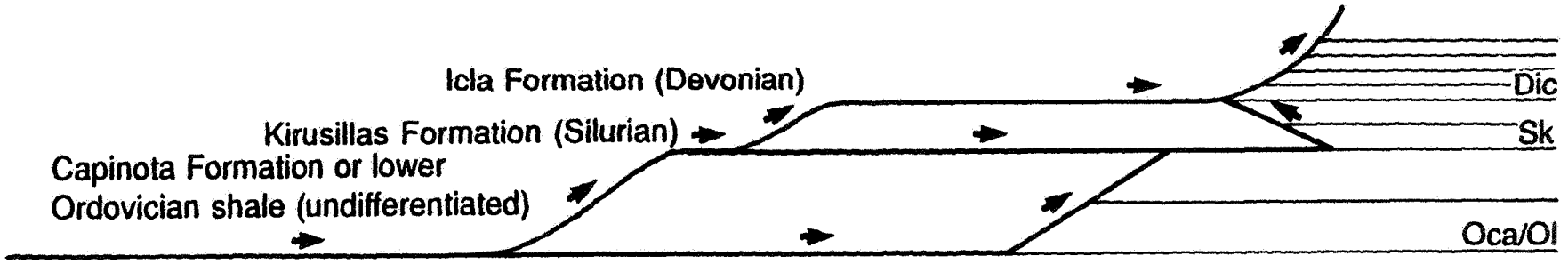

Figure 5.3

Stratigraphic levels
defined by surface geology
in the Subandean Zone, East Vallegrande region

Stratigraphic levels
defined by well and seismic reflection data
in the foreland

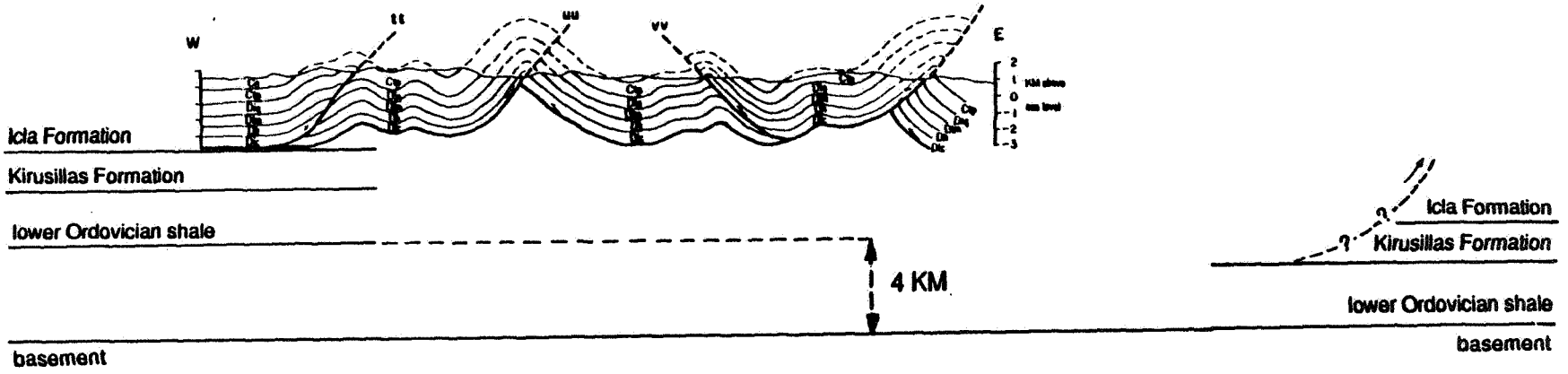

Figure 5.4

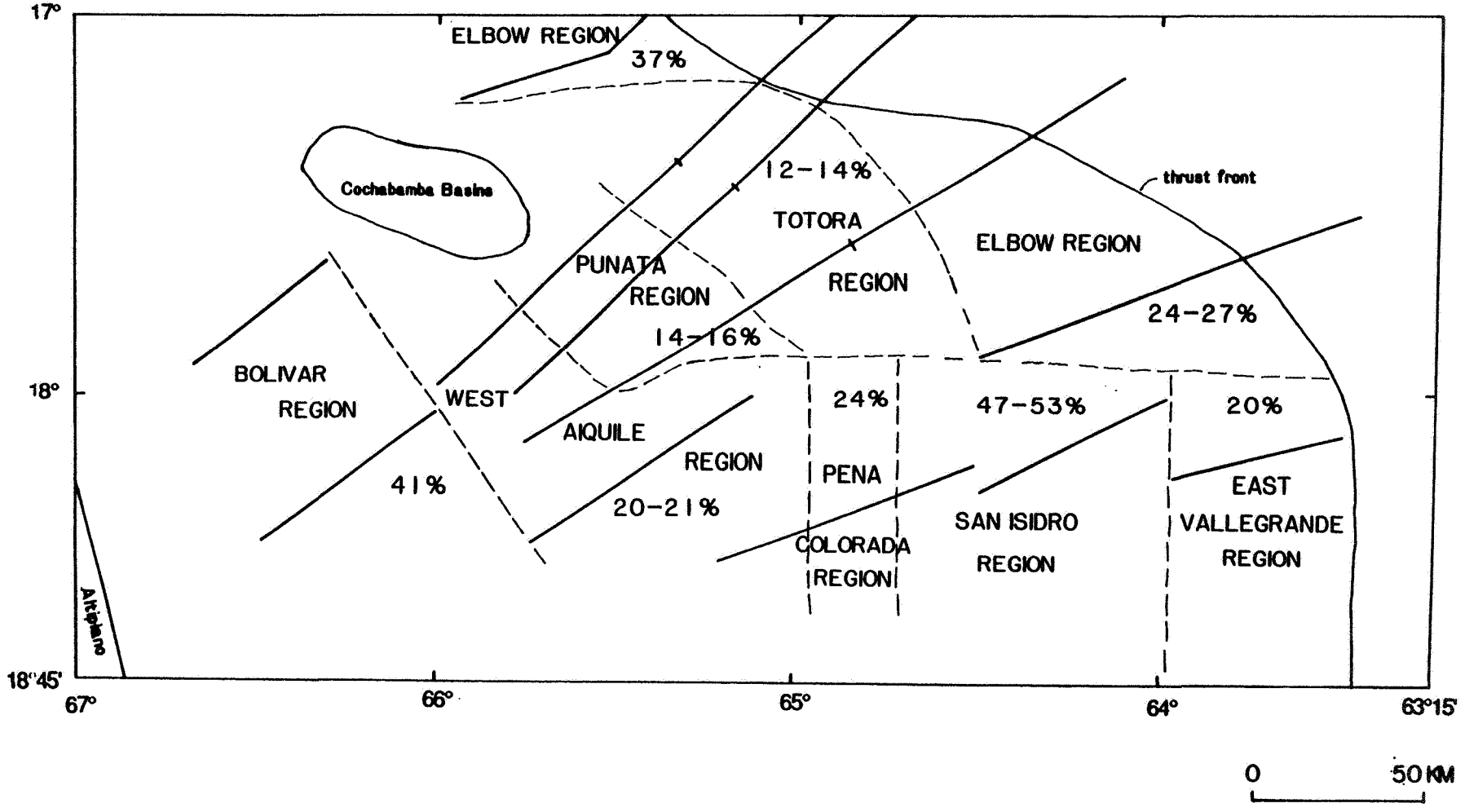
17°
18°
18°45'
67°
66°
65°
64°
63°15'
ELBOW REGION
37%
Cochabamba Basins
12-14%
TOTORA
REGION
thrust front
ELBOW REGION
PUNATA
REGION
14-16%
24-27%
BOLIVAR
REGION
WEST
AIQUILE
REGION
20-21%
41%
24%
PENA
47-53%
20%
EAST
VALLEGRANDE
REGION
SAN ISIDRO
REGION
COLORADA
REGION
Altiplano
0
50 KM

Figure 5.5

Legend of stratigraphic units for cross sections

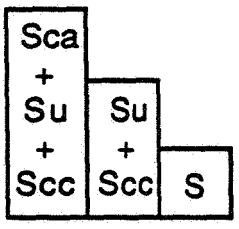

Catavi, Uncia, and Cancaniri formations

T	undifferentiated Tertiary sedimentary rocks
K	undifferentiated Cretaceous sedimentary rocks
Ctp	Tupambi and Itacua formations
Diq	Iquiri Formation
Dlm	Los Monos Formation
Dh	Huamampampa Formation
Dic	Icla Formation
Dsr + St	Santa Rosa and Tarabuco formations
Sk + Scc	Kirusillas and Cancaniri formations
Ou	upper Ordovician
Ol	lower Ordovician
C	Limbo Group

Figure 5.6

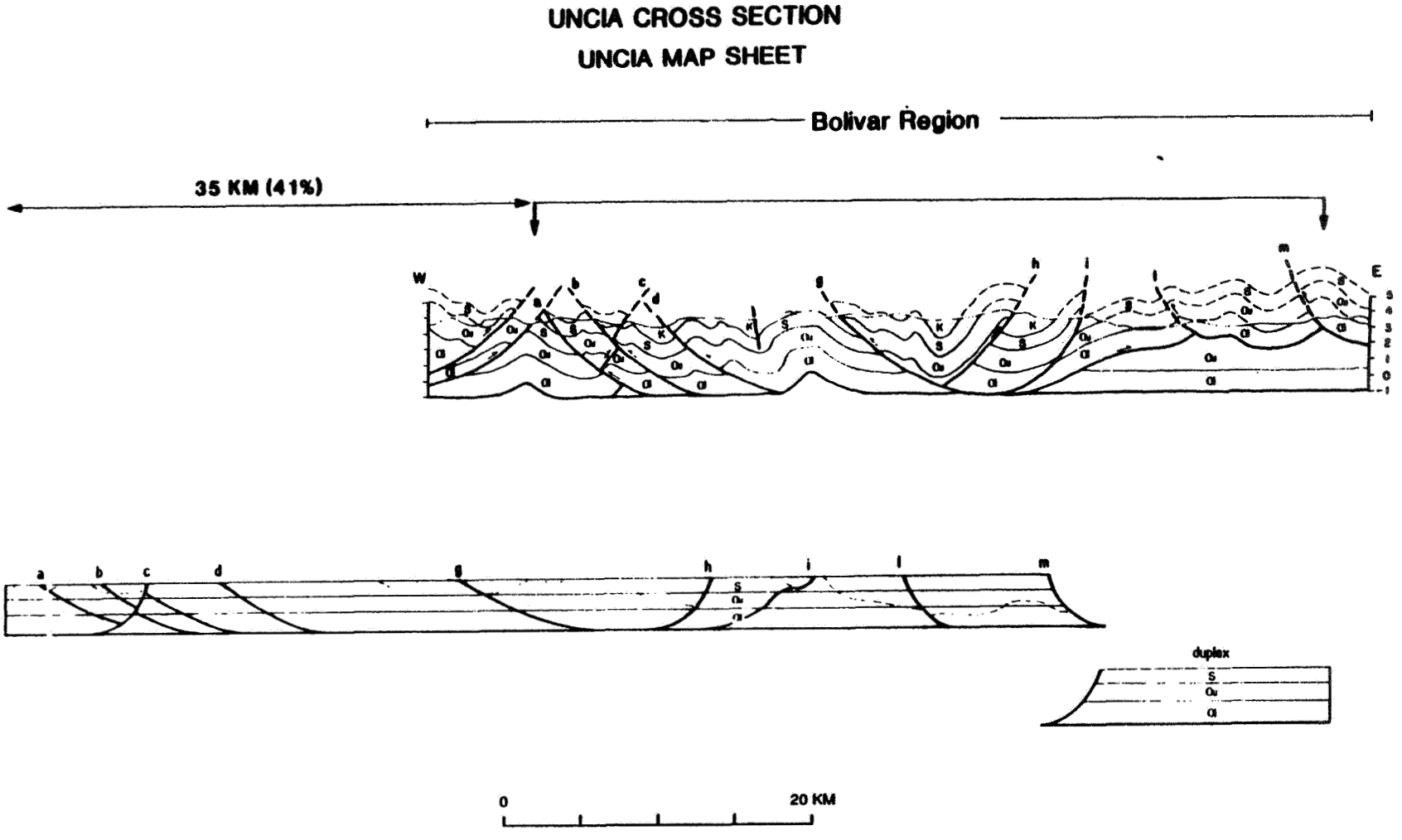
UNCIA CROSS SECTION
UNCIA MAP SHEET
Bolivar Region
35 KM (41%)
W
E
a
b
c
d
g
h
i
l
m
duplex
0
20 KM

Figure 5.7

COCHABAMBA CROSS SECTION

COCHABAMBA MAP SHEET

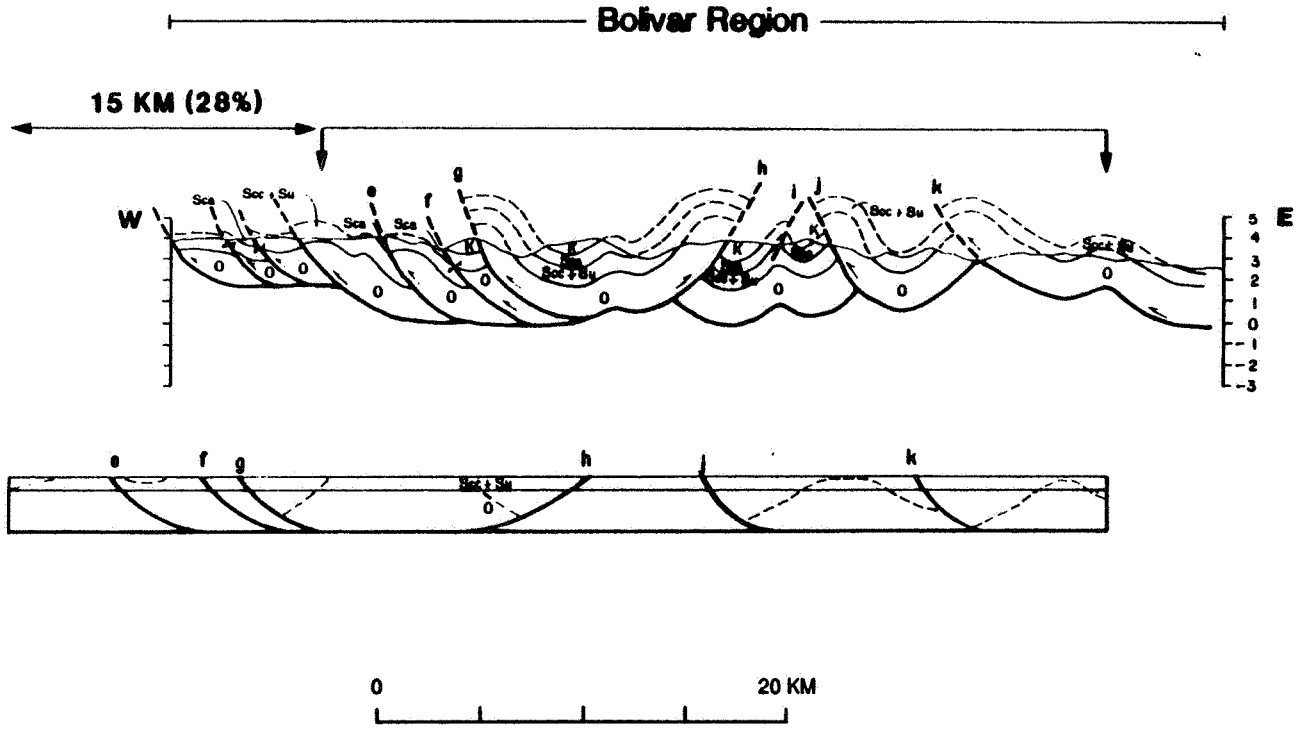

Figure 5.8

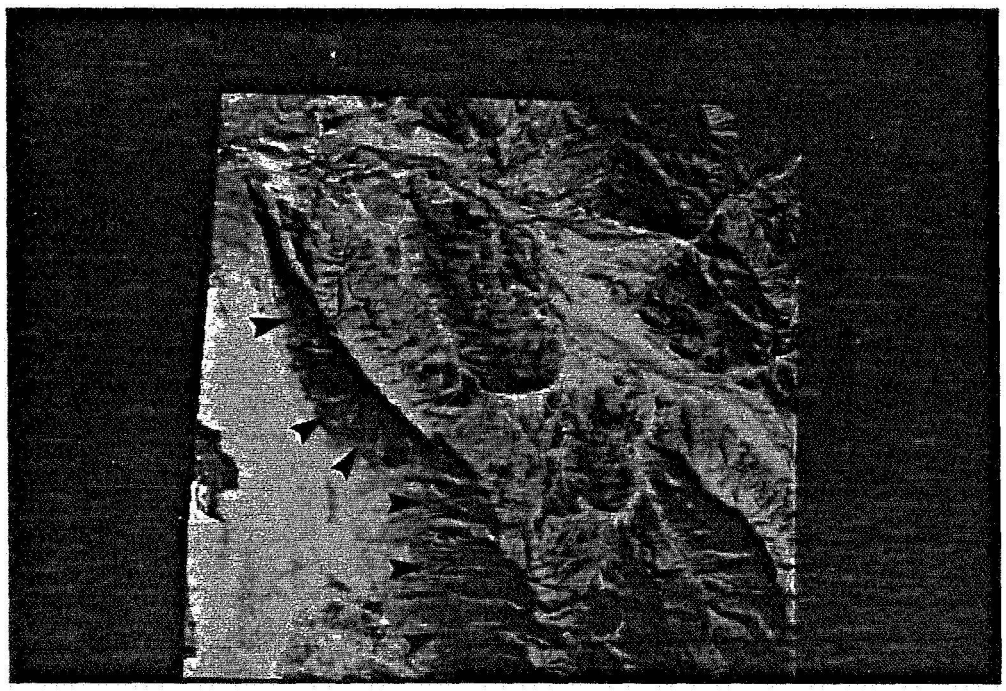

Figure 5.9

NORTH PUNATA CROSS SECTION

PUNATA MAP SHEET

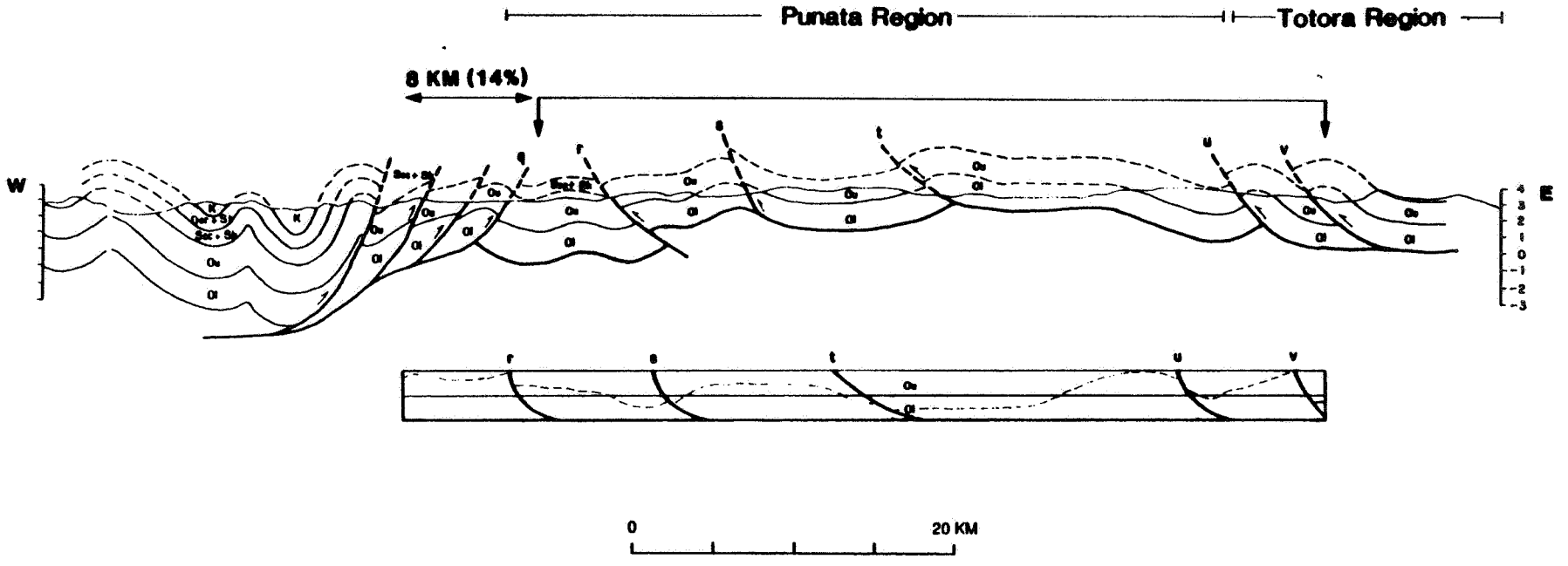

Figure 5.10

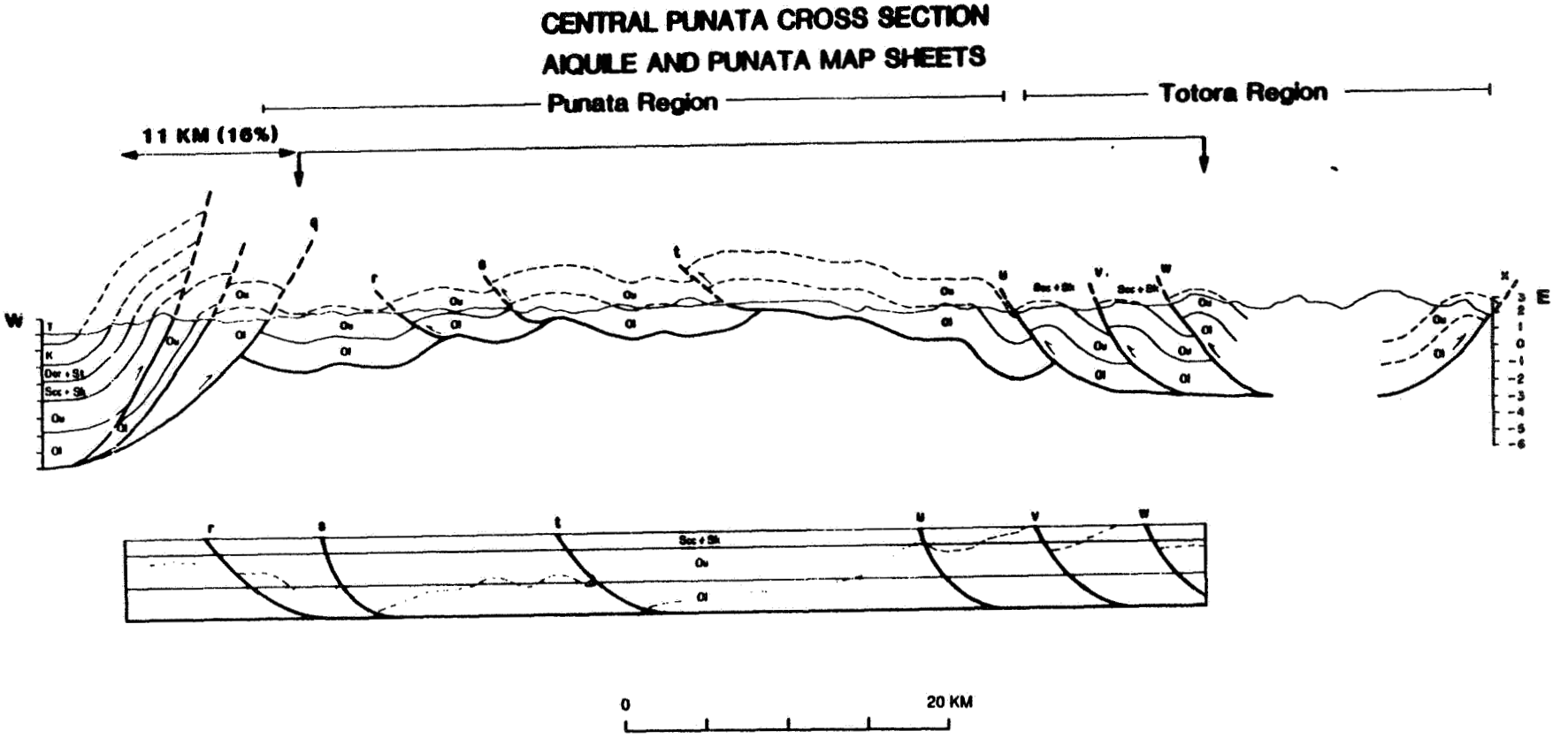
CENTRAL PUNATA CROSS SECTION
AIQUILE AND PUNATA MAP SHEETS
Punata Region
Totora Region
11 KM (16%)
W
E
0
20 KM

Figure 5.11

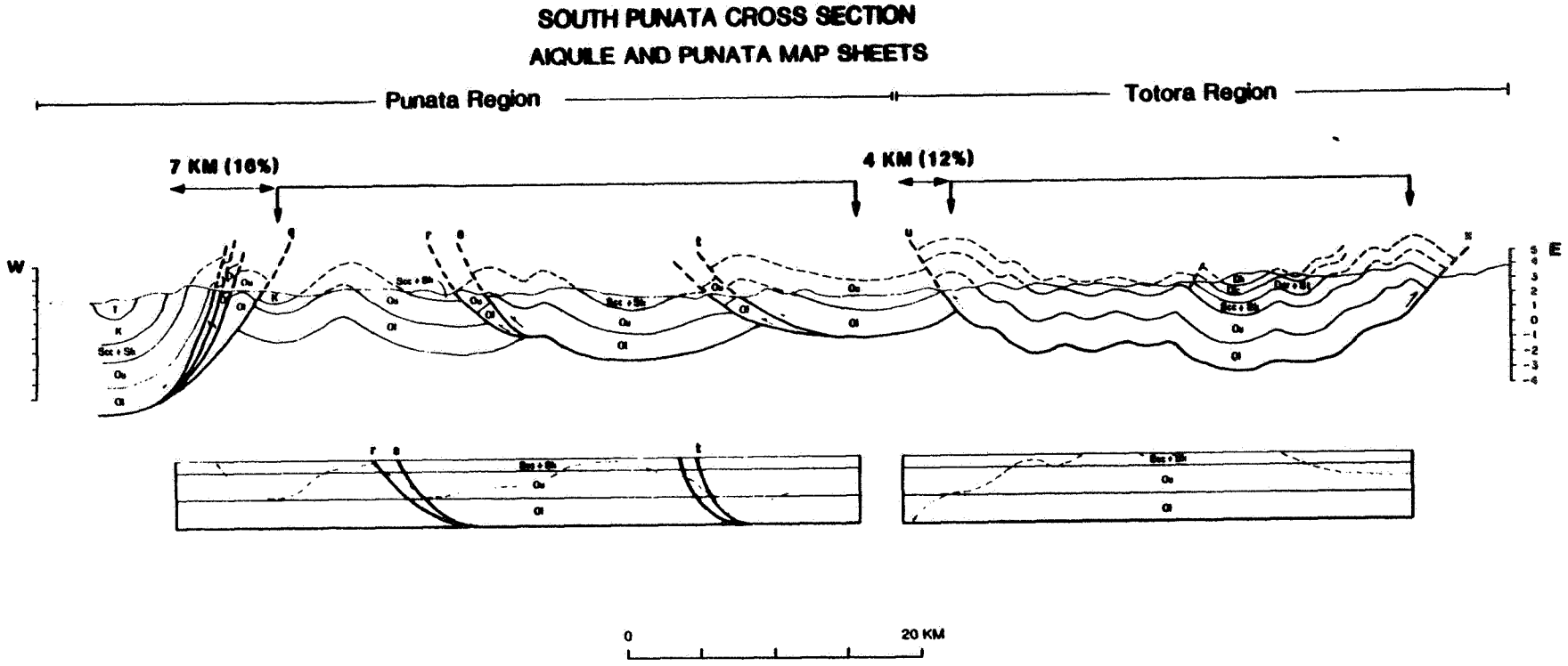
SOUTH PUNATA CROSS SECTION
AIQUILE AND PUNATA MAP SHEETS
Punata Region
Totora Region
7 KM (16%)
4 KM (12%)
W
E
0
20 KM

Figure 5.12

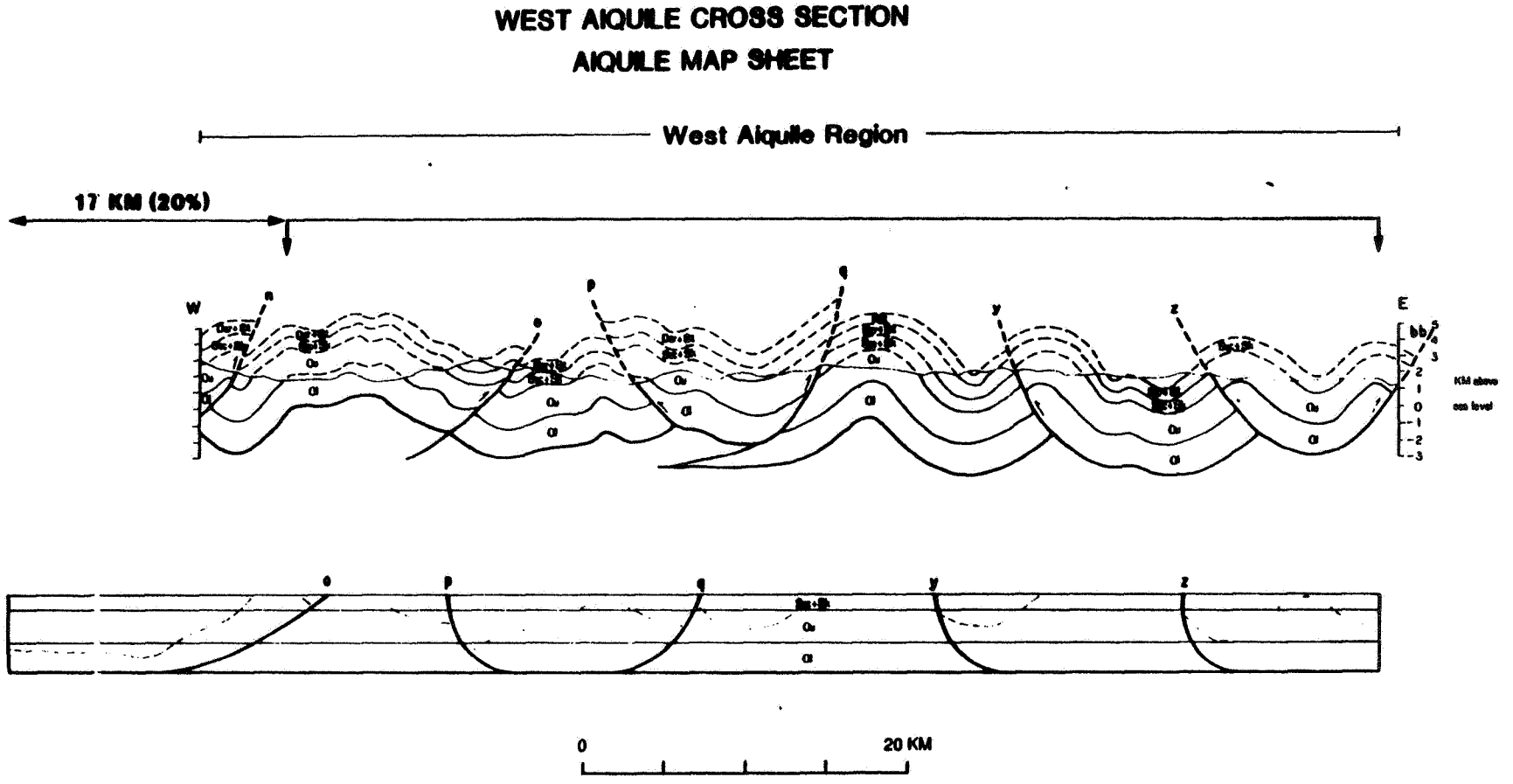
WEST AIQUILE CROSS SECTION
AIQUILE MAP SHEET
West Aiquile Region
17 KM (20%)
W
E
0
20 KM

Figure 5.13

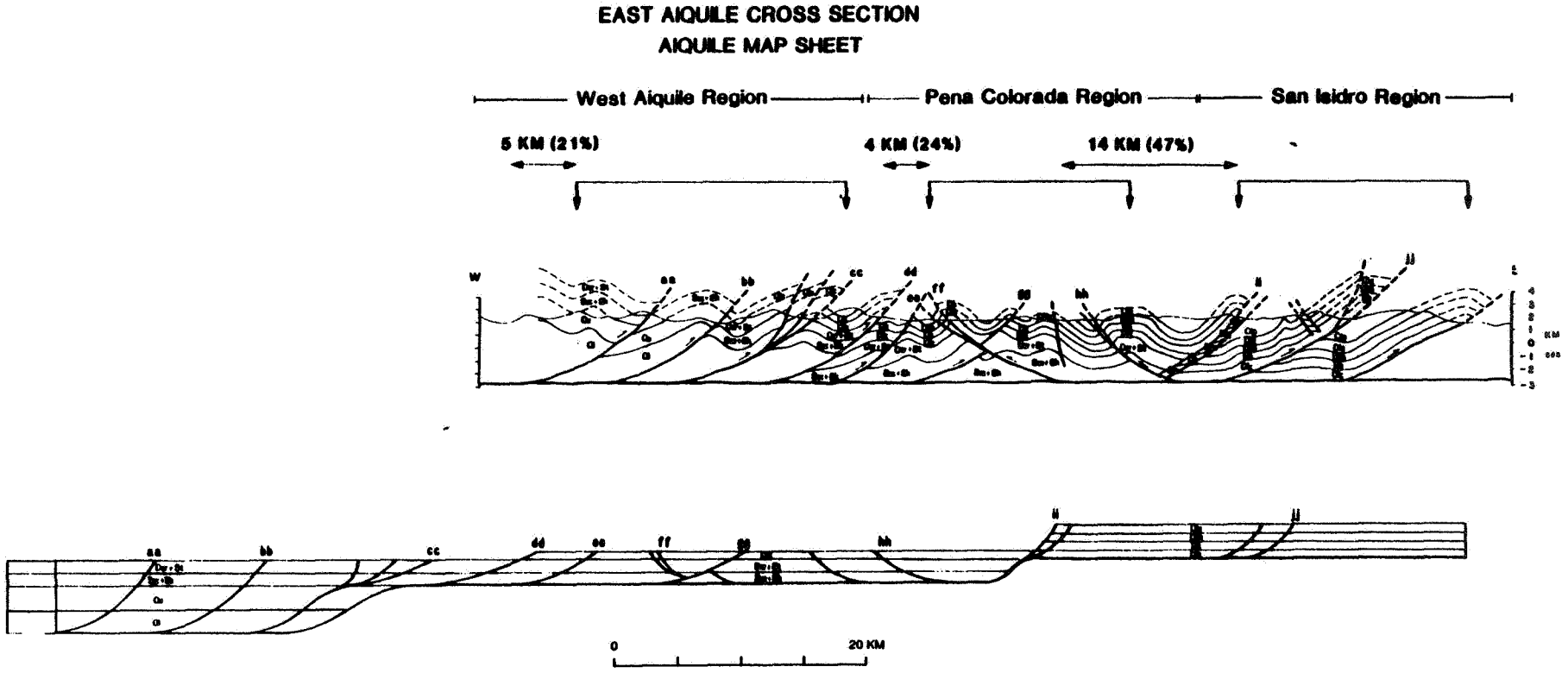
EAST AIQUILE CROSS SECTION
AIQUILE MAP SHEET
West Aiquile Region
Pena Colorada Region
San Isidro Region
5 KM (21%)
4 KM (24%)
14 KM (47%)
W
E
aa
bb
cc
dd
ee
ff
gg
hh
ii
jj
0
20 KM

Figure 5.14

NORTH TOTORA CROSS SECTION
PUNATA MAP SHEET

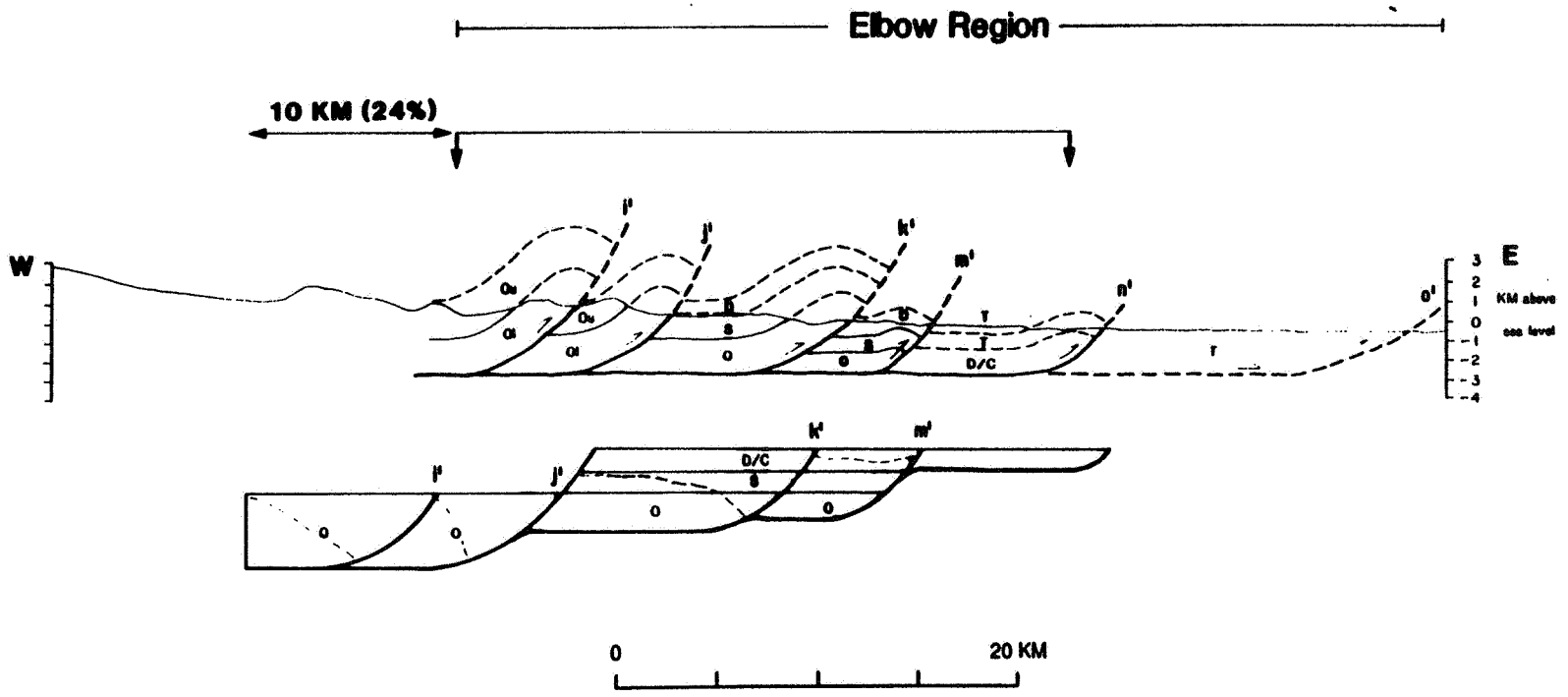

Figure 5.15

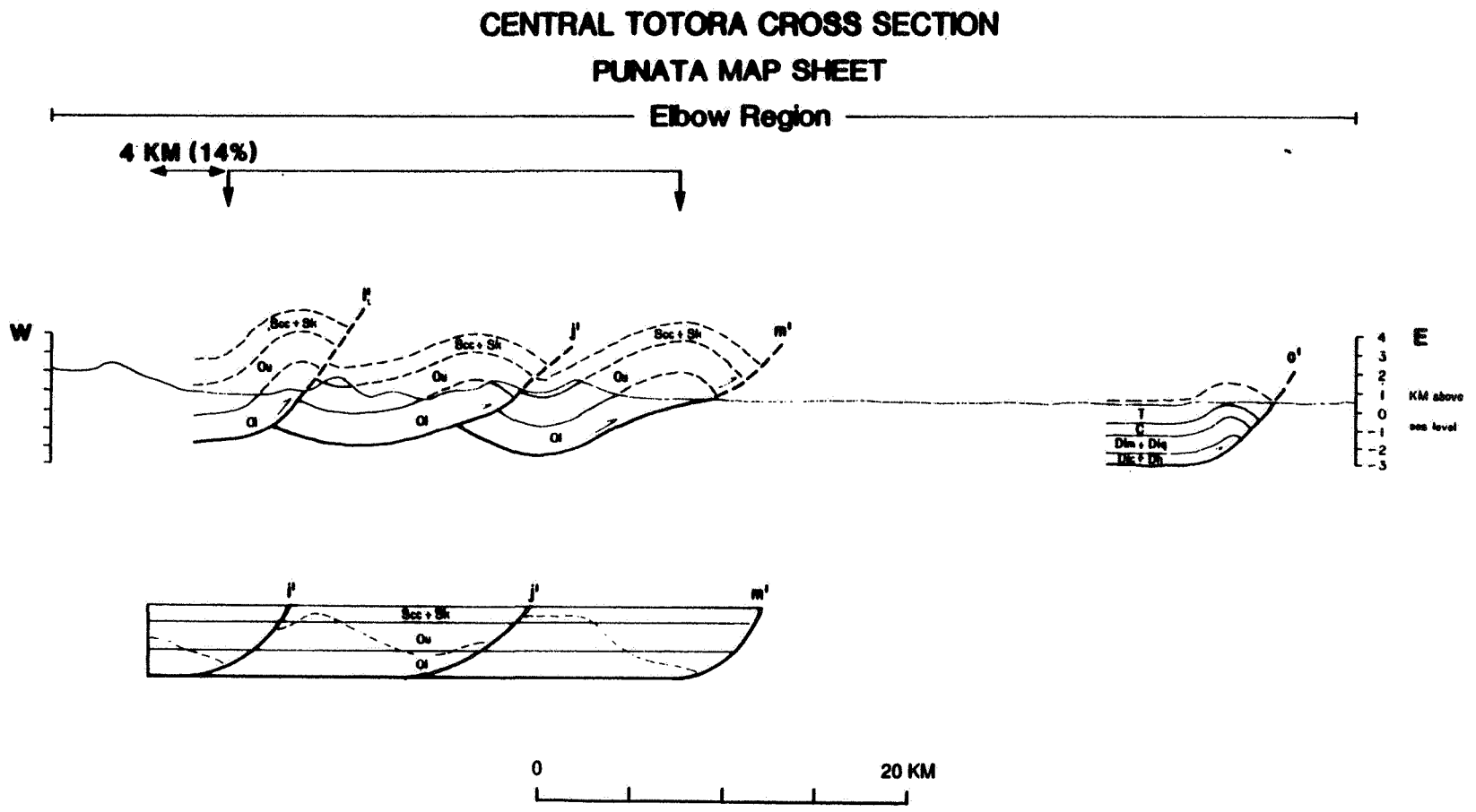
CENTRAL TOTORA CROSS SECTION
PUNATA MAP SHEET
Elbow Region
4 KM (14%)
W
E
KM above sea level
0
20 KM

Figure 5.16

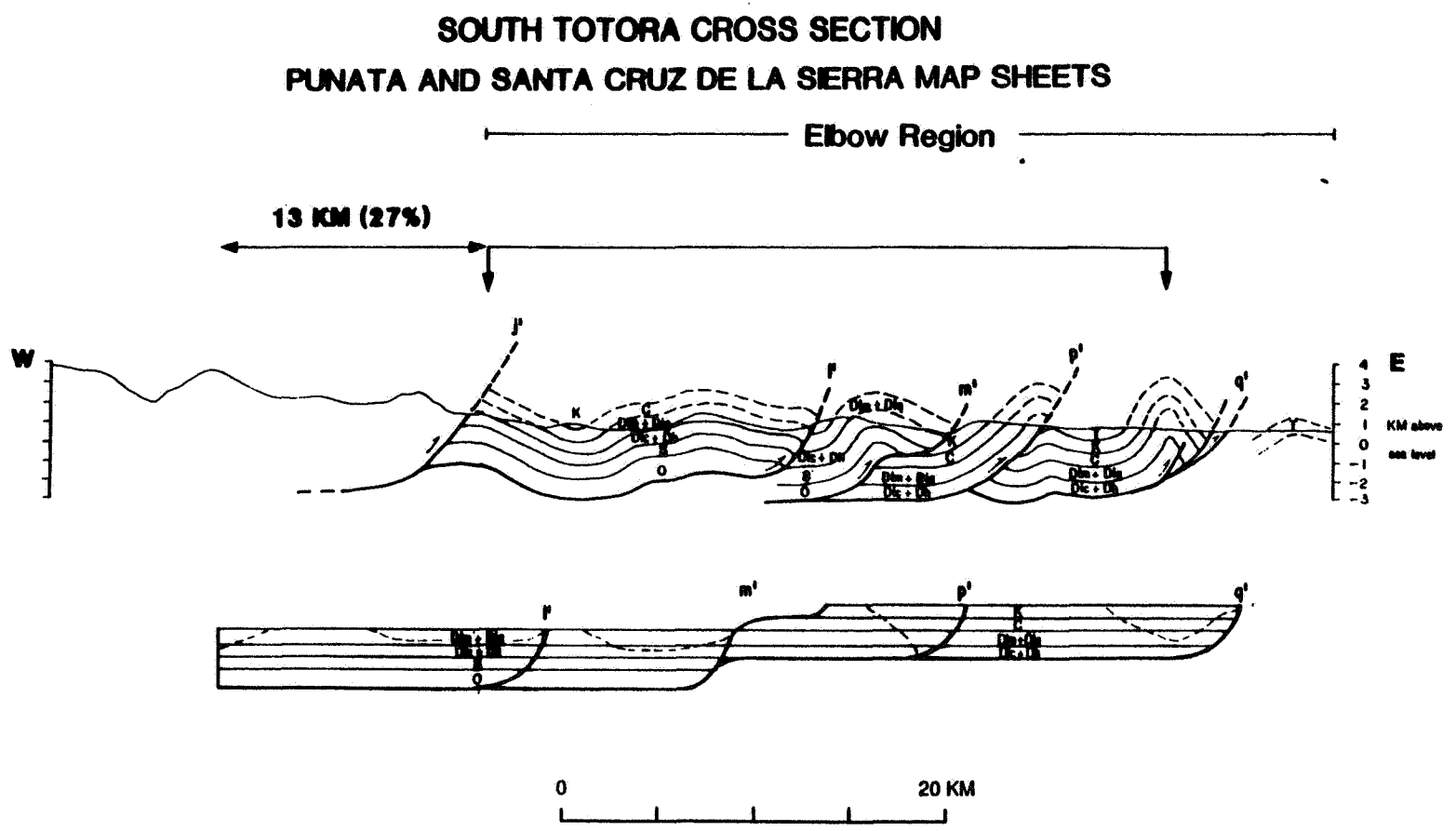
SOUTH TOTORA CROSS SECTION
PUNATA AND SANTA CRUZ DE LA SIERRA MAP SHEETS
Elbow Region
13 KM (27%)
W
E
KM above sea level
0
20 KM

Figure 5.17

WEST VALLEGRANDE CROSS SECTION
VALLEGRANDE MAP SHEET

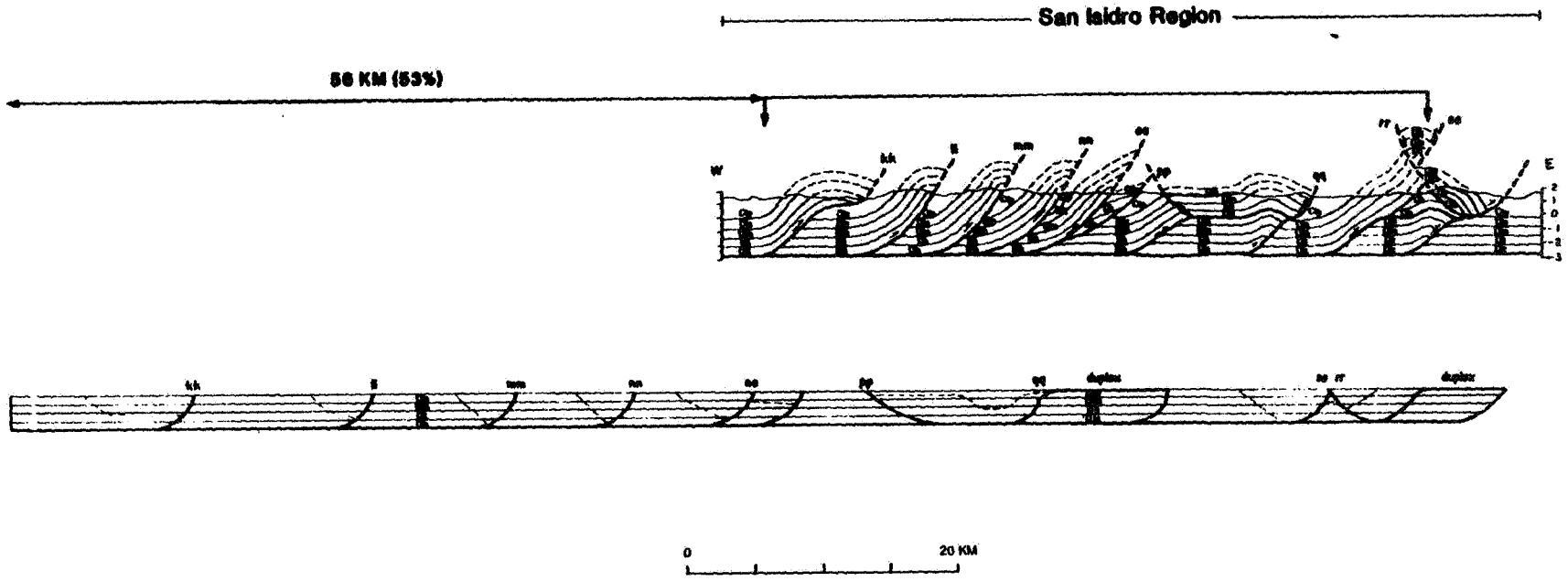

Figure 5.18

EAST VALLEGRANDE CROSS SECTION
VALLEGRANDE MAP SHEET

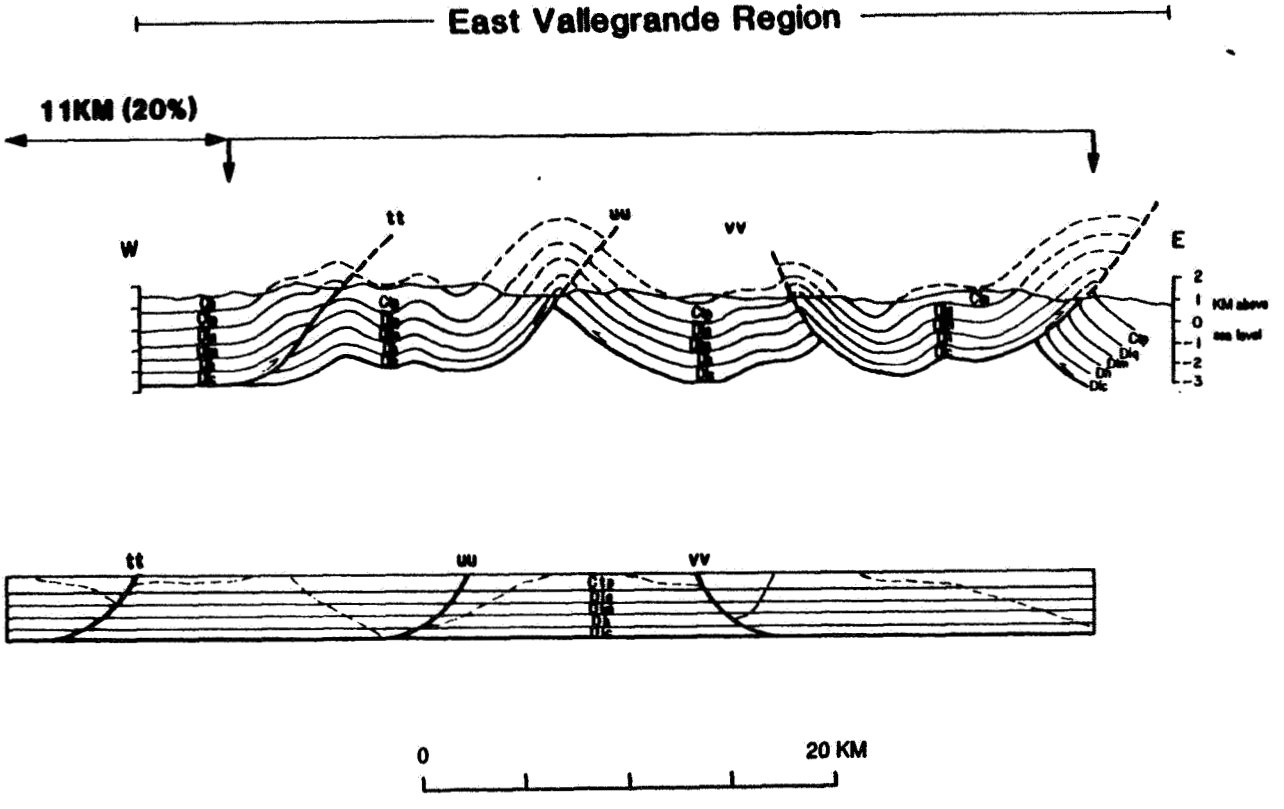

Figure 5.19

SOUTH SANTA CRUZ CROSS SECTION
SANTA CRUZ DE LA SIERRA MAP SHEET

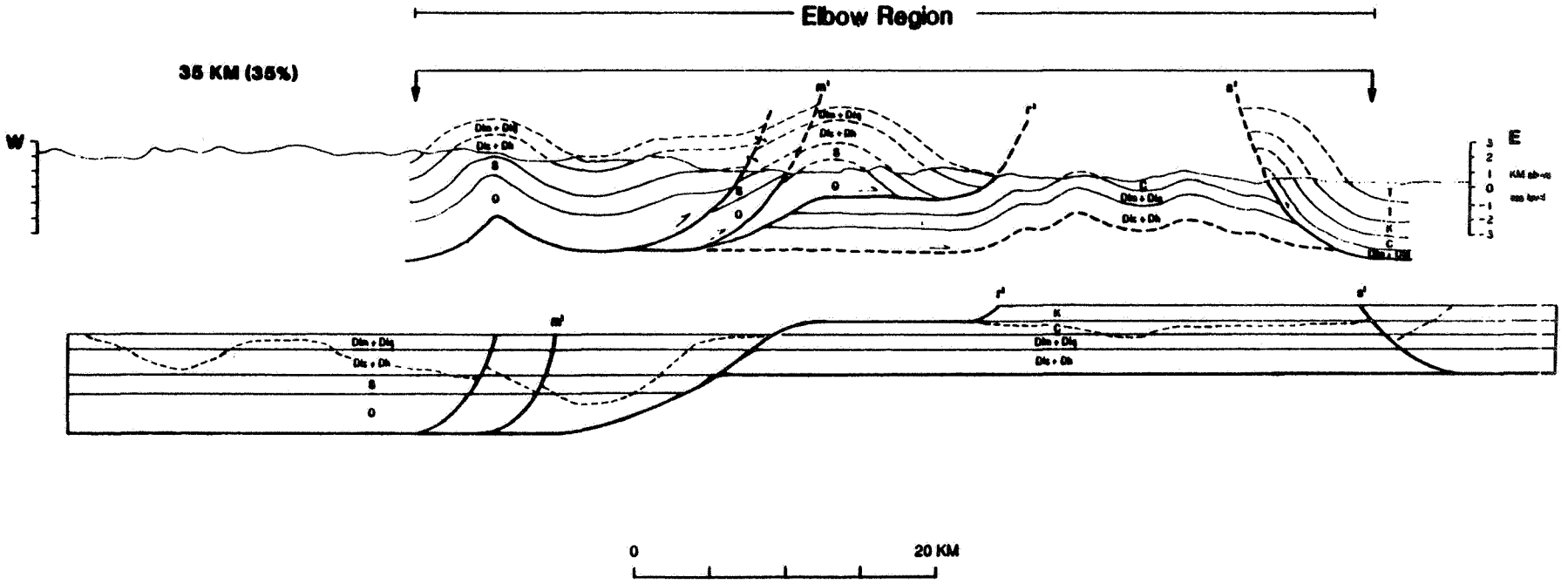

Figure 5.20

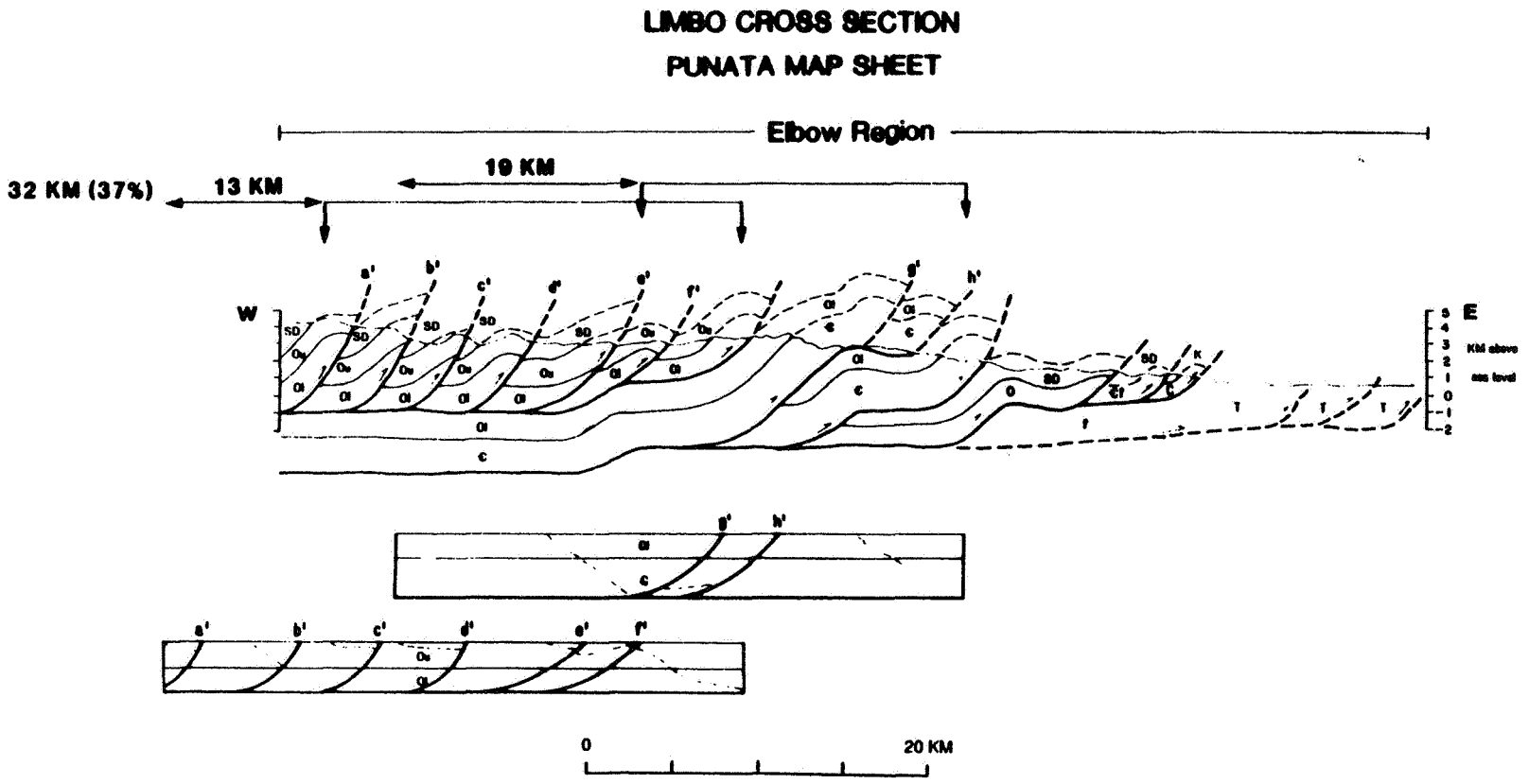
LIMBO CROSS SECTION
PUNATA MAP SHEET
Elbow Region
32 KM (37%)
13 KM
19 KM
W
E
KM above sea level
0
20 KM

Figure 5.21

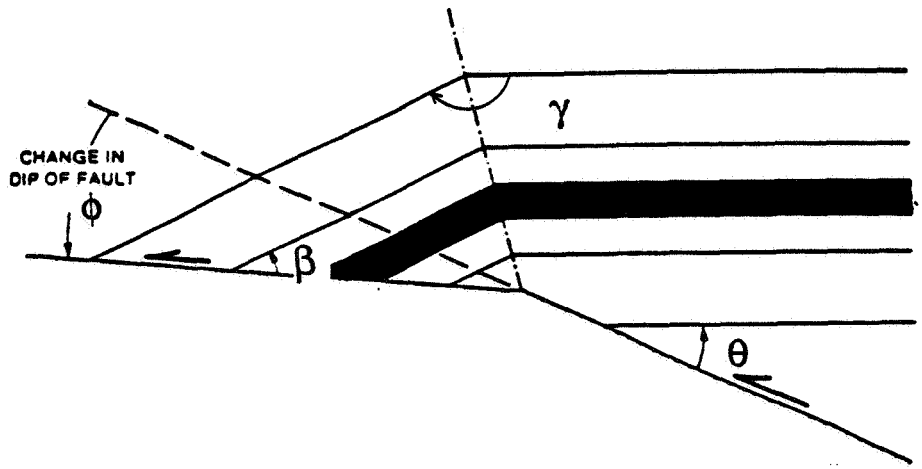

Figure 5.22

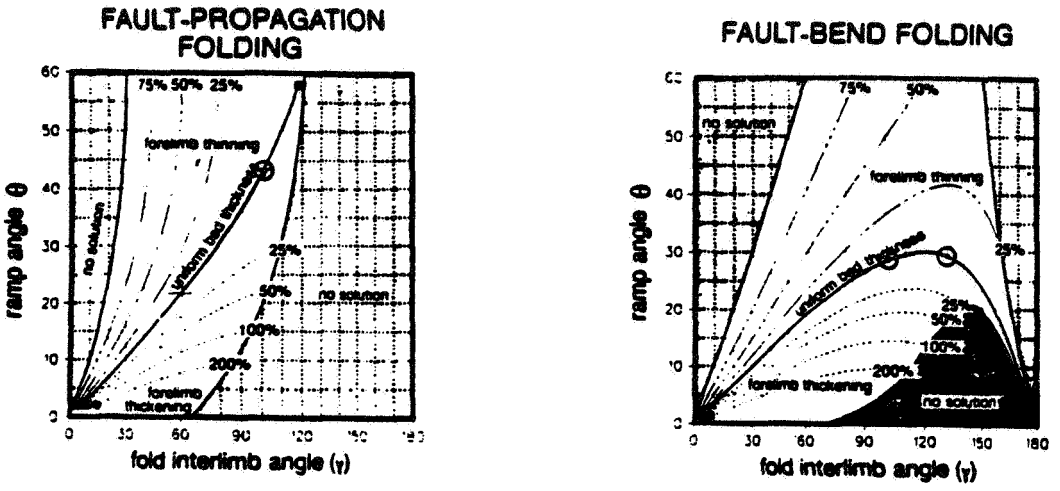

from Jamison (1987)

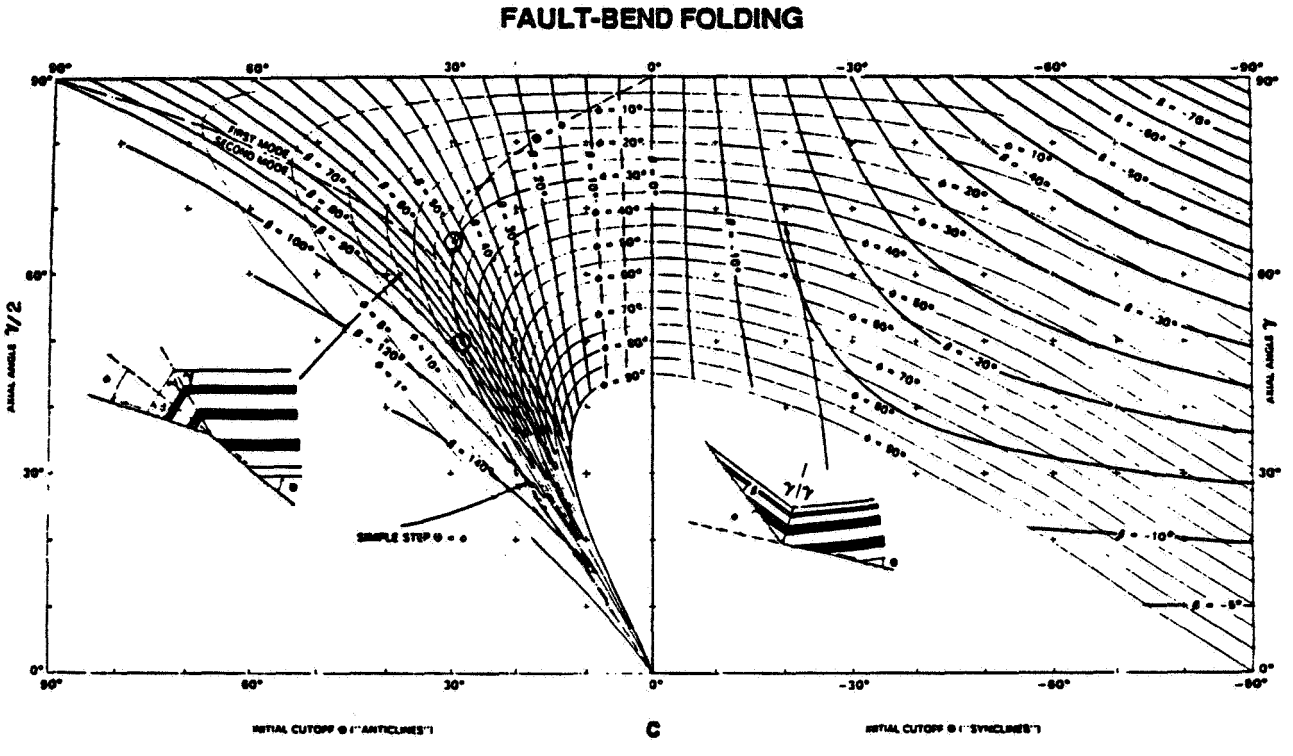

from Suppe (1983)

Figure 5.23

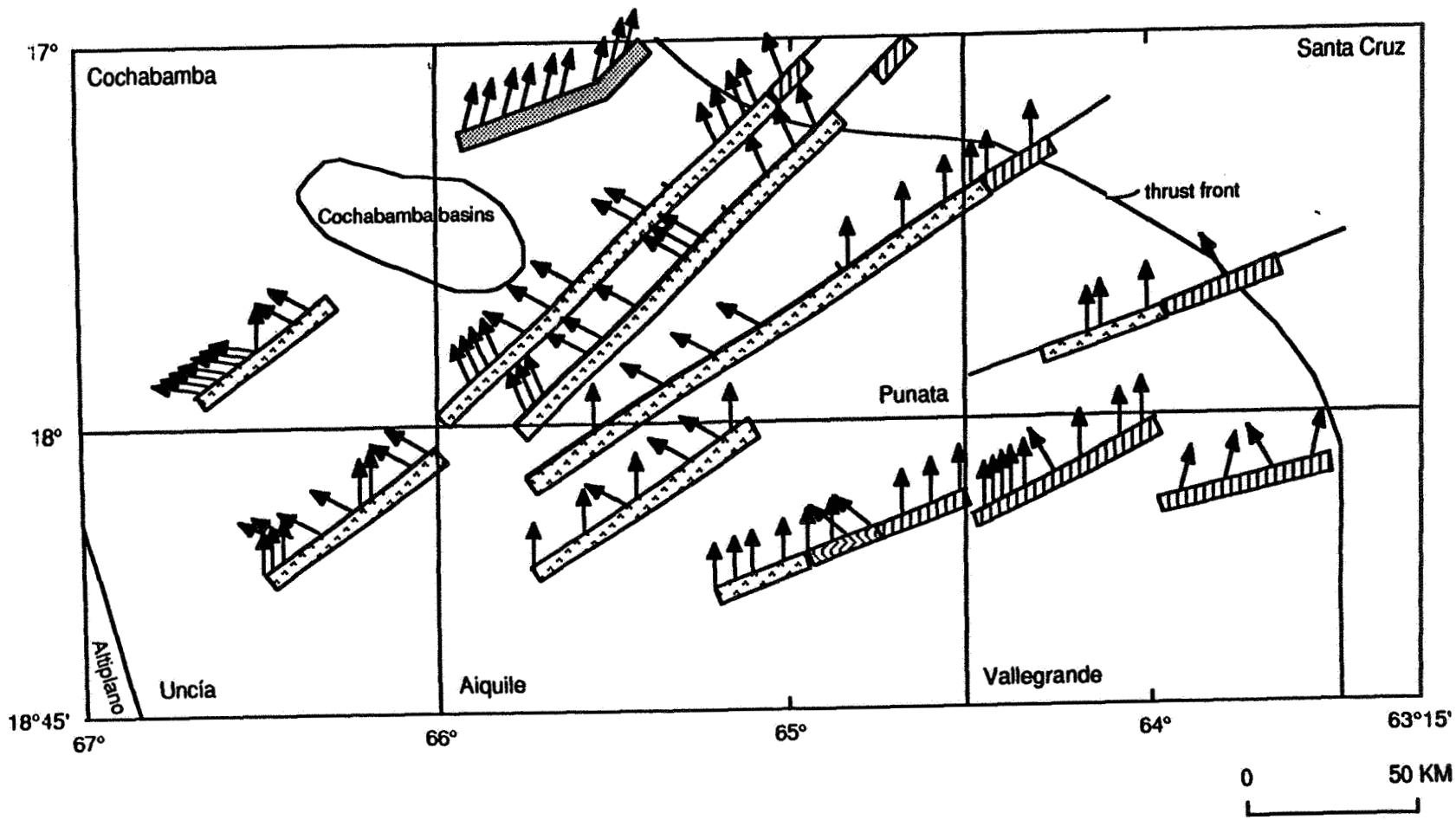
17°
18°
18°45'
67°
66°
65°
64°
63°15'
Cochabamba
Santa Cruz
Cochabamba basins
thrust front
Punata
Altiplano
Uncía
Aiquile
Vallegrande
0
50 KM
Level of Decollement
Icla Formation
Kirusillas Formation
Lower Ordovician
Limbo Group
East-vergent (west-dipping) thrust fault
West-vergent (east-dipping) thrust fault

Figure 5.24

Oruro-Punata-Chapare Profile--Emergent thrust front

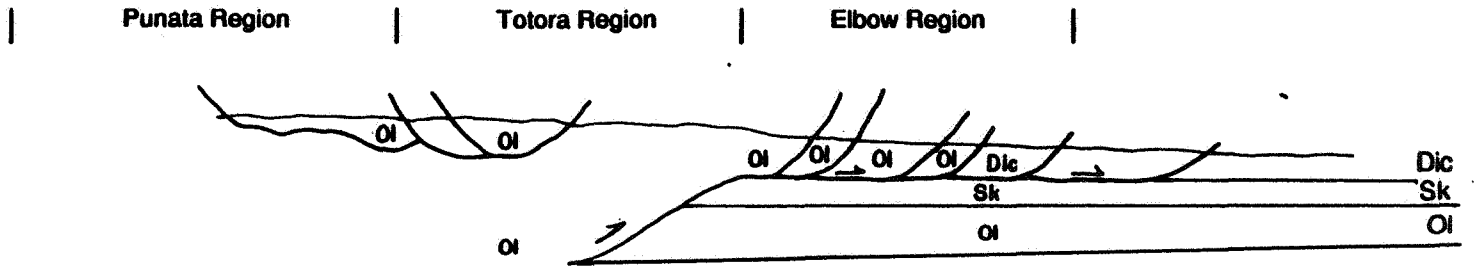

Oruro-Santa Cruz Profile--Triangle zone

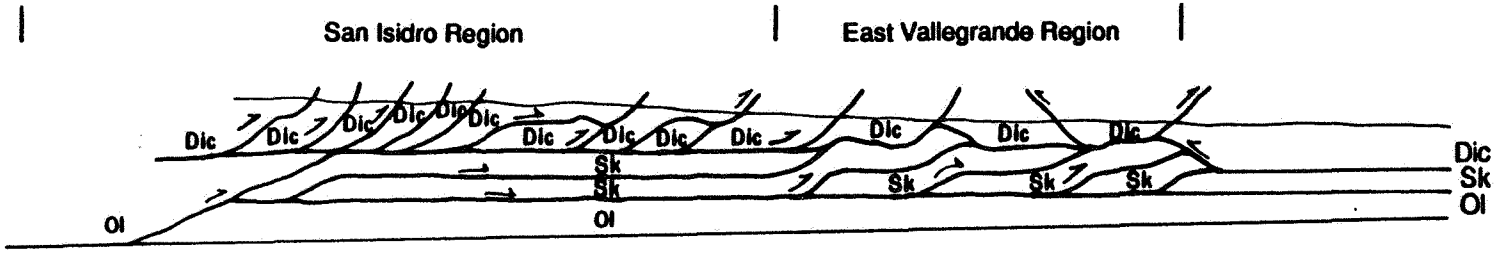

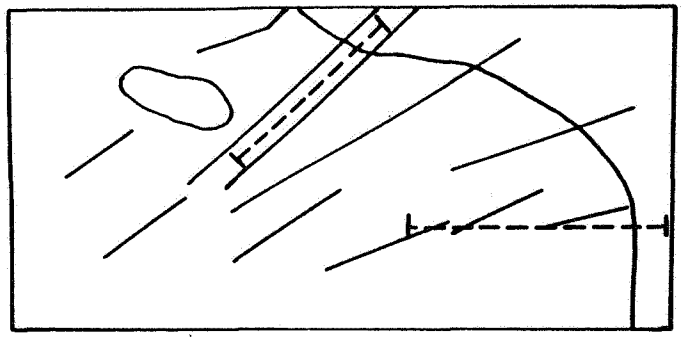

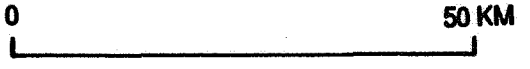

Figure 5.25

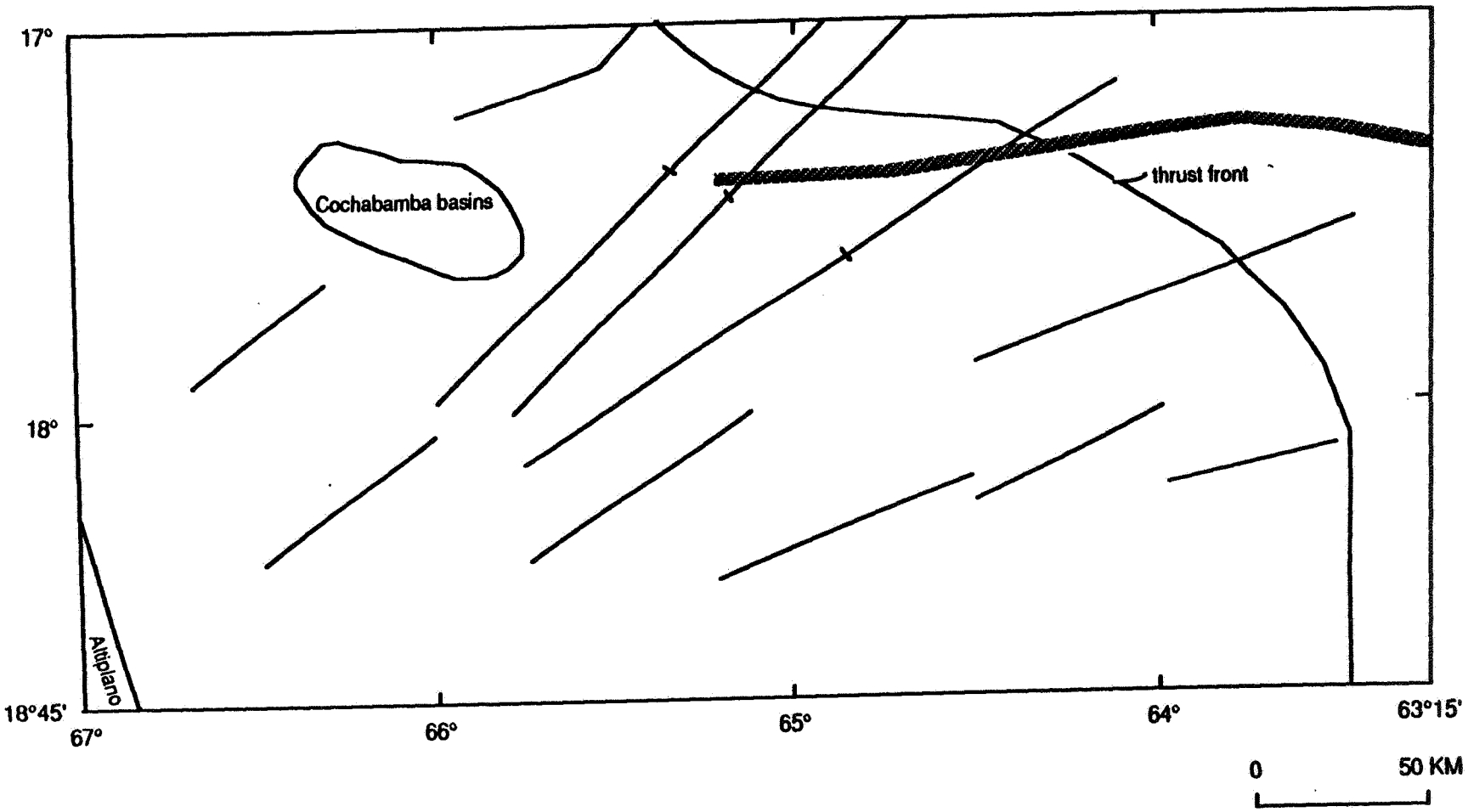

Northern limit of the Silurian, Devonian and Carboniferous basin

Figure 5.26

CHAPTER SIX

The importance of crustal shortening in the formation of the central Andes

Introduction

The central Andes are an ideal place to study orogenesis because they constitute an active, type example of an Andean margin. An Andean margin is comprised of an orogenic belt that is the result of subduction of oceanic lithosphere beneath continental lithosphere. Orogeny in the central Andes is characterized by the extremely thickened crust that underlies two active belts of magmatism and crustal deformation: the magmatic arc of the Cordillera Occidental and the folded and faulted Cordillera Oriental and Subandean Zone that flank the high plateau of the Altiplano. Which of these two processes, magmatism or crustal deformation, has contributed more to the thickened crust continues to be controversial, in part because quantification of magmatic contributions from the mantle is largely unconstrained. Balanced cross sections, however, enable us to quantify the amount of crustal shortening, and therefore to assess its significance in the process of mountain-building.

In the Bolivian Andes, the mapping completed for this study provides the basis for such a calculation. The determination of a lower bound on shortening involves the careful construction of balanced cross sections. Balanced area calculations based on this minimum estimate and estimates of plausible additional shortening indicate that crustal shortening has

probably played the dominant, but not the only, role in orogenesis in the central Andes.

Determination of a minimum amount of shortening

Several composite cross sections have been constructed from the individual balanced cross sections (Plates 7 and 8), crossing the Cordillera Oriental and Subandean Zone both north and south of the elbow region, at approximately 18°S (Figure 2.2). The minimum total shortening from the combined individual balanced cross sections is calculated by dividing the composite cross section into lengths subject to different deformational styles and applying the appropriate percent shortening to calculate the minimum total shortening for those lengths (Figure 5.5). The shortening that has occurred above the different surfaces of detachment in Devonian, Silurian and Ordovician rocks may be combined in this way because the thrust sheets that sole into Ordovician shale carry a structural package that includes the Silurian and Devonian strata, and therefore none of the observed thrust sheets that sole into the Ordovician shale are structural "basement" to the thrust sheets that sole into either Silurian or Devonian shale.

The composite cross sections fall into two categories: profiles that cross the mountain belt in an approximately east-west direction, which are averaged for analysis into the Oruro-Santa Cruz profile, and those that cross the mountain belt in a northeast-southwest direction, whose average is represented in the Oruro-Punata-Chapare profile. I consider first the Oruro-Santa Cruz profile, which crosses the mountain belt at its widest, lies entirely within the mapped area of this study, and lies south of the bend in the mountain belt. A later discussion will address the minimum

total shortening along the Punata profile, and the complications of the bend in the mountain belt.

The minimum amounts of crustal shortening across the Bolivian Andes measured along the east-west trending cross sections are 207 and 213 km. For purposes of discussion below, I use the average of these two numbers, 210 km. Before discussing the significance of the minimum total shortening, I briefly review the precision of this number and emphasize the reasons it is a minimum.

The precision of the minimum total shortening was discussed in Chapter 4. First, measurement errors are small. Second, errors due to non-plane strain are negligible with respect to metamorphism or pressure solution, and are probably negligible due to strike-slip faulting. No significant metamorphism or pressure solution is observed in the mapped area. The evidence for strike-slip faulting is present in only a few areas and does not include obviously offset features that would allow quantification of the amount of slip that has occurred. If present, such slip would be in the sense of decreasing the amount of shortening observed, and therefore biasing the calculated estimate towards underestimation.

Three assumptions are necessary for the construction of the cross sections. These have been chosen to ensure that the shortening implied in these sections is a minimum.

First, where hanging wall cutoffs are eroded, the measured displacement along thrust faults is a minimum. This erosion is common throughout the mapped area, and it can be demonstrated, where cross sections overlap along strike, that displacements along thrust faults are underestimated. Where two structures merge along strike, displacement that was distributed over both structures must become concentrated on a

single one. In such a case, a minimum displacement will be an underestimate.

Second, the angles between faults and bedding have been depicted in the cross sections as steeper than theoretical and observational data would predict for most fold and thrust belts (Suppe, 1983; Jamison, 1987), but have been based on evidence for large hanging wall cutoff angles from within the mapped area. These geometries result in an underestimation of the shortening because a greater amount of shortening is implicit in cross sections drawn with small angles between faults and bedding than in cross sections with large cutoff angles. For example, two balanced cross sections for the east Vallegrande region are shown in Figure 6.1. A balanced cross section that allows high cutoff angles implies 11 km of absolute shortening or 20% shortening over a distance of 53 km. Over the same distance, a significantly greater amount of shortening, 17 km or 32%, is calculated from a balanced cross section which is drawn with low cutoff angles of 20°, as constrained by fore- and back-dips (Suppe, 1983). Although the latter case is probably the more realistic of the two, at least for the footwall cutoff angles, the conservative interpretation that high cutoff angles are present in the study area has been made because the footwall cutoff angles were not observed during field work and because the field evidence indicates large hanging wall cutoff angles.

Third, no shortening of material below the thrust sheets exposed at the surface or from blind thrusts is included in the minimum estimate of shortening. All of the cross sections require additional deformation at depth. The surface of detachment defined in the cross sections does not coincide with the top of the basement and it is often folded, indicating that that surface has been uplifted and deformed by slip along deeper faults.

The geometry of faults at depth, however, is unconstrained by the surface geology and therefore no attempt is made to calculate its contribution to the minimum estimate of shortening initially.

In summary, a minimum total shortening of 210 kilometers is a conservative estimate of the shortening that has occurred across this mountain belt.

Balanced area calculations--Oruro-Santa Cruz profile

Introduction

Comparison of the deformed cross sectional area implied by the minimum total amount of crustal shortening with the present-day crustal structure suggests that crustal shortening has been the primary mechanism of orogenesis. Estimates of plausible additional shortening indicate, in fact, that virtually the entire mountain belt could have been built by crustal shortening, particularly if the basement is substantially involved. The contribution of basement involvement to the present-day crustal thickness appears to become important in the western Cordillera Oriental and in the Altiplano. The assessment of the range of likely amounts of crustal shortening indicate that mantle-derived magmas may have contributed from 0 to 30% of the observed crustal thickness. These results are discussed in light of the isotopic and geochemical constraints on the petrogenesis of the intrusive and extrusive rocks exposed in the central Andes.

Calculations

A comparison of the restored length with respect to present-day tectonic provinces provides an initial assessment of the importance of crustal shortening in Andean orogenesis (Figure 6.2). The minimum total shortening of 210 kilometers represents 36% shortening of a belt that was

initially 580 kilometers wide. From the foreland, where undeformed sediments lie on basement, this restored length would extend beneath the Cordillera Occidental, or more than 80% of the present-day width of the Bolivian Andes. If undeformed, the basement of the shortened, detached cover would have been underthrust beneath the entire width of the Altiplano and 30 kilometers of the Cordillera Occidental, implying that net convergence, between the trench and the undeformed foreland, of the same amount has occurred and that the thickened crust beneath the Altiplano is composed entirely of detached material.

Calculations that balance cross sectional areas provide another means of assessing the significance of a minimum total shortening of 210 km. I compare initial cross sectional areas of an undeformed sedimentary sequence or of the entire crust with the present-day deformed area in order to assess the contribution due to shortening.

Several assumptions are basic to any calculations that balance cross sectional areas, and the results are strongly dependent on even small variations in those assumptions. The most general of these is that the cross sectional area has not changed during deformation. In the case of calculations that balance crustal cross sectional areas, this assumption means specifically that none of the lower crust has been subducted into the asthenosphere as a result of crustal shortening, and that none of the crust has experienced strike-slip deformation or lateral flow out of the plane of the cross sections. Tectonic erosion at the trench is ignored as a first approximation. Additional assumptions specific to each of the two following calculations are discussed below.

Crustal cross sections at a scale of 1:1,000,000 were constructed across the northern and southern parts of the mountain belt in the mapped

area, in the same locations as the regional cross sections (Figure 2.2). The present day crustal structure in the central Andes is defined by gravity and seismic data (Figure 6.3). Normal crustal thicknesses of 30 to 35 kilometers in the foreland east of the Subandean Zone and along the Pacific coast are inferred from nearby seismic refraction studies (Aldrich et al., 1958; Lomnitz, 1962). Beneath the Bolivian Altiplano and parts of the Cordilleras Oriental and Occidental, however, the Moho has not been well-imaged in refraction studies due to abnormally high attenuation, but a combination of gravity, refraction, and surface wave data indicates that the crust is thickened to as much as 60-70 km. Refraction studies indicate poorly-constrained depths of 46 to 60 km along various profiles crossing northern Chile, southern Peru and southern Bolivia (Aldrich et al., 1958; Lomnitz, 1962;). Surface wave data (James, 1971) define similar crustal thicknesses. In addition, a negative Bouguer gravity anomaly of -400 mgal centered over the Bolivian Altiplano indicates that the crust is thickest there and that this thickness could be as much as 70 km. The crust thins along strike, returning to normal crustal thicknesses north and south of the Altiplano. The contour map of crustal thickness of James (1971) as reproduced in Wilson (1985) was used to define the base of the crust along the two profiles. Thickening to 70 kilometers for a 150 kilometer width below the Altiplano and Cordillera Occidental is assumed, with crustal thickness thinning to 35 kilometers at the coast. At the thrust front, the depth to the Moho is allowed to vary between 35 and 45 kilometers because crustal thickness is not defined more precisely than "normal crustal thickness".

Theoretical estimates of the amount of shortening involving the entire crust that would be required to build this thickened crust vary, reflecting

the uncertainty in the present-day crustal structure at the thrust front. For the crustal structure assumed in this study and the range of initial crustal thicknesses discussed above, shortening of as little as 215 kilometers up to as much as 446 kilometers, for initial crustal thicknesses of 45 and 35 kilometers, respectively, would account for the entire present-day crustal thickness. For the average initial crustal thickness of 40 kilometers, shortening by 316 kilometers is calculated. This value is in agreement with that calculated by Lyon-Caen et al. (1985) and Isacks (1988), who found that between 300 and 350 kilometers of shortening would be required to build the thickened crust.

All of these calculations assume that the average shortening of the basement is the same as that of the sediments. If we considered just the foreland portions of mountain belts, this assumption would not be justified: basement is observed to be undeformed for great lengths below foreland fold and thrust belts. On the other hand, over the entire width of a mountain belt, shortening of the basement may be great enough in the interior of the mountain belt to justify this assumption. Basement involvement in this case will be discussed in more detail below.

The importance of the minimum total shortening, 210 kilometers, with respect to the above numbers can be assessed from the results of balanced area calculations. The first set of calculations (Table 1) considers the entire width of the mountain belt, and assumes that the present-day crustal thickness can be attributed to shortening of the basement and sedimentary cover by the same amount. An excess area is determined by subtracting from the observed area a minimum cross sectional area of crust assumed to have been present prior to deformation. This area is equal to crustal thickness (35, 40, or 45 kilometers) multiplied by the

present width of the mountain belt, 720 kilometers. The excess area, if undeformed, would have a length equal to 215, 316, and 446 kilometers for crust of 45-, 40-, or 35-kilometer thickness (Figure 6.4). Comparison of this excess area with that corresponding to shortening of 210 kilometers indicates how significant this minimum amount of shortening has been in the formation of the thickened crust. The results depend strongly on the initial crustal thickness assumed: shortening of crust that was initially 35 kilometers thick accounts for only 47% of the excess area, while that percentage increases to 98% for crust initially 45 kilometers thick (Figure 6.4; Table 1). For the average initial value of crustal thickness of 40 kilometers, 210 kilometers of shortening accounts for 67% of the excess area. Even though the observed shortening is a minimum, it is at least two-thirds of the shortening required to produce the crustal cross sectional area observed today, if crust that was initially 40 kilometers thick was shortened.

A more general calculation does not assume that basement of constant thickness extends across the entire present-day width of the mountain belt. If the entire cross sectional area is composed of crustal material, then this assumption allows the basement and sedimentary cover to deform independently and shorten by different amounts. In this case, shortening of 210 kilometers yields a restored length of 580 kilometers that implies, for initial crustal thicknesses of 35, 40, and 45 kilometers, cross sectional areas that are 50, 56, or 62% of the total crustal cross sectional area, respectively (Figure 6.5). These estimates are poorly-constrained because the true restored length cannot be determined; the restored length used is assumed to be equal to the restored length of the sedimentary cover, which is clearly an underestimate if basement extends across the

range as indicated by field and well data (Mégard, 1987; Cobbing, 1985; Thorpe, 1984). These results show the sensitivity of these calculations to the initial assumptions made: we do not have enough information to determine the role of the basement, and therefore we must assume either that basement and sedimentary cover are shortened by the same amount or that there is less basement present than indicated by surface observations.

The second set of calculations assesses the contribution to crustal thickness due to shortening of just the sedimentary cover over only part of the width of the Bolivian Andes. A thickened, deformed wedge beneath the Cordillera Oriental and Subandean Zone only is considered to be the result of shortening of the observed sedimentary sequence. Two important assumptions must be made in these calculations.

First, the deformed cross sectional area is dependent on the thickness and extent of the continental basement beneath the mountain belt. Neither of these quantities in the Bolivian Andes is well-defined by independent data. From its exposure 200 kilometers east of the thrust front, the Brazilian shield dips approximately 1.2° to the west, as imaged by seismic reflection data up to thirty kilometers away from the thrust front (Yacimientos Petrolíferos Fiscales Bolivianos (YPFB) seismic reflection profile interpretation). Analysis of Bouguer gravity anomalies indicates that the Bolivian Andes are regionally supported by the underthrust Brazilian shield towards the west for a distance of at least 150 and possibly 200 kilometers (Lyon-Caen et al., 1985). The lack of exposed basement within the mapped area, or along strike from it for several hundred kilometers suggests that basement may remain uninvolved beneath the entire width of the Cordillera Oriental and Subandean Zone. In other fold and thrust belts, undeformed basement extending for approximately

200 kilometers below the deformed sedimentary cover is documented by seismic, gravity, and magnetic data. For example, in the Canadian Rockies, seismic, gravity, magnetic, electrical conductivity, and structural data indicate that continental basement at present 40 kilometers thick dips gently westward beneath that mountain belt for 200 km (Price, 1981). For the purposes of these calculations, and in the absence of any constraints on the position or extent of basement involvement within the Cordillera Oriental and Subandean Zone, the assumption is made that undeformed basement extends for 370 kilometers beneath the Cordillera Oriental and Subandean Zone. The possibility of basement involvement is discussed in more detail later.

The thickness of this basement is assumed to vary between 25 and 35 km, based on its 10 kilometer depth at the thrust front, as defined by well and refraction data from the foreland at the latitude of Santa Cruz, and the permissible range of normal crustal thicknesses of 35 to 45 kilometers. The trapezoidally-shaped area that comprises the deformed cross sectional area beneath the Cordillera Oriental and Subandean Zone is a maximum if the basement is 25 kilometers thick, and a minimum if it is 35 kilometers thick.

The second assumption that is required for these balanced area calculations relates to the undeformed cross sectional area, which is dependent on the thickness of sediments prior to deformation. An average sedimentary thickness ranging from 8 to 10 kilometers is assumed. These thicknesses correspond to trapezoidal geometries for which the depth at the eastern end may vary from 0 to 4 kilometers. At the western end, the minimum thickness is equal to 12 kilometers, the observed thickness of the sedimentary sequence, whose base is never exposed, and the maximum

thickness is 20 kilometers, a reasonable upper bound for this sedimentary sequence (Lyon-Caen et al., 1985; and this study). The length of the initial cross sectional area is determined by the observed minimum shortening.

The results of this set of balanced area calculations also show that crustal shortening accounts for a majority of the observed crustal thickness (Figure 6.6; Table 2). Shortening of a sedimentary package initially an average of 8 kilometers thick, overlying a basement that is 25 or 35 kilometers accounts for 51 or 70% of the observed thickening of the sedimentary wedge, respectively (Table 2). Correspondingly, 64 or 87% of the deformed area is accounted for by shortening of a sequence initially an average of 10 kilometers thick. For basement that is assumed to be 30 kilometers thick, 59 to 74% of the observed deformed area is accounted for by shortening of a sedimentary sequence initially an average of 8 to 10 kilometers thick. These calculations show that, at a minimum, from 51 to 87% of the crustal thickening in the Cordillera Oriental and Subandean Zone can be accounted for by shortening of 210 kilometers.

Whether the cross sectional area of the entire mountain belt or just that area plausibly related to deformation of the sedimentary cover is considered, the minimum amount of shortening of 210 kilometers accounts for a substantial portion of the crustal thickening, suggesting that crustal shortening has played an important role in the formation of the Bolivian Andes.

Plausible Additional Amounts of Shortening

Less conservative interpretations of the cross sections increase the amount of shortening calculated and therefore strengthen the argument that crustal shortening is probably the primary mechanism of orogeny in the Bolivian Andes. Substantial increases in the amount of shortening

depicted in balanced cross sections can be made if the underlying assumptions are varied (e.g. Roeder, 1988). Two of the assumptions in this study that bias the minimum total estimate of shortening toward a smaller value are reconsidered in order to estimate plausible amounts of additional shortening.

First, the underestimation due to large cutoff angles is assessed. As discussed in Chapter 2, theoretical considerations suggest that cross sections drawn with small cutoff angles might be more realistic representations of the deformation in the Bolivian Andes. It is not possible to draw such cross sections over much of the width of the mountain belt without making unconstrained assumptions about the deep fault structure. However, along the East Vallegrande cross section near the thrust front, an alternative cross section can be drawn because the surface of detachment is decoupled from and therefore independent of the deeper structure (Figure 6.2). Shortening calculated from the cross section drawn with small cutoff angles is 55% larger than in the original cross section. If we assume that the shortening along all of the cross sections is underestimated by the same amount, the new estimate for the minimum total shortening would be 325 km for the Oruro-Santa Cruz profile.

Second, an estimate of the contribution to total crustal shortening from slip along deeper, buried thrust faults can be made. This calculation is determined from calculations that balance areas of the regional cross sections (Figure 6.7). The area below the basal surfaces of detachment of the balanced cross sections and above projections of undeformed basement is attributed to shortening of sedimentary cover. As above, the calculations are made for thicknesses of basement varying between 25 and 35 kilometers, and the result is combined with the minimum estimate of

210 kilometers of shortening determined from the thrust sheets above this area. Shortening of 805 kilometers and of 540 kilometers is calculated for 25- and 35-kilometer-thick basement, respectively. For the average initial basement thickness of 30 kilometers, 673 kilometers of shortening would account for the entire area above undeformed basement. While the magnitude of these amounts of shortening suggests that they may be too large, the total crustal area implied by these amounts of shortening approximates that observed in all three cases (Table 1; Figure 6.5). It is possible that the amount of shortening is overestimated by these calculations because the assumption of undeformed basement is not valid, and this possibility will be discussed below. These estimates of shortening, however, provide upper bounds on the amount of shortening possible in the Bolivian Andes. The assumption that all of the area is filled by sedimentary cover yields the maximum amount of shortening of the sedimentary cover possible. Alternatively, if basement-involved thrusts occupy this area, the minimum amount of shortening is exactly that calculated from the balanced cross sections previously, or 210 kilometers.

The contribution of these increased estimates of crustal shortening to the present-day crustal thickness is proportionately larger, as detailed in Tables 1 and 2. For example, shortening of a 40-kilometer-thick crust by 325 kilometers would account for all of the excess area observed today across the entire mountain belt, or shortening of a sedimentary sequence 10 kilometers thick, on the average, by 325 kilometers would account for 88% of the deformed area presumably comprised of thrust sheets of sedimentary cover. The importance of crustal shortening as a mechanism of orogeny in the Bolivian Andes, substantial at a minimum, only increases with more realistic estimates of its magnitude. Percentages in excess of

100 indicate, if the estimated shortening is correct, loss of lithospheric material to the asthenosphere, possibly via tectonic erosion, or strike-slip motion out of the plane of the section. These increased estimates indicate that crustal shortening could have built virtually the whole mountain range.

Deformation in the Altiplano

Consideration of the style of deformation in the Altiplano provides an independent indication that crustal shortening is probably more important than indicated by the minimum amount of shortening that has occurred in the Cordillera Oriental and Subandean Zone. The lack of exposure within the Altiplano, however, means that much of the evidence is inferential. Two main lines of evidence indicate that thin-skinned deformation extends into the Altiplano. First, where Paleozoic and younger rocks are exposed, outcrops within the Altiplano are made up of folded and thrust-faulted strata, and structures at the boundary between the Cordillera Oriental and the Altiplano are observed to plunge steeply beneath the upper Tertiary and Quaternary sediments that cover much of the Altiplano. Furthermore, seismic reflection profiles show that at approximately 18°S latitude, the eastern sixty kilometers of the Altiplano is deformed in the same thin-skinned style as is observed in the Cordillera Oriental (M. Cirbian, pers. comm., 1986). The timing of this deformation is of the same age as that to the east, as indicated by involvement of Oligocene sedimentary rocks in the deformation (M. Cirbian, pers. comm. 1986). In the northern Altiplano, seismic reflection profiles document the existence of a west-verging thrust belt across the width of the tectonic province (Roeder, 1988). If the high plateau of the Altiplano, beneath which the maximum crustal thickening is observed, has also been formed by shortening of the crust, then almost all of the Bolivian Andes have been formed by this mechanism.

Balanced area calculations--Oruro-Punata-Chapare profile

The same type of calculations that balance cross sectional areas, carried out for the Oruro-Punata-Chapare profile, indicate the extent of the underestimation that is possible due to the assumptions made in drawing the balanced cross sections. Composite cross sections along the Oruro-Punata-Chapare profile indicate a minimum of approximately 100 kilometers of shortening (Table 3). In the absence of other information, this estimate might be regarded as reflecting a real difference in the amount of shortening and/or the percent shortening of the mountain belt north and south of the bend, as is indicated by a decrease in crustal thickness to the north. There are several indications, however, that the estimate of 100 kilometers is a gross underestimate of the amount of shortening that has occurred. The broad area of high structural elevation in the Punata region constitutes the clearest example of buried overthrusting at depth, and suggests that this amount of shortening is artificially low. In addition, the calculation of shortening is strongly biased towards underestimation because the cross sections across the Elbow region cannot be rigorously balanced.

Most importantly, the results of the calculations that balance cross sectional areas show that amounts of shortening comparable to those observed along the Oruro-Santa Cruz profile are possible. The crustal scale cross section (Figure 6.8) was constructed in the same way as that of the Oruro-Santa Cruz profile. The theoretical amounts of shortening of crust of various thicknesses, required to account for the cross sectional area across the width of the Andes are 441, 314, and 216 kilometers for crust initially of 35-, 40-, and 45-kilometer thickness. These estimates of shortening are virtually identical to those calculated for the Oruro-Santa

Cruz profile. Large estimates of shortening calculated from the regional cross section, assuming that the basement is undeformed and that all area above it is comprised of thrust sheets that sole into Ordovician shale, account for all but 10% of the observed cross sectional area (Table 4).

The minimum total estimate of 100 kilometers accounts for only small portions of the observed deformational area (Table 4). If the basement and sedimentary cover are shortened by the same amount over the width of the mountain belt, deformation of crust of various thicknesses accounts for a range between 23 to 46% of the present-day crustal cross sectional area. If the basement and sedimentary cover are allowed to shorten independently, the shortening of crust 35 to 45 kilometers thick accounts for 35 to 44% of the deformed area. Shortening of just the sedimentary cover beneath the Cordillera Oriental and Subandean Zone accounts for only 10 to 17% of the deformed area (Table 5). An increased estimate of shortening of 155 kilometers, that incorporates the effect of smaller cutoff angles, increases the above ranges to 35 to 72% in the first case, to 40 to 51% in the second case, and to 16 to 26% in the third case.

The underestimation of shortening, derived from upper thrust sheets only, is only corrected when the shortening due to faults at depth is included. The estimates of shortening from area-balancing of the regional cross sections account for from 69 to 86% of the deformed area possibly due to shortening of the sedimentary cover. If the entire crust is shortened, but the basement and sedimentary cover shorten independently and by different amounts, these estimates account for 90% of the present-day crustal thickness for all values of initial crustal thickness. If basement and sedimentary cover shorten by the same amount, these

estimates are clearly too large, as they would account for 156 to 228% of the excess crustal area.

Other sources of cross sectional area, such as magmatism or basement involvement within the Cordillera Oriental, must also be considered.

Basement involvement

The implicit assumption that basement is undeformed beneath the Cordillera Oriental and Subandean Zone, which has been the basis of much of the above discussion, is the result of a lack of information on the position and extent of basement involvement. Various lines of evidence from published maps as well as the above calculations, indicate that shortened basement could contribute substantially to the thickened crust. Continental basement is postulated to underlie the entire width of the Andes, including the Cordillera Occidental and the Altiplano, based on surface exposures in southern Peru, isotopic signatures in volcanic rocks of the Cordillera Occidental (Thorpe et al., 1982), and well data in the Altiplano (Pitcher, 1984; Lehmann, 1978; Roeder, 1988). The probable extension of thin-skinned deformation into the Altiplano (J. Lowell, 1988, pers. comm.; Roeder, 1988), based on the exposure of folded and faulted Paleozoic rocks within the Altiplano and on seismic reflection lines, may imply, by its distance from the thrust front, basement-involved thrusting. Finally, the large magnitude of shortening calculated from area balancing of the regional cross sections suggests that basement-involved thrusts may instead occupy some of the area between the projection of undeformed basement and the base of my cross sections, thereby reducing the amount of shortening in the sedimentary cover. Possible indications of basement involvement include a gravity high within the Subandean Zone, or any of the regions of high structural relief within the Cordillera Oriental, e.g. the

Punata region. This area comprises either deformed sedimentary cover, at one extreme, or deformed basement, at the other extreme; the magnitude of this area implies that the possibility exists for greater basement involvement in this fold and thrust belt in general, and specifically in the external parts of the belt, than observed in other fold and thrust belts. No data that positively supports basement involvement in the fold and thrust belt, however, exists.

Magmatic addition

The formation of mountain belts above subduction zones is viewed by some workers (Gill, 1981; Thorpe et al., 1982) as directly related to "orogenic" andesitic volcanism. Volcanic arcs are an almost ubiquitous feature above subducting plates. The andesitic volcanism that characterizes volcanic arcs is thought to represent mantle-derived additions to the crust, based on observed geochemical and isotopic patterns and the unique association of volcanic arcs with steeply-dipping subduction zones. Andesitic volcanism, then, is "orogenic" because it is thought to be responsible for the growth of the continental crust through underplating and other magmatic additions to the crust (Weaver and Tarney, 1982; Brown, 1982). In the central Andes, the thickened crust is often attributed to these additions. Cobbing (1985) advocates the extreme view that magmatic processes alone have built the thickened crust of the central Andes. Others suggest that the addition of large volumes of mantle-derived magmas to the crust may secondarily cause crustal shortening (Hamilton, 1988; Smith, 1981).

The amount of crustal shortening documented throughout the central Andes indicates that neither of the above views is appropriate for the central Andes. Minimum estimates of 210 kilometers of shortening from

balanced cross sections in this study show that addition of mantle-derived magmas can contribute at most, only one-third of the excess cross sectional area observed in the Bolivian Andes, and that probably their contribution is substantially less. A similar conclusion is likely in Peru and Argentina, where thin-skinned deformation involving on the order of 100 kilometers of shortening is also documented (Megard, 1984; Pardo, 1982; Allmendinger et al., 1983). The size of the volumetric contribution of shortened crust rules out the possibility that magmatic addition alone could have formed the thickened crust.

The importance of crustal components in the intrusive and extrusive rocks exposed today, as indicated by isotopic and geochemical signatures, provides additional evidence that crustal shortening has played the dominant role in orogeny in the central Andes. Although a mantle component is apparently a requirement for the occurrence of any andesitic volcanism above a subduction zone (Barazangi and Isacks, 1976), isotopic signatures indicate that orogenic andesites are rarely primary melts of the mantle wedge only (Gill, 1981), and the petrogenesis of the magmas of volcanic arcs remains controversial. Crustal contamination, magma mixing, crustal fusion, and fractional crystallization may occur together or separately during the ascent of melt formed from fusion of either or both the mantle and subducted slab. Isotopic signatures provide indications of the combinations of the above processes that have been operative, but it is difficult to determine the relative importance of the different proposed processes (Weaver and Tarney, 1982).

Isotopic and geochemical evidence from the central Andes verifies the importance of crustal components, and documents an increase in their proportion since the mid-Tertiary. Evidence for crustal contamination

includes shoshonitic compositions, enrichment of incompatible LIL trace elements, silica, and K, high initial $^{87}Sr/^{86}Sr$ ratios (.705-.710), low $^{143}Nd/^{144}Nd$ ratios (less than .5127), high $d^{18}O$ values (6.9 to 14%), and the large range of and generally high values of lead isotope ratios ($^{206}Pb/^{204}Pb$=17.35 to 19.01, $^{207}Pb/^{204}Pb$=15.57 to 15.69, $^{208}Pb/^{204}Pb$=38.47 to 39.14) (Harmon and Hoefs, 1984; Thorpe, 1982; Barreiro, 1984). Thus, throughout the history of magmatism in the central Andes, there has been a crustal contribution to the volcanic rocks exposed. Furthermore, a major change in source type and/or petrogenetic processes in the early Miocene (Thorpe, 1984; Hawkesworth et al., 1982) coincides with the onset of crustal shortening. Thorpe (1984) indicated the increased importance of assimilation associated with fractional crystallization since the Pliocene and possibly since the late Cretaceous. Hawkesworth et al. (1982) interpreted a suite of isotopic ratios and trace element enrichment patterns as indicating probable crustal melting, although the data could also be explained by mixing crust and mantle magmas. The coincidence of at least increased crustal contamination, if not a change to crustal source volumes, with the initiation of Andean deformation in the mid-Tertiary suggests the following two conclusions. First, crustal shortening, in creating the thickened crust, had a major effect on the source volumes for the active volcanic arc. Second, the older, less contaminated magmas present could not have contributed to the crustal thickening because their emplacement predates the major episode of crustal shortening

In summary, the importance of crustal shortening in the formation of the central Andes is not only indicated by the volumetric proportions indicated by the amount of shortening, but also is reflected in the extent of

involvement of crustal components in magmatism, and their increase in time.

Table 6.1. Oruro-Santa Cruz Profile---Balancing of Crustal Cross Sectional Areas

x_{crust}, crustal thickness	35	40	45
Present-day cross sectional area, A_{total} (km^2)	40801	41426	42051
720 x x_{crust} (km^2)	25200	28800	32400
$A_{excess} = A_{total} - 720 \times x_{crust}$ (km^2)	15601	12626	9651
theoretical shortening, s_{theor} (km)	446	316	215
Percent of A_{excess} (s_{calc} = 210 km)	47	67	98
Percent of A_{total} (s_{calc} = 210 km)	50	56	62
Percent of A_{excess} (s_{calc} = 325 km)	73	103	152
Percent of A_{total} (s_{calc} = 325 km)	60	67	74
Percent of A_{excess} (s_{calc} = 805, 673, 540 km)*	181	213	252
Percent of A_{total} (s_{calc} = 805, 673, 540 km)	101	101	97
* Area-Balance calculations for regional cross section (Figure 6.7)			
Area of buried deformation	4484	3559	2634
restored length of area of buried deformation (7 km sedimentary thickness)	641	509	376
shortening calculated from balanced cross sections	194	194	194
total shortening	805	673	540

Table 6.2. Oruro-Santa Cruz Profile, Cordillera Oriental and Subandean Zone
Balancing of cross sectional areas

x_{crust}, crustal thickness (km)	35		40		45	
Present-day cross sectional area, A_{total} (km^2)	9100		7875		6650	
Initial sedimentary thickness, x_{sed} (km)	8	10	8	10	8	10
Percent of A_{total} (s_{calc} = 210 km)	51	64	59	74	70	87
Percent of A_{total} (s_{calc} = 325 km)	61	76	71	88	84	105
theoretical shortening	768	540	614	418	461	295

Table 6.3 Estimates of minimum total shortening
Oruro-Punata-Chapare Transects

Cross section	percent shortening	s(km)	s(km)	s(km)	s(km)	s(km)
Uncía	41%	72	72	72	72	
Cochabamba	28%					38
West Aiquile	20%	8	8	8	8	31
East Aiquile	21%					
North Punata	14%	10				
Central or South Punata (western half)	16%		11	11	11	
South Punata or Totora (eastern half)	12%			8	8	
Central Totora	14%		9			
South Totora	27%			15		
North Totora	24%	14				
South Santa Cruz	26%				28	
East Aiquile	24%					9
E. Aiquile & W. Vallegrande	50%					89
East Vallegrande	20%					12
Minimum Total Shortening		104	100	114	127	179

s = amount of shortening calculated for a given length of the transect

Table 6.4. Oruro-Punata-Chapare Profile
Balancing of Crustal Cross Sectional Areas

x_{crust}, crustal thickness	35	40	45
Present-day cross sectional area, A_{total} (km^2)	37768	38093	38418
638 x x_{crust} (km^2) (present-day width = 638km)	22330	25520	28710
$A_{excess} = A_{total} - 638 \times x_{crust}$ (km^2)	15438	12573	9708
theoretical shortening, s_{theor} (km)	441	314	216
Percent of A_{excess} (s_{calc} = 100 km)	23	32	46
Percent of A_{total} (s_{calc} = 100 km)	35	40	44
Percent of A_{excess} (s_{calc} = 690, 591, 491 km)*	156	188	228
Percent of A_{total} (s_{calc} = 690, 591, 491 km)	90	91	90
* Area-Balance calculations for regional cross section			
Area of buried deformation	4536	3841	3146
restored length of area of buried deformation (7 km sedimentary thickness)	648	549	449
shortening calculated from balanced cross sections	239	239	239
total shortening	690	591	491

Table 6.5. Oruro-Punata-Chapare Profile, Cordillera Oriental and Subandean Zone
Balancing of cross sectional areas

xcrust, crustal thickness (km)	35		40		45	
Present-day cross sectional area, A_{total} (km^2)	8021		6961		5901	
Initial sedimentary thickness, xsed (km)	8	10	8	10	8	10
Percent of A_{total} (s_{calc} = 100 km)	10	13	12	14	14	17
Percent of A_{total} (s_{calc} = 690,591,491km)	69	86	68	85	67	83
theoretical shortening	725	524	592	418	460	312

Figure Captions

Figure 6.1. Two interpretations of the surface geology along the east Vallegrande cross section. The lower cross section is the one used in this study; 20% shortening is calculated. The upper cross section has been redrawn with small (<30°) hanging wall and footwall cutoff angles; the percent shortening is then 32%.

Figure 6.2. The minimum amount of shortening, 210 kilometers, yields a restored length of 580 kilometers. This length is shown superimposed on a 1:1 cross section across the central Andes. The minimum restored length extends into the tectonic province of the Cordillera Occidental.

Figure 6.3. Crustal thickness beneath the Andes along the Oruro-Santa Cruz profile. Crustal thicknesses of 35 and 40 kilometers at the thrust front are shown.

Figure 6.4. The percent of the excess deformed crustal cross sectional area accounted for by crustal shortening assuming different amounts of shortening and different crustal thicknesses is shown by the ruled areas superimposed on the excess area. These calculations assume that the basement and the sedimentary cover are shortened by the same amount. The deformed crustal cross section and its restoration to undeformed crust that is initially 35-, 40-, or 45-kilometers thick are shown at the top. Percentages in excess of 100 mean either that the estimate of shortening is too large or that some cross sectional area has been removed, i.e. by tectonic erosion.

Figure 6.5. The percent of the total deformed crustal cross sectional area accounted for by crustal shortening, assuming different amounts of shortening and different crustal thicknesses is shown by the ruled areas superimposed on the total area. These calculations assume that the basement and the sedimentary cover deform independently. Percentages in excess of 100 mean either that the estimate of shortening is too large or that some cross sectional area has been removed, i.e. by tectonic erosion.

Figure 6.6. The percent of the deformed cross sectional area within the Cordillera Oriental and Subandean Zone that is accounted for by shortening within the sedimentary cover only is shown by the ruled areas. Different amounts of shortening correspond to the minimum calculated from the cross sections and two estimates of plausible additional shortening. Percentages in excess of 100 mean either that

the estimate of shortening is too large or that some cross sectional area has been removed, i.e. by tectonic erosion.

Figure 6.7. An estimate of additional shortening may be calculated by area-balancing the area below the shallowest levels of decollement and the projection of undeformed basement from the foreland. All of the area above the projection of undeformed basement is assumed to comprise deformed thrust sheets of the sedimentary cover.

Figure 6.8. Crustal thickness along the Oruro-Punata-Chapare profile. Alternative crustal thicknesses at the thrust front are shown.

EAST VALLEGRANDE CROSS SECTION

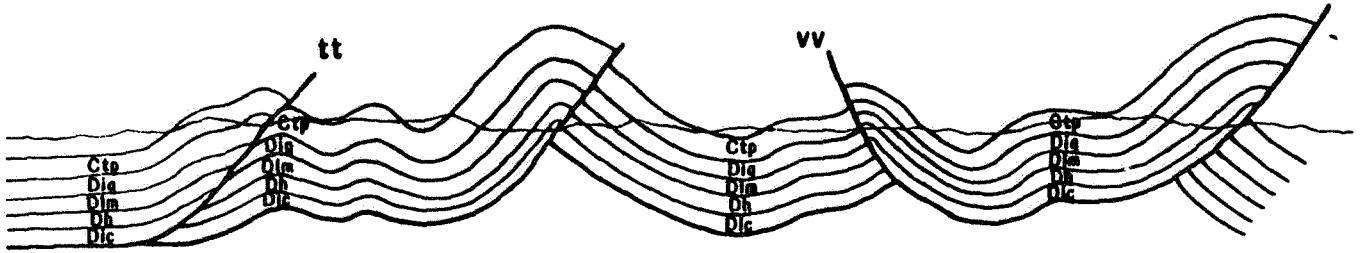

LARGE CUTOFF ANGLES
SHORTENING: 11 KM (20%)

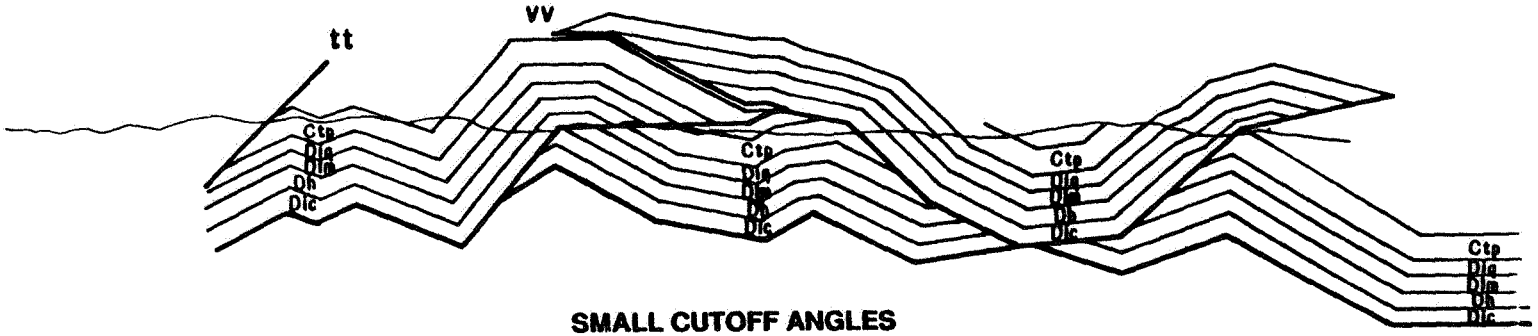

SMALL CUTOFF ANGLES
SHORTENING: 17 KM (32%)

Figure 6.1

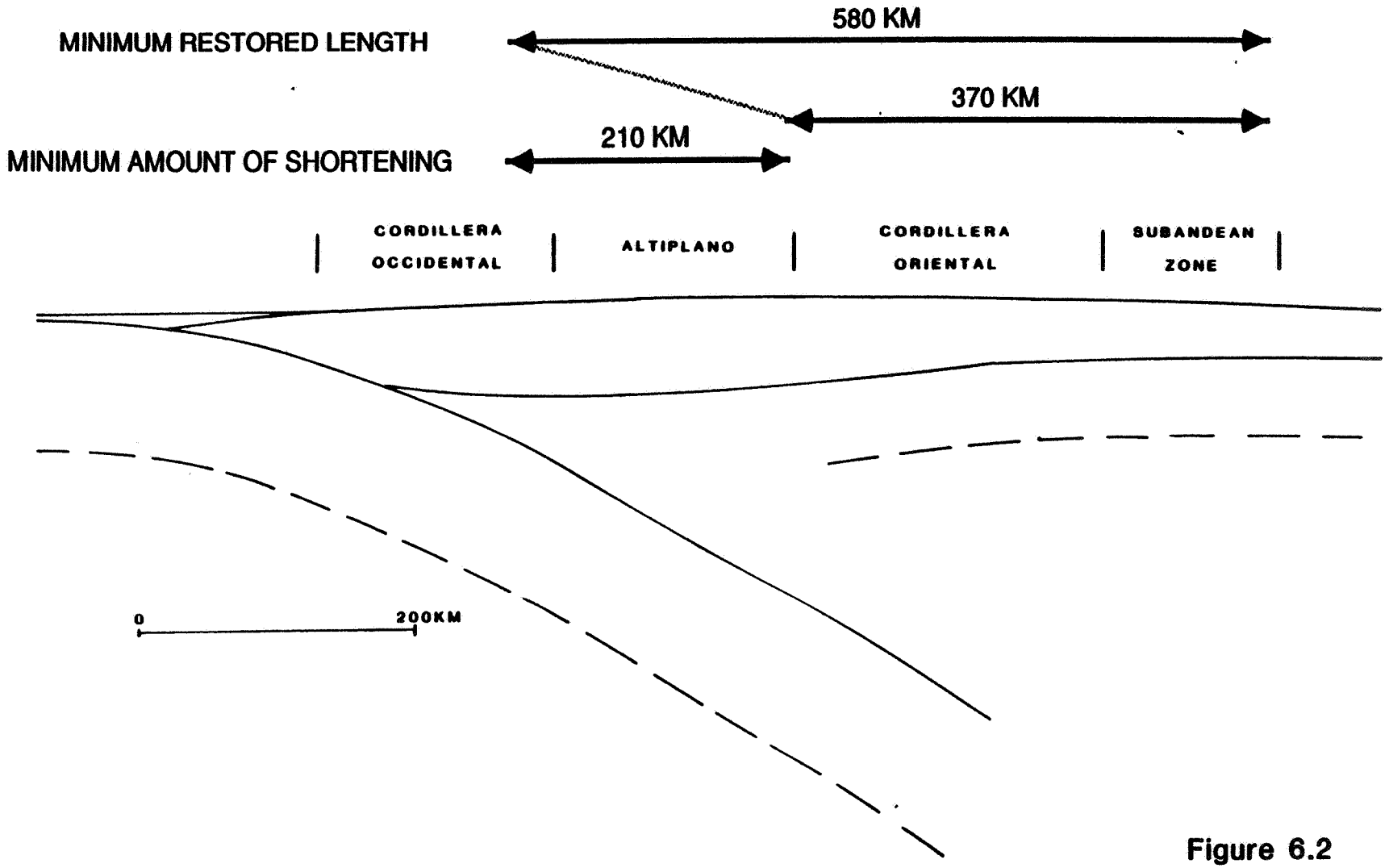
MINIMUM RESTORED LENGTH
580 KM
370 KM
210 KM
MINIMUM AMOUNT OF SHORTENING
CORDILLERA OCCIDENTAL
ALTIPLANO
CORDILLERA ORIENTAL
SUBANDEAN ZONE
0
200KM

Figure 6.2

CRUSTAL THICKNESS ALONG THE ORURO-SANTA CRUZ PROFILE

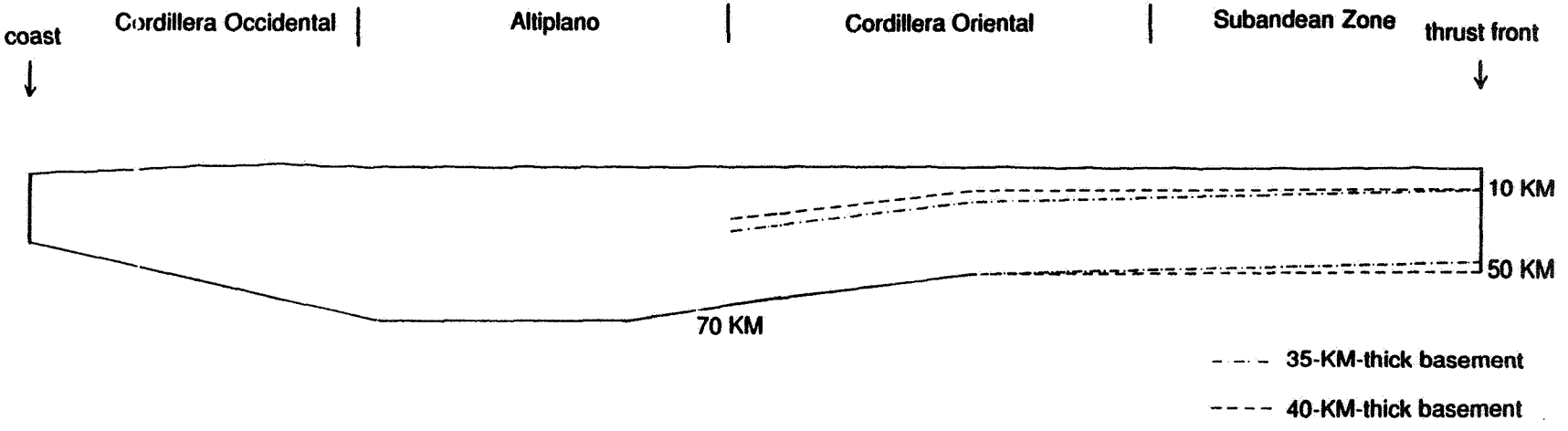

Figure 6.3

Comparison of actual and theoretical excess crustal cross sectional areas

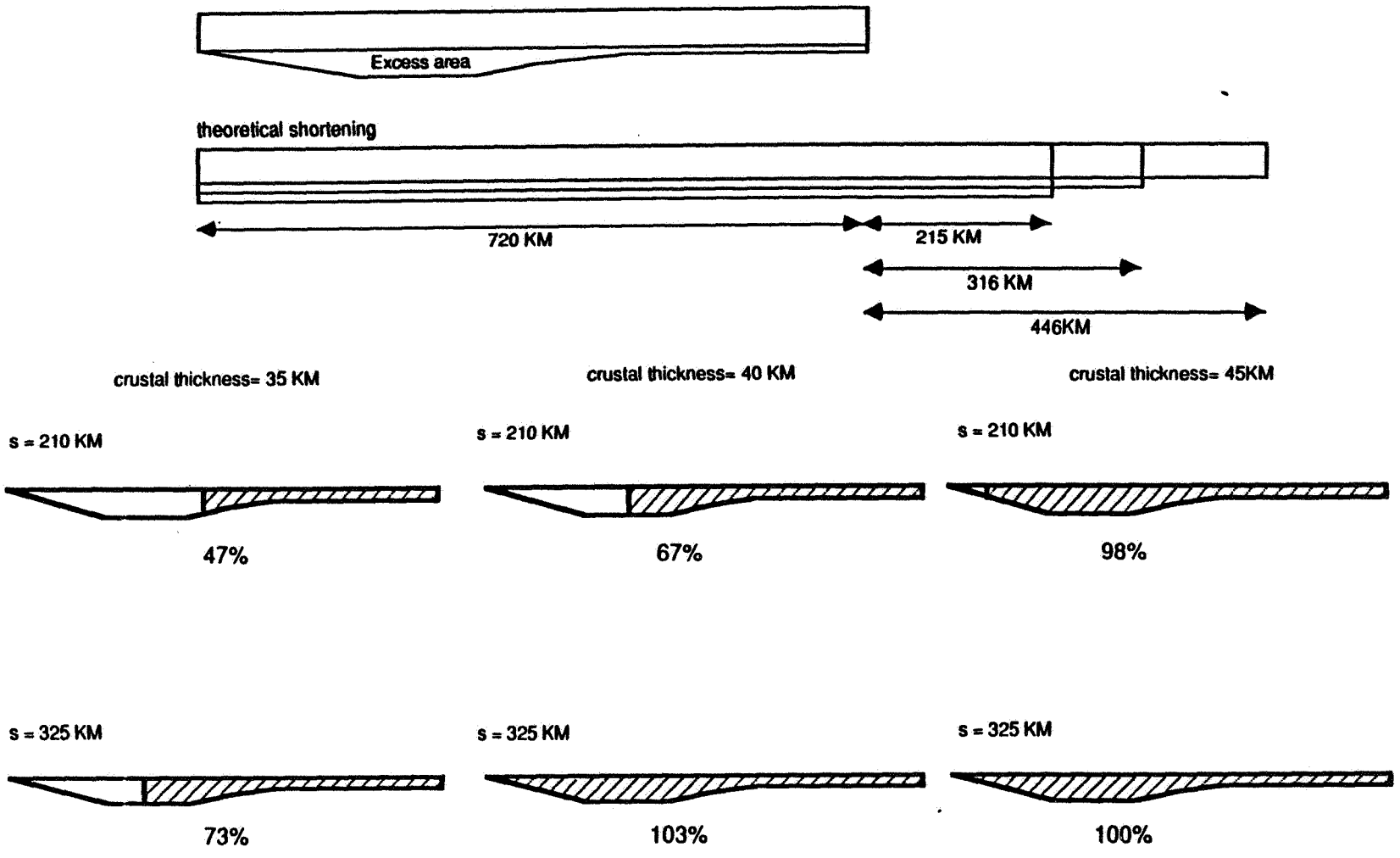

Figure 6.4

Comparison of actual and theoretical total crustal cross sectional areas

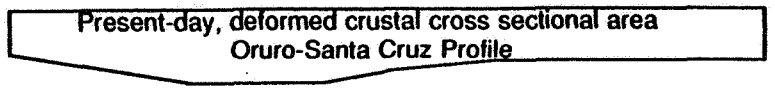

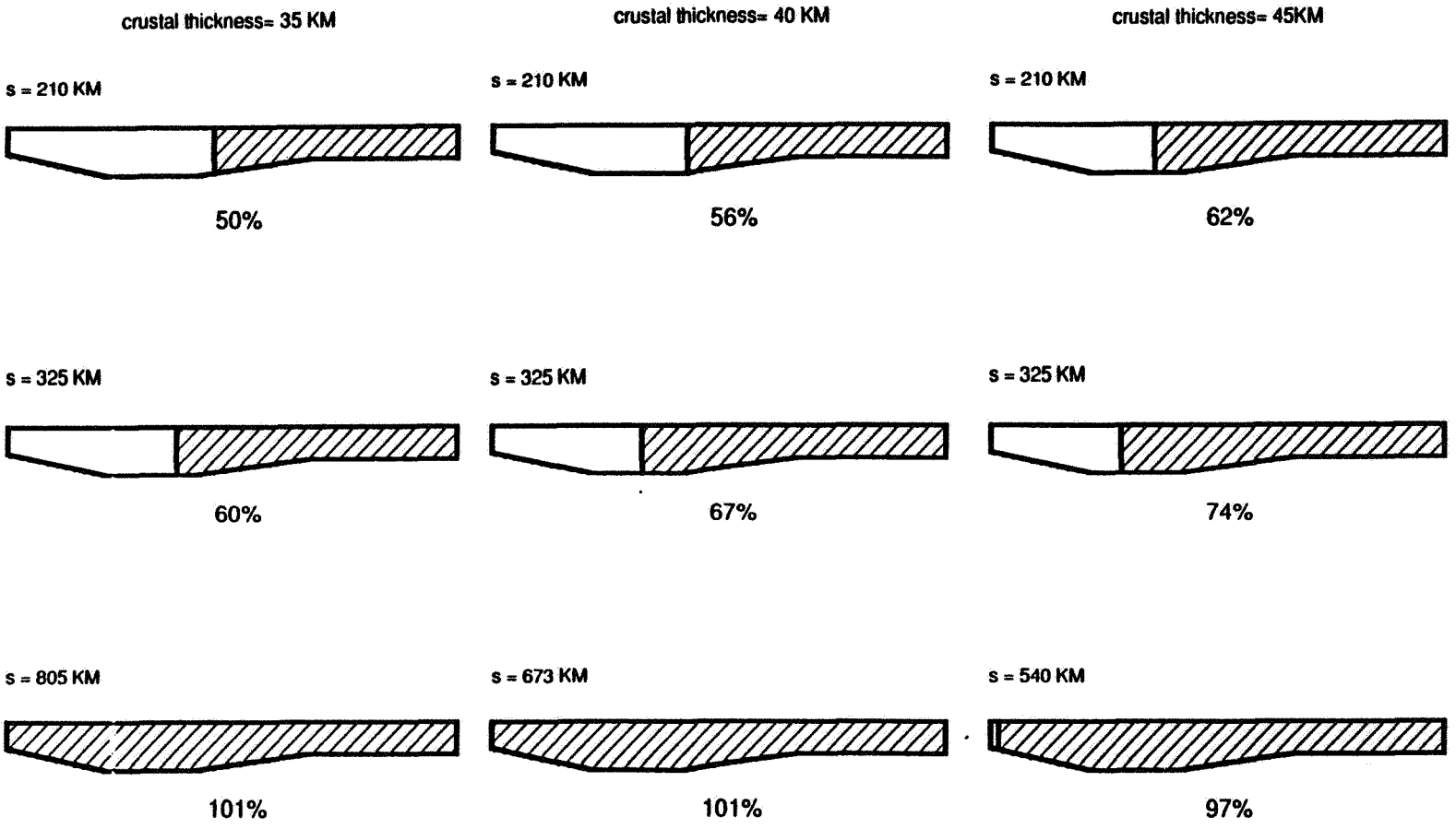

Figure 6.5

Comparison of actual and theoretical upper crustal cross sectional areas,
Cordillera Oriental and Subandean Zone

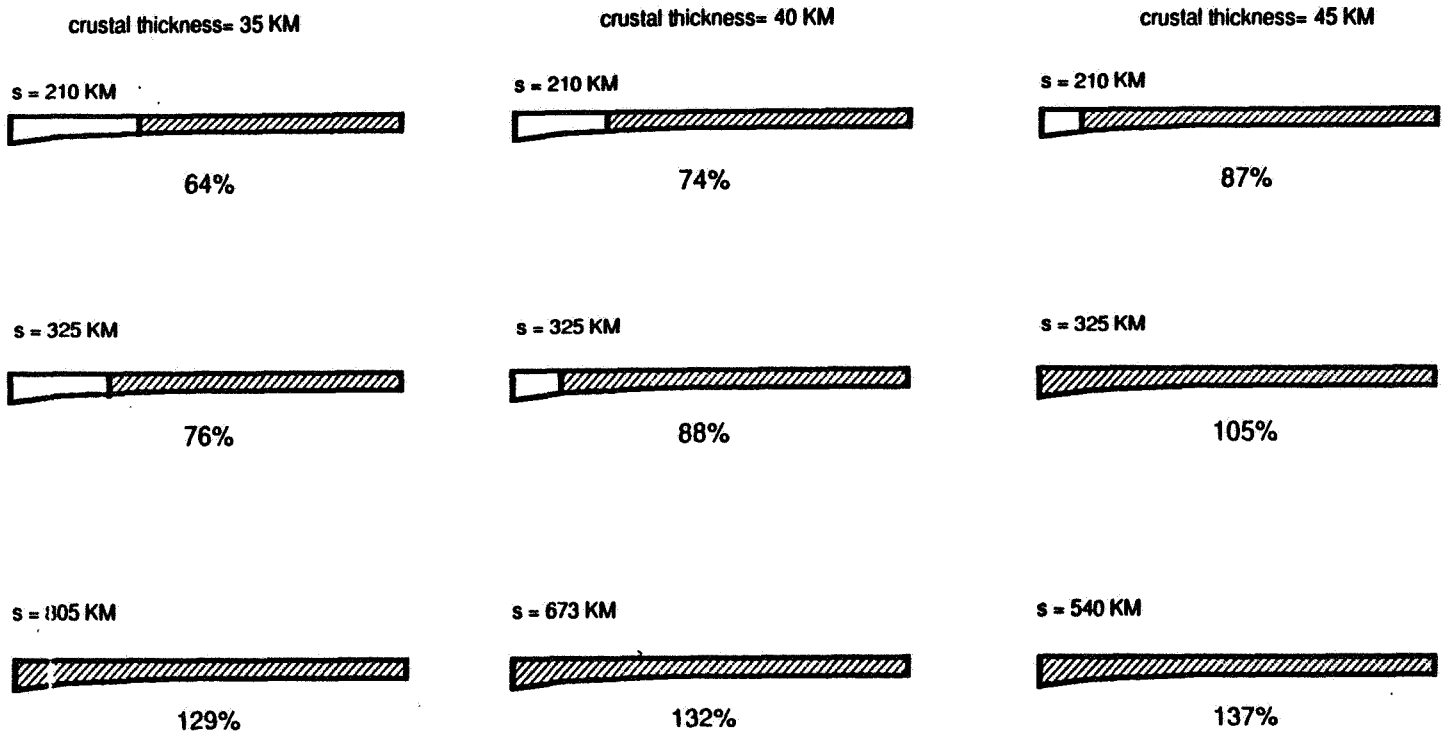

Figure 6.6

Oruro-Santa Cruz Profile

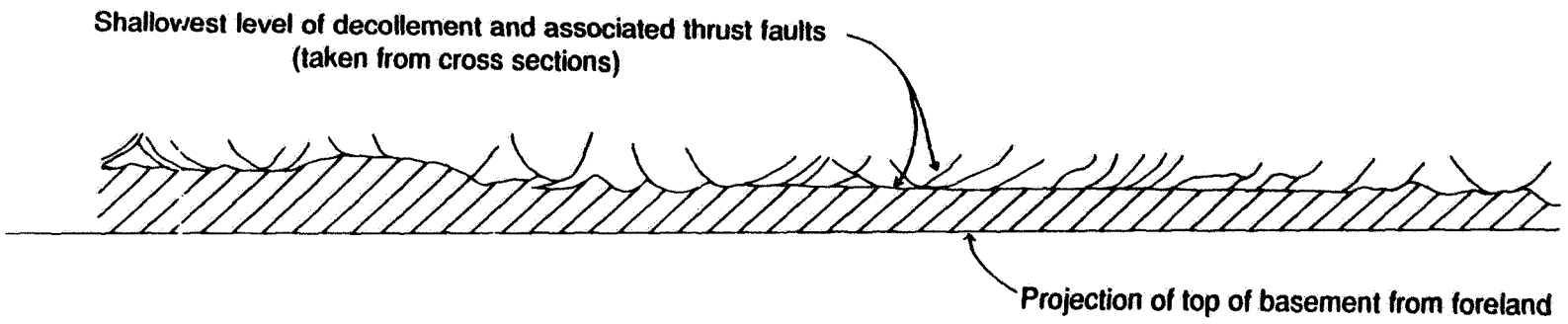

Area deformed by buried thrusting. Area-balancing of this area yields an estimate of additional shortening, assuming all of the concealed deformation involves the sedimentary cover.

Figure 6.7

CRUSTAL THICKNESS ALONG THE ORURO-PUNATA-CHAPARE PROFILE

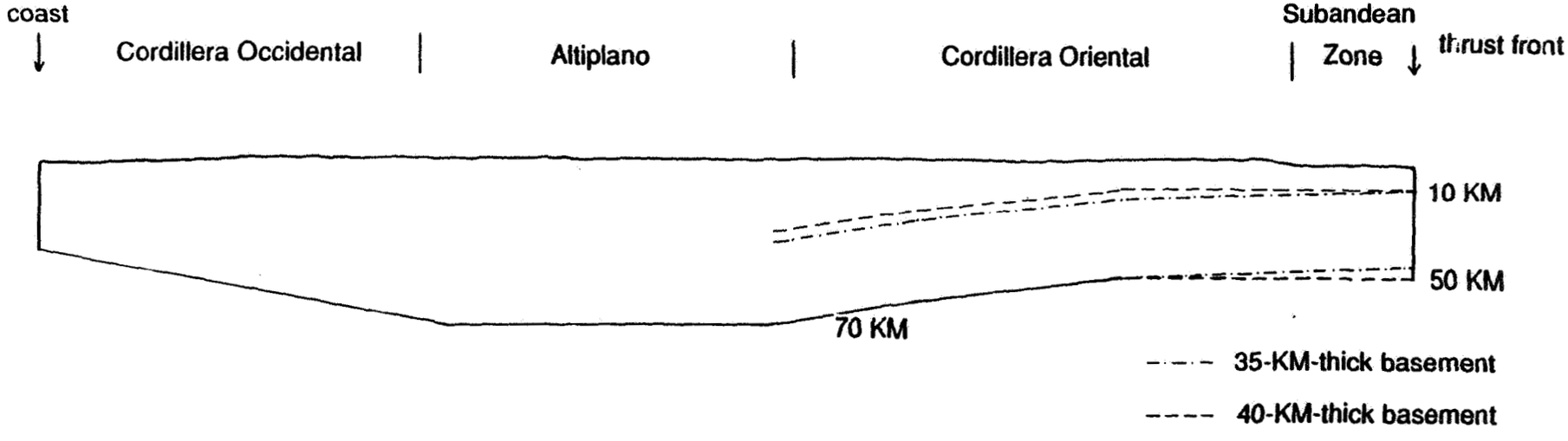

Figure 6.8

CHAPTER SEVEN

Back-arc fold and thrust belts along Andean and other plate margins

Introduction

The complexity and variety of responses of the continental lithosphere to plate interactions has impeded the definition of quantitative relations describing the behavior of the continental lithosphere. For example, orogenesis above subduction zones remains poorly understood, even though it is the focus of numerous qualitative generalizations about plate behavior. These generalizations are rarely tested. With the addition of the results of this study to the existing body of knowledge about the central Andes, however, three hypotheses regarding the formation of back-arc fold and thrust belts can be tested. Primarily on the basis of the quantification of the amount of shortening that has occurred in the Bolivian Andes, it is shown that orogeny involving significant shortening in a back-arc tectonic setting is not uniquely driven by either continental collision or magmatic intrusion, that significant shortening can occur within back-arc fold and thrust belts that display a sense of overthrusting antithetic to that of subduction, and that loss of the lower continental lithosphere into the asthenosphere is required.

Driving forces of the formation of back-arc fold and thrust belts

Recent thinking about orogenesis has emphasized the role of collision in mountain building. The recognition of accreted terrains along the North American margin (Jones et al., 1977; Monger et al., 1982; Davis et al., 1982; Coney et al., 1980), in conjunction with the effects of known continental collisions, has led some workers (Nur and Ben-Avraham, 1983;

Ben-Avraham and Nur, 1987) to question whether orogeny could occur without collision, namely in an Andean margin in response to subduction of oceanic lithosphere only. Specifically, some workers have attributed the approximately 200 kilometers of crustal shortening that has occurred along west-dipping thrust faults in the back-arc fold and thrust belt of the Canadian Cordillera entirely to the collision of exotic terrains, and have hypothesized that shortening of this magnitude in a back-arc setting is only possible in a collisional setting. The large minimum amount of shortening calculated in this study, however, definitively contradicts this generalization. A subduction regime along the western South American margin could have been established since at least 60 Ma (Pardo-Casas and Molnar, 1987) and possibly since 190 Ma (Zeil, 1979). Although there is evidence for a Paleozoic history of accretion of exotic terrains along the South American margin (Ramos et al., 1986), Mesozoic overlap sequences show that accretion was completed by the end of the Devonian Period and has not been important in the central Andes subsequently (Dalziel, 1985; Ramos et al., 1986). During the period of orogenesis involving crustal shortening in the Bolivian Andes, then, an Andean margin existed seaward of the back-arc setting. Since there is no temporal overlap of accretionary events with orogenesis in the central Andes, accretion of exotic terrains could not have caused the development of the thin-skinned thrust fault system. The subduction of oceanic lithosphere alone must be a sufficient cause of back-arc antithetic thrust faulting.

An alternative view of the formation of fold and thrust belts proposes that the uplift and lateral spreading of batholiths in the interior of a mountain belt may drive shortening (Hamilton, 1979, 1988; Smith, 1981). This interpretation requires that the volume of the batholiths be large

enough to displace a volume of crust equal to that shortened, and that intrusion and shortening be contemporaneous. Evidence from the central Andes indicates that this scenario is inappropriate. Were this scenario to apply to the Bolivian Andes, it would require that the mountain belt has been shortened by a maximum of 200 kilometers, and that there is no other contribution to crustal cross sectional area (e.g. tectonic erosion). Shortening of 200 kilometers is, however, the minimum that could have occurred; more likely estimates of shortening account for more than two-thirds of the deformed cross sectional area. Therefore, the volume of magmatic material is too small to have generated the amount of crustal shortening observed.

The response of the lower lithosphere to crustal shortening

Net convergence between the forearc and the Brazilian shield in the central Andes, as indicated by the amount of crustal shortening measured, requires a corresponding convergence within the lower lithosphere. In the plane strain case, balancing of the wedge-shaped area above the subducting Nazca plate shows that some of the South American plate must be subducted, where subduction refers to the incorporation of lithospheric material into the asthenosphere in response to shortening and thickening within the lithosphere.

Substantial shortening in synthetic and antithetic fold and thrust belts

Mattauer and Collot (1986) and Mattauer et al. (1983) hypothesize that all thin-skinned fold and thrust belts that have experienced a substantial amount of shortening should have an orientation synthetic to that of subduction, that is, that the sense of overthrusting in a fold and thrust belt must be the same as that observed in the corresponding subduction zone. This hypothesis has been used to interpret the tectonic setting of ancient

orogenic belts. The long history of eastward subduction of oceanic lithosphere beneath South America in the central Andes, and the magnitude of antithetic back-arc thrusting measured in the central Andes clearly indicates, however, that the sense of overthrusting in a substantially shortened orogenic belt is not diagnostic of the sense of contemporary subduction.

In summary, the documentation of a thin-skinned antithetic back-arc fold and thrust belt in the Bolivian Andes, which has accomodated a substantial amount of shortening, validates the concept of Andean orogeny. Neither continental collision nor magmatic intrusion are necessary causes of large amounts of crustal shortening. The corresponding convergence of the lower lithosphere is accomodated by loss of at least the lower lithosphere into the asthenosphere.

CHAPTER EIGHT

Conclusions

A quantitative interpretation of the structural style of the Bolivian Andes, based on a combined field and photogeologic study of a transect across the mountain belt between approximately 17.5 and 19°S, shows that the Cordillera Oriental and Subandean Zone comprise a thin-skinned fold and thrust belt that has accomodated a large amount of crustal shortening. The fold and thrust belt occupies a back-arc position and its sense of overthrusting is antithetic to the sense of subduction. Timing relationships suggest that the main deformational events within the Cordillera Oriental and Subandean Zone are post-Oligocene, although eastward subduction beneath the margin of South America is postulated to have begun as early as early Jurassic time.

Classic geometric arguments indicate that the deformation is thin-skinned. The surfaces of decollement are localized in three Paleozoic shale formations: undifferentiated Lower Ordovician shale, the Silurian Kirusillas Formation, and the Devonian Icla Formation. The decollement ramps up to progressively younger beds toward the foreland.

Much of the observed deformation is typical of foreland fold and thrust belts, but some of the features are unique to the Bolivian Andes. An unexposed, deep fault system that involves structural packages of unknown lithological composition underlies the upper, decoupled thrust sheets. This relationship may explain the unusual number of backthrusts and the unusually steep dips of the thrust faults that characterize the Bolivian Andes. Many hanging wall cutoff angles are large (70°). The geometry of

the thrust front changes at the bend in the mountain belt from a triangle zone in southern Bolivia to an emergent thrust front in northern Bolivia. The inferred triangle zone does not correlate with a retarded advance of the thrust belt, with a reduced width of the thrust belt, or with changes in facies in the units containing the surfaces of decollement, contrary to observations in other mountain belts. The bend in the Bolivian Andes at approximately 18°S is apparently due, at least in part, to the presence of a wider pre-orogenic sedimentary basin south of 18°S. Although left-lateral tear faulting and lateral ramps accomodate changes in the number and level of surfaces of decollement at the latitude of the bend, it does not extend across the width of the mountains. The change in the trend of the mountain belt may require a component of left-lateral faulting, parallel to the mountain belt, north of the bend. The Cochabamba basins are interpreted as thin-skinned pull-apart basins formed due to a left step in a left-lateral tear fault system.

The amount of crustal shortening is calculated from balanced cross sections across the mapped area. Balanced cross sections can be drawn accurately in this tectonic setting because there has been no significant penetrative strain within the deformed units and no regional dynamic metamorphism. The estimates are biased towards underestimation of the amount of shortening. A minimum amount of shortening of 210 kilometers across the Cordillera Oriental and Subandean Zone is calculated; the actual amount is probably much larger.

The amount of shortening that has occurred across the Bolivian Andes allows the determination of the mechanism of formation of the mountain belt and the evaluation of models of orogeny and subduction. Calculations of balanced crustal cross sectional areas based on the minimum amount of

shortening require that crustal shortening has been more important in forming the thickened crust than addition of mantle-derived magmas to the crust. For assumptions of an average crustal thickness, 210 kilometers of shortening accounts for at least two-thirds of the present-day cross sectional area of the crust of the Andes at 18°S. Plausible estimates of shortening calculated with less conservative assumptions and the consideration of the probable extension of the thin-skinned style of deformation into the Altiplano indicate that virtually all of the mountain range could have been built by crustal shortening. The importance of crustal shortening is further indicated by the temporal coincidence of a change to a crustal source for young melts and the onset of thrust faulting, and the degree of crustal contamination and its increase in time in the exposed volcanic rocks.

The minimum estimate of crustal shortening provides a key piece of evidence that can be used to evaluate hypotheses of orogenesis. First, the magnitude of the shortening indicates loss of at least some of the lower continental lithosphere into the mantle. Second, the documentation of eastward subduction of oceanic lithosphere contemporaneous with a west-dipping thin-skinned thrust fault system verifies the occurrence of antithetic back-arc fold and thrust belts across which a large amount of shortening has occurred. Finally, the validity of the concept of Andean orogeny is shown by the contemporaneous occurrence of substantial crustal shortening in a back-arc setting and the subduction of only oceanic lithosphere. Neither continental collision nor magmatic intrusion are necessary driving forces for orogenesis.

REFERENCES

Ahlfeld, F.E., 1972, Geología de Bolivia, La Paz, Bolivia: Los Amigos del Libro, 190p.

Allenby, R.J., 1987, Origin of the Bolivian Andean orocline: a geologic study utilizing Landsat and Shuttle Imaging Radar: Tectonophysics, v. 142, p. 137-154.

Allmendinger, R.W., V.A. Ramos, T.E. Jordan, M. Palma, and B.L. Isacks, 1983, Paleogeography and Andean structural geometry, northwest Argentina: Tectonics, v. 2, p.1-16.

Anderson, E.M., 1951, The Dynamics of Faulting and Dyke Formation with Applications to Britain: Edinburgh, Oliver and Boyd, 2nd.edition.

Bally, A.W., P.L. Gordy, and G.A. Stewart, 1966, Structure, seismic data, and orogenic evolution of the southern Canadian Rocky Mountains: Bulletin of Canadian Petroleum Geology, v. 14, p. 337-381.

Banks, C.J. and J. Warburton, 1986, "Passive-roof" duplex geometry in the frontal structures of the Kirthar and Sulaiman mountain belts, Pakistan: Journal of Structural Geology, v. 8, p. 229-237.

Barazangi, M. and B.L. Isacks, 1976, Spatial distribution of earthquakes and subduction of the Nazca plate beneath South America : Geology, v. 4, p. 686-692.

Barazangi, M. and B.L. Isacks, 1979, Subduction of the Nazca plate beneath Peru: evidence from spatial distribution of earthquakes : Geophysical Journal of the Royal Astronomical Society, v. 57, p. 537-555.

Barreiro, B.A., 1984, Lead isotopes and Andean magmagenesis, in Harmon, R.S. and B.A. Barreiro, Andean Magmatism: Chemical and Isotopic Constraints: Cambridge, Mass., USA, Shiva Publishing Limited, p. 21-31.

Beck, M.E., Jr., 1988, Analysis of Late Jurassic-Recent paleomagnetic data from active plate margins of South America: Journal of South American Earth Sciences, v. 1, p. 39-53.

Ben-Avraham, Z. and A. Nur, 1987, Effects of collision at trenches on oceanic ridges and passive margins, in Monger, J.W.H. and J. Francheteau,

Circum-Pacific Orogenic Belts and Evolution of the Pacific Basin: Washington, D.C., American Geophysical Union, Geodynamics Series Volume 18 , p. 9-19.

Benjamin, M.T., N.M. Johnson and C.W. Naeser, 1987, Recent rapid uplift inthe Bolivian Andes: evidence from fission-track dating: Geology, v. 15, p. 680-683.

Bjorklund, L., 1985, The Middle and Lower Allochthons in the Akkajaure-Tysfjord area, northern Scandinavian Caledonides, in Gee, D.G. and B.A. Sturt, The Caledonide Orogen--Scandinavia and Related Areas: Chichester, John Wiley and Sons, p. 515-528.

Boyer, S.E. and D. Elliott, 1982, Thrust Systems: American Association of Petroleum Geologists Bulletin, v. 66, p. 1196-1230.

Brockmann, C., A. Castanos, R. Suarez, and P. Tomasi, 1972, Estudio geológico de la Cordillera Oriental de los Andes, en la zona central de Bolivia (región del Chapare): Soc. Geol. Bol., v. 18, p. 1-36.

Brown, G.C., 1982, Calc-alkaline intrusive rocks: their diversity, evolution, and relation to volcanic arcs, in Thorpe, R.S., Andesites: Orogenic Andesites and Related Rocks: New York, John Wiley & Sons Ltd., p. 437-464.

Burchfiel, B.C. and L.H. Royden, 1988, Structure of an A-type subduction zone, Northern Scandinavian Caledonides: GSA abstracts with programs, Northeastern Section Mtg., v. , p. .

Butler, R.W.H., 1982, The terminology of structures in thrust belts: Journal of Structural Geology, v. 4, p. 239-245.

Buxtorf, A., 1916, Prognosen und Befunde beim Hauensteinbasin--und Grenchenbergtunnel und die Bedeutung der letzteren für die Geologie des Juragebirges: Verhandl. Naturforsch. Gesellsch. Basel, v. 27, p. 184-254.

Carey, S.W., 1958, A tectonic approach to continental drift: Symp. Continental Drift, Hobart, 177-355.

Cirbian K., M., R. Marocco, J. Oller V., and T. Sempéré, 1986, Evidencia de una discontinuidad sedimentaria fundamental en el eoTerciario andino de Bolivia: Bolivian Geological Society, Abstracts, p.45.

Cobbing, E.J., 1985, The tectonic setting of the Peruvian Andes, in Pitcher, W. S., Atherton, M. P., Cobbing,E., and J.R.D. Beckinsale, Magmatism at a Plate Edge: the Peruvian Andes: Glasgow, Blackie, p. 3-13.

Coney, P.J., D.L. Jones, and J.W.H. Monger, 1980, Cordilleran suspect terranes : Nature, v. 288, p. 329-333.

Cooper, M.A. and P.M. Trayner, 1986, Thrust-surface geometry: implications for thrust-belt evolution and section-balancing techniques: Journal of Structural Geology, v. 8, p. 305-312.

Crowell, J.C., R. Suarez S., and A.C. Rocha C., 1981, The Silurian Cancaniri (Zapla) Formation of Bolivia, Argentina and Peru, in Hambray, M.J. and W.B. Harland, Earth's Pre-Pleistocene Glacial Record: Cambridge, England, Cambridge University Press, p. 902-907.

Dahlen, F.A., J. Suppe and D. Davis, 1984, Noncohesive critical Coulomb wedges, an exact solution: Journal of Geophysical Research, v. 89, p. 10087-10101.

Dahlstrom, C. D. A., 1969, Balanced Cross Sections: Canadian Journal of Earth Sciences v. 6, p. 743-757.

Dalziel, I.W.D., 1986, Collision and Cordilleran orogenesis: an Andean perspective, in Coward, M.P. and A.C. Ries, Collision Tectonics: Geological Society of London Special Publication 19 , p. 389-404.

Davis, D. and T. Engelder, 1985, The role of salt in fold-and-thrust belts: Tectonophysics, v. 119, p. 67-88.

Davis, D., J. Suppe, and F.A. Dahlen, 1983, Mechanics of fold-and-thrust belts and accretionary wedges: Journal of Geophysical Research, v. 88, p. 1153-1172.

Davis, G.A., J.W.H. Monger and B.C. Burchfiel, 1978, Mesozoic construction of the Cordilleran "collage", central British Columbia to central California, in Howell, D.C. and K.A. McDougall, Mesozoic Paleogeography of the western United States: Pacific Sect., Soc. Econ. Paleo. Min. , p. 1-32.

DePaor, Declan G., 1987, Stretch in shear zones: implications for section balancing: Journal of Structural Geology, v. 9, p. 893-895.

Dewey, J.F. and J.M. Bird, 1970, Mountain belts and the new global tectonics: Journal of Geophysical Research, v. 75, p. 2625-2647.

Dunne, W.M. and D.A. Ferrill, 1988, Blind thrust systems: Geology, v. 16, p. 33-36.

Elliott, D., 1983, The construction of balanced cross sections: Journal of Structural Geology, v. 5, p. 101.

Elliott, D. and M.R.W. Johnson, 1980, Structural evolution in the northern part of the Moine thrust belt, NW Scotland: Trans. Roy. Soc. Edin., v. 71, p. 69-96.

Farrar, E., A.H. Clark, D.J. Kontak, D.A. Archibald, 1988, Zongo-San Gabán zone: Eocend foreland boundary of the Central Andean orogen, northwest Bolivia and southeast Peru, Geology, v. 16, pp. 55-58.

Fernandez G., Cesar A., 1981, Late Paleozoic Tarija Formation, southern Bolivia and northern Argentina, in Hambray, M.J. and W.B. Harland, Earth's Pre-Pleistocene Glacial Record: Cambridge, England, Cambridge University Press, p. 853-854.

Gill, J., 1981, Orogenic Andesites and Plate Tectonics: New York, Springer-Verlag, p. 390.

Grange, F., P. Cunningham, J. Gagnepain, D. Hatzfeld, P. Molnar, L. Ocola, A. Rodrígues, S.W. Roecker, J.M. Stock, G. Suárez, 1984, The configuration of the seismic zone and the downgoing slab in southern Peru, Geophysical Research Letters, v. 11, p. 38-41.

Hamilton, W., 1978, Mesozoic tectonics of the western United States: Pac. Sec., Soc. Econ. Paleo. Min., v. 2, p. 33-70.

Hamilton, W., 1987, Plate-tectonic evolution of the western U.S.A.: Episodes, v. 10, p. 271-276.

Hamilton, W., 1988, Tectonic setting and variations with depth of some Cretaceous and Cenozoic structural and magmatic systems of the western United States, in Ernst, W.G., Metamorphism and crustal evolution of the western United States: Prentice-Hall, p. in press.

Harmon, R.S. and J. Hoefs, 1984, Oxygen isotope ratios in Late Cenozoic Andean volcanics, in Harmon, R.S. and B.A. Barreiro, Andean Magmatism: Chemical and Isotopic Constraints: Cambridge, Mass., USA, Shiva Publishing Limited, p. 9-21.

Hasegawa, A. and I.S. Sacks, 1981, Subduction of the Nazca plate beneath Peru as determined from seismic observations, Journal of Geophysical Research, v. 86, p. 4971-4980.

Hawkesworth, C.J., 1982, Isotope characteristics of magmas erupted along destructive plate margins, in Thorpe, R.S., Andesites: Orogenic

Andesites and Related Rocks: New York, John Wiley & Sons Ltd., p. 549-574.

Hawkesworth, C.J., Hammill, M., Gledhill, A.R., van Calsteren, P., and Rogers, G., 1982, Isotope and trace element evidence for late-stage intra-crustal melting in the High Andes: Earth and Planetary Science Letters, v. 58, p. 240-254.

Hayashida, A., L.A. Rodrigo, and A. Saavedra, 1984, Fission track dating and paleomagnetic study of the Cenozoic continental deposits at Salla, Bolivian Andes: Reports of New World Monkeys, Kyoto University Primate Research Institute, v. 4, p. 89-98.

Heki, K., Y. Hamano, H. Kinoshita, A. Taira, and M. Kono, 1984, Paleomagnetic study of Cretaceous rocks of Peru, South America: Tectonophysics, v. 108, p. 267-281.

Helwig, James, 1972, Stratigraphy, sedimentation, paleogeography, and paleoclimates of Carboniferous ("Gondwana") and Permian of Bolivia: American Association of Petroleum Geologists Bulletin, v. 56, p. 1008-1033.

Herail, G., M. Fornari, G. Viscarra, G. Laubacher and J. Argollo, 1987, Geodinamica de una cuenca intramontana del frente andino: la cuenca de Tipuani-Mapiri: Decimo Congreso Geológico Argentino, Actas II, p. 93-96.

Isaacson, Peter E., 1975, Evidence for a western extracontinental land source during the Devonian period in the central Andes: Geological Society of America Bulletin, v. 86, p. 39-46.

Isacks, B.L., 1988, Uplift of the central Andean plateau and bending of the Bolivian orocline: Journal of Geophysical Research, v. 93, p. 3211-3231.

Jaeger, J.C. and N.G.W. Cook, 1979, Fundamentals of Rock Mechanics: London, Chapman and Hall, Ltd., 593 p.

James, D.E., 1971, Plate tectonic model for the evolution of the central Andes: Geological Society of America Bulletin, v. 82, p. 3325-3346.

Jamison, W.R., 1987, Geometric analysis of fold development in overthrust terranes: Journal of Structural Geology, v. 9, p. 207-219.

Jarrard, R.D., 1986, Relations among subduction parameters: Reviews of Geophysics, v. 24, p. 217-284.

Jones, D.L., N.J. Silberling, and J. Hillhouse, 1977, Wrangellia--a displaced terrane in northwestern North America: Canadian Journal of Earth Science, v. 14, p. 2565-2577.

Jones, P.B., 1982, Oil and gas beneath east-dipping underthrust faults in the Alberta Foothills, Canada, in R.B. Powers, Geologic studies of the Cordilleran thrust belt: Denver, Rocky Mountain Association of Geologists, p. 61-74.

Jordan, T.E. and R.N. Alonso, 1987, Cenozoic stratigraphy and basin tectonics of the Andes Mountains, 20°-28°S: American Association of Petroleum Geologists Bulletin, v. 71, p. 49-64.

Jordan, T.E., B.L. Isacks, R. W. Allmendinger, J.A. Brewer, V. A. Ramos, and C.J. Ando, 1983, Andean tectonics related to geometry of subducted Nazca plate: Geological Society of America Bulletin, v. 94, p. 341-361.

Lehmann, B., 1978, A Precambrian sample from the Altiplano, Bolivia: Geol. Rundsch., v. 67, p. 270-278.

Lohmann, H.H., 1970, Outline of the tectonic history of Bolivian Andes: American Association of Petroleum Geologists Bulletin, v. 54, p. 735-757.

Lyon-Caen, H., P. Molnar, and G. Suárez, 1985, Gravity anomalies and flexure of the Brazilian shield beneath the Bolivian Andes: Earth and Planetary Science Letters, v. 75, p. 81-92.

Marocco, R., T. Sempéré, M. Cirbian and J. Oller, 1987, Mise en évidence d'une déformation paléocène en Bolivie du Sud: sa place dans l'évolution géodynamique des Andes Centrales: C.R. Acad. Sc. Paril, Série II, v. 304, no.18, p. 1139-1143.

Martínez, C., 1980, Structure et évolution de la chaîne hercynienne et de la chaîne andine dans le nord de la Cordillère des Andes de Bolivie: Paris, France, O.R.S.T.O.M., Travaux et documents de L'O.R.S.T.O.M., no. 119 , p. 352.

Mather, K.F., 1922, Front ranges of the Andes between Santa Cruz, Bolivia and Embarcacion, Argentina: Geological Society of America Bulletin, v. 33, p. 703-764.

Mattauer, M. and B. Collot, 1986, Continental subduction, thrusting and strike-slip faulting in the Canadian Cordillera: Bull. Soc. Géol. France, v. 8, p. 899-909.

Mattauer, M., B. Collot and J. Van den Driessche, 1983, Alpine model for the internal metamorphic zones of the North American Cordillera: Geology, v. 11, p. 11-15.

Mégard, F., 1987a, Structure and Evolution of the Peruvian Andes, in Schaer, Jean-Paul and J. Rodgers, The Anatomy of Mountain Ranges: Princeton, New Jersey, Princeton University Press, p. 179-211.

Mégard, F., 1987b, Cordilleran Andes and Marginal Andes: A review of Andean geology north of the Arica Elbow (18°S), in Monger, J.W.H. and J. Francheteau, Circum-Pacific Orogenic Belts and Evolution of the Pacific Basin: Washington, D.C., American Geophysical Union, Geodynamics Series Volume 18, p. 71-97.

Mégard, F., 1984, The Andean orogenic period and its major structures in central and northern Peru: Journal of the Geological Society of London, v. 141, p. 893-900.

Mégard, F, D.C. Noble, E.H. McKee, and H. Bellon, 1984, Multiple pulses of Neogene compressive deformation in the Ayacucho intermontane basin, Andes of central Peru: Geological Society of America Bulletin, v. 95, p. 1108-1117.

Mitra, S., 1988, Three-dimensional geometry and kinematic evolution of the Pine Mountain thrust system, southern Appalachians: Geological Society of America Bulletin, v. 100, p. 72-95.

Molnar, P. and T. Atwater, 1978, Interarc spreading and Cordilleran tectonics as alternates related to the age of subducted oceanic lithosphere: Earth and Planetary Science Letters, v. 41, p. 330-340.

Monger, J.W.H., R.A. Price and D.J. Tempelman-Kluit, 1982, Tectonic accretion and the origin of the two major metamorphic and plutonic welts in the Canadian Cordillera: Geology, v. 10, p. 70-75.

Morley, C.K., 1986, A classification of thrust fronts: American Association of Petroleum Geologists Bulletin, v. 70, p. 12-25.

Nur, A. and Z. Ben-Avraham, 1982, Oceanic plateaus, the fragmentation of continents, and mountain building: Journal of Geophysical Research, v. 87, p. 3644-3661.

Nur, A. and Z. Ben-Avraham, 1983, Displaced Terranes and Mountain Building, in K.J. Hsu, Mountain Building Processes: London, Academic Press, p. 73-85.

Pardo A., A., 1982, Caracteristicas estructurales de la faja subandina del norte del Peru: Asociación Colombiano de geologos y geofisicos del petróleo, Sério 13726, Simposio "Exploración petrolera en las cuencas subandinas de Venezuela, Colombia, Ecuador y Peru", p. 17.

Pardo-Casas, F. and P. Molnar, 1987, Relative motion of the Nazca (Farallon) and South American plates since late Cretaceous time: Tectonics, v. 6, p. 233-248.

Pareja L., J., Vargas F., C., Suárez S., R., Ballón A., R., Carrasco C., R., and Villaroel A., C., 1978, Mapa Geológico de Bolivia y Memoria Explicativa: La Paz, Bolivia, Yacimientos Petroliferos Fiscales Bolivianos y Servicio Geológico de Bolivia, 27p.

Paulsen, O.L., 1988, El limite interno del plegamiento andino en Bolivia y su relación con los campos productores de la llanura Chaco-Beniana, III Simposio Bolivariano, Exploración Petrolera de las Cuencas Subandinas, Caracas, 1988, p. 475-502.

Pearce, J.A., 1982, Trace element characteristics of lavas from destructive plate boundaries, in Thorpe, R.S., Andesites: Orogenic Andesites and Related Rocks: New York, John Wiley & Sons Ltd., p. 525-548.

Pitcher, W. S. and Cobbing, E. J. , 1985, Phanerozoic plutonism in the Peruvian Andes, in Pitcher, W. S., Atherton, M. P., Cobbing, E., and J.R.D. Beckinsale, Magmatism at a Plate Edge: the Peruvian Andes: Glasgow, Blackie, p. 19-25.

Pitcher, W.S., 1984, Phanerozoic plutonism in the Peruvian Andes, in Harmon, R.S. and B.A. Barreiro, Andean Magmatism: Chemical and Isotopic Constraints: Cambridge, Mass., USA, Shiva Publishing Limited, p. 152-168.

Plafker, G., 1962, Geology of the "Elbow Area": Bolivia California Petroleum Company, Unpublished Report , p. 47.

Price, R.A., 1981, The Cordilleran foreland thrust and fold belt in the southern Canadian Rocky MountainsThrust and Nappe Tectonics: Geol. Soc. London Spec. Pub. 9 , p. 427-448.

Ramos, V.A., T.E. Jordan, R.W. Allmendinger, C. Mpdozis, S.M. Kay, J.M. Cortés, and M. Palma, 1986, Paleozoic terranes of the central Argentine-Chilean Andes: Tectonics, v. 5, p. 855-880.

Rich, J.I., 1934, Mechanics of low-angle overthrust faulting as illustrated by Cumberland thrust block, Virginia, Kentucky, and Tennessee: American Association of Petroleum Geologists Bulletin, v. 18, p. 1584-1596.

Rod, E., 1960, Strike-slip fault of continental importance in Bolivia: American Association of Petroleum Geologists Bulletin, v. 43, p. 772-789.

Rodgers, J., 1987, Differences between mountain ranges, in Schaer, Jean-Paul and J. Rodgers, The Anatomy of Mountain Ranges: Princeton, New Jersey, Princeton University Press, p. 11-19.

Rodrigo G., L.A. and A. Castaños, 1978, Sinopsis estratigráfica de Bolivia, I Parte Paleozoico: La Paz, Bolivia, Academía Nacional de Ciencias de Bolivia, p. 146.

Roeder, D., 1988, Andean-age structure of Eastern Cordillera (Province of La Paz, Bolivia): Tectonics, v. 7, p. 23-39.

Sempéré, T., 1987, Contribución a la estratigrafía del Mesozoico Boliviano en el Domino Andino: La Paz, Bolivia, Misión O.R.S.T.O.M. en Bolivia, 34 p.

Sempéré, T., H. Chavez F., and M. Perez L., 1986, Estudio sedimentologico preliminar de la parte superior de la formación Mondragon en las cercanias de Leñas, Depto. de Potosi, consecuencias geodinamicas: Bolivian Geological Society, Abstracts, p.45.

Serra, S., 1977, Styles of deformation in the ramp regions of overthrust faults, 29th Annual Field Conference, Wyoming Geological Association Guidebook, p. 487-498.

Sheffels, B.M. and D.W. Klepacki, 1985, The Cochabamba Fault System: a left-slip fault system in the elbow region of the Andes [abs.]: EOS (American Geophysical Union Transactions), v. 66, p. 1088.

Smith, A.G., 1981, Subduction and coeval thrust belts, with particular reference to North America, in McClay, K.R. and N.J. Price, Thrust and Nappe Tectonics: Geological Society of London Spec. Pub. 9 , p. 111-124.

Stauder, W., 1975, Subduction of the Nazca plate under Peru as evidenced by focal mechanisms and by seismicity: Journal of Geophysical Research, v. 80, p. 1053-1064.

Suarez S., R., 1976, El Sistema Ordovícico en Bolivia: Revista Técnica, Y.P.F.B., v. V, p.111-223.

Suppe, J., 1983, Geometry and kinematics of fault-bend folding: American Journal of Science, v. 283, p. 684-721.

Thormann, W., 1966, Investigaciones preliminares sobre la geotectónica y metalogénesis de la zona Challapata-Caxata, Bolivia: Servicio Geológico de Bolivia, Boletín No. 7, v. , p. 118.

Thorpe, R. S., Francis, P.W., Hammill, M., and Baker, M.C.W., 1982, The Andes, in Thorpe, R.S., Andesites: Orogenic Andesites and Related Rocks: New York, John Wiley & Sons Ltd., p. 187-206.

Thorpe, R.S., 1984, The tectonic setting of active Andean magmatism, in Harmon, R.S. and B.A. Barreiro, Andean Magmatism: Chemical and Isotopic Constraints: Cambridge, Mass., USA, Shiva Publishing Limited, p. 4-9.

Tilke, P., 1986, Caledonian structure, metamorphism, geochronology and tectonics of the southern Rombak Window, Northern Sweden: Ph.D. Thesis, M.I.T., Cambridge, MA , 308 p.

Tosdal, R.M., A.H. Clark and E. Farrar, 1984, Cenozoic polyphase landscape and tectonic evolution of the Cordillera Occidental, southernmost Peru: Geological Society of America Bulletin, v. 95, p. 1318-1332.

Vann, I.R., R.H. Graham and A.B. Hayward, 1986, The structure of mountain fronts: Journal of Structural Geology, v. 8, p. 215-227.

Weaver, B.L. and Tarney, J., 1982, Andesitic magmatism and continental growth, in Thorpe, R.S., Andesites: Orogenic Andesites and Related Rocks: New York, John Wiley & Sons Ltd., p. 639-662.

Wilson, D. V., 1985, The deeper structure of the Central Andes and some geophysical constraints, in Pitcher, W. S., Atherton, M. P., Cobbing, E,.and J.R.D. Beckinsale, Magmatism at a Plate Edge: the Peruvian Andes: Glasgow, Blackie, p. 13-18.

Woodward, N.B., S.E. Boyer, and J. Suppe, 1985, An Outline of Balanced Cross Sections: GSA Short Course Notes, GSA Annual Mtg., Orlando, Florida, 172 p.

Yacimientos Petroliferos Fiscales Bolivianos,, 1983, Guia de la excursión geologica, II Reunion Internacional Proyecto IGCP-193, Silurico-Devonico de Latinoamerica: Santa Cruz, Bolivia, YPFB, 25 p.

Ybert, J.P. and M. Pérez L., 1986, Datos palinologicos del Cretacico superior y limite Cretacico-Terciario de la seccion de carata, Departamento de Potosi, Bolivia: Bolivian Geological Society, Abstracts, p.38.

Zeil, W., 1979, The Andes, a geological review: Berlin, Gebruder Borntraeger, 260 p.

APPENDIX

LOCATION MAP OF EXAMPLE AIR PHOTOS

EXAMPLE AIR PHOTO A--WESTERN CORDILLERA ORIENTAL

EXAMPLE AIR PHOTO B--CENTRAL CORDILLERA ORIENTAL

EXAMPLE AIR PHOTO C--SUBANDEAN ZONE

LOCATION OF THE EXAMPLE AIR PHOTOS, A, B, AND C ON THE
SIMPLIFIED GEOLOGIC MAP OF THE BOLIVIAN ANDES
17°S to 18°45'S

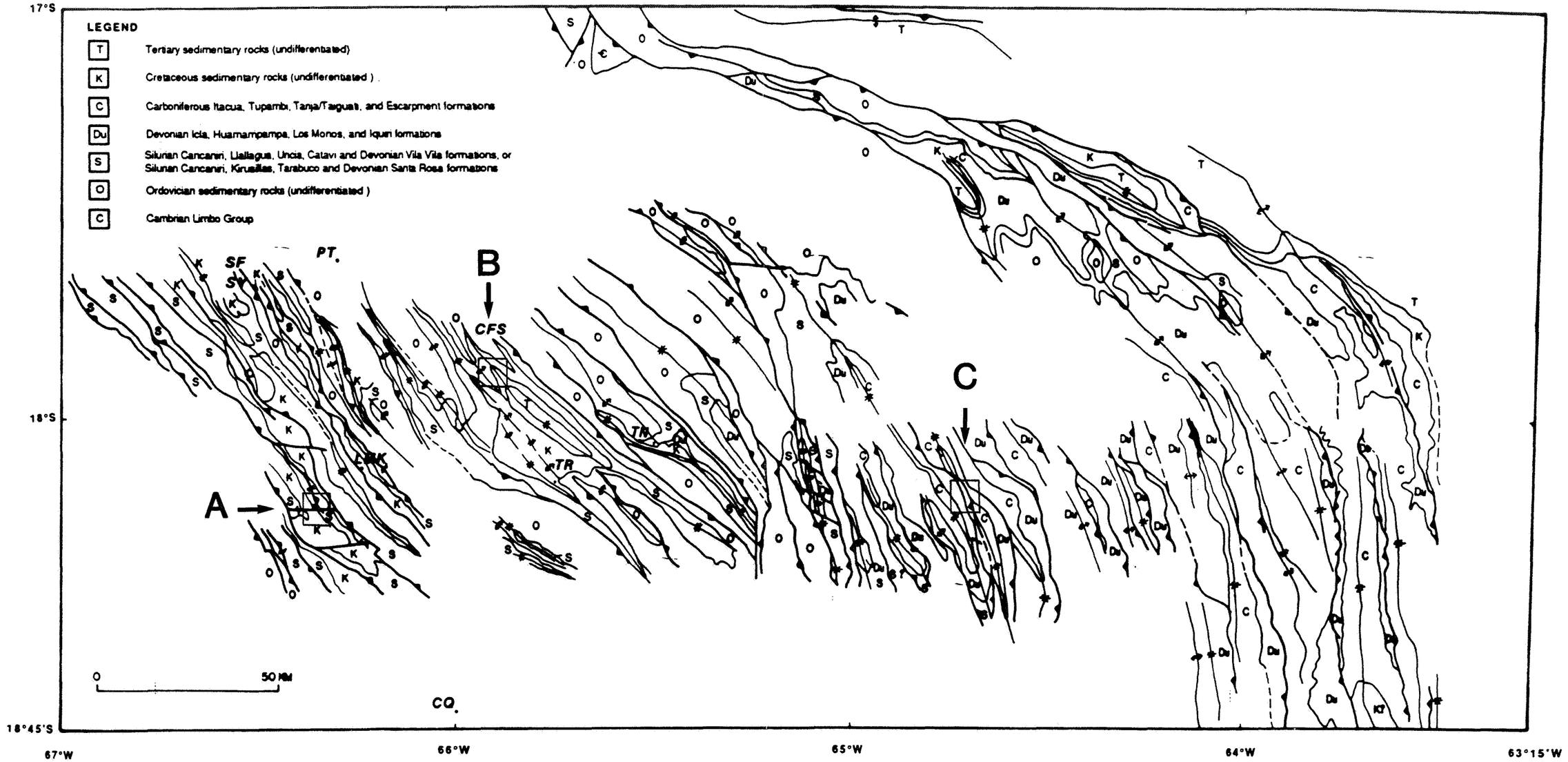

Figure 5.1

A

B

C

PREVIOUS PUBLICATIONS RELATED TO WORK SUPPORTED BY THIS GRANT

Sheffels, B. M., 1987, Back-Arc Tectonic Style in the type-Andean margin: Constraints from balanced cross sections of the Bolivian Andes (abs.), GSA Abstr. with Programs, 19, 840.

Sheffels, B. M., B.C. Burchfiel, and P. Molnar, 1986, Deformational Style and crustal shortening in the Bolivian Andes (abs.), EOS, Trans. Amer. Geophys. Union, 67, 1242.

Sheffels, B.M. and D.W. Klepacki, 1985, The Cochabamba fault system: a left-slip fault system in the elbow region of the Andes (abs.), EOS, Trans. Amer. Geophys. Union, 66, 1088.

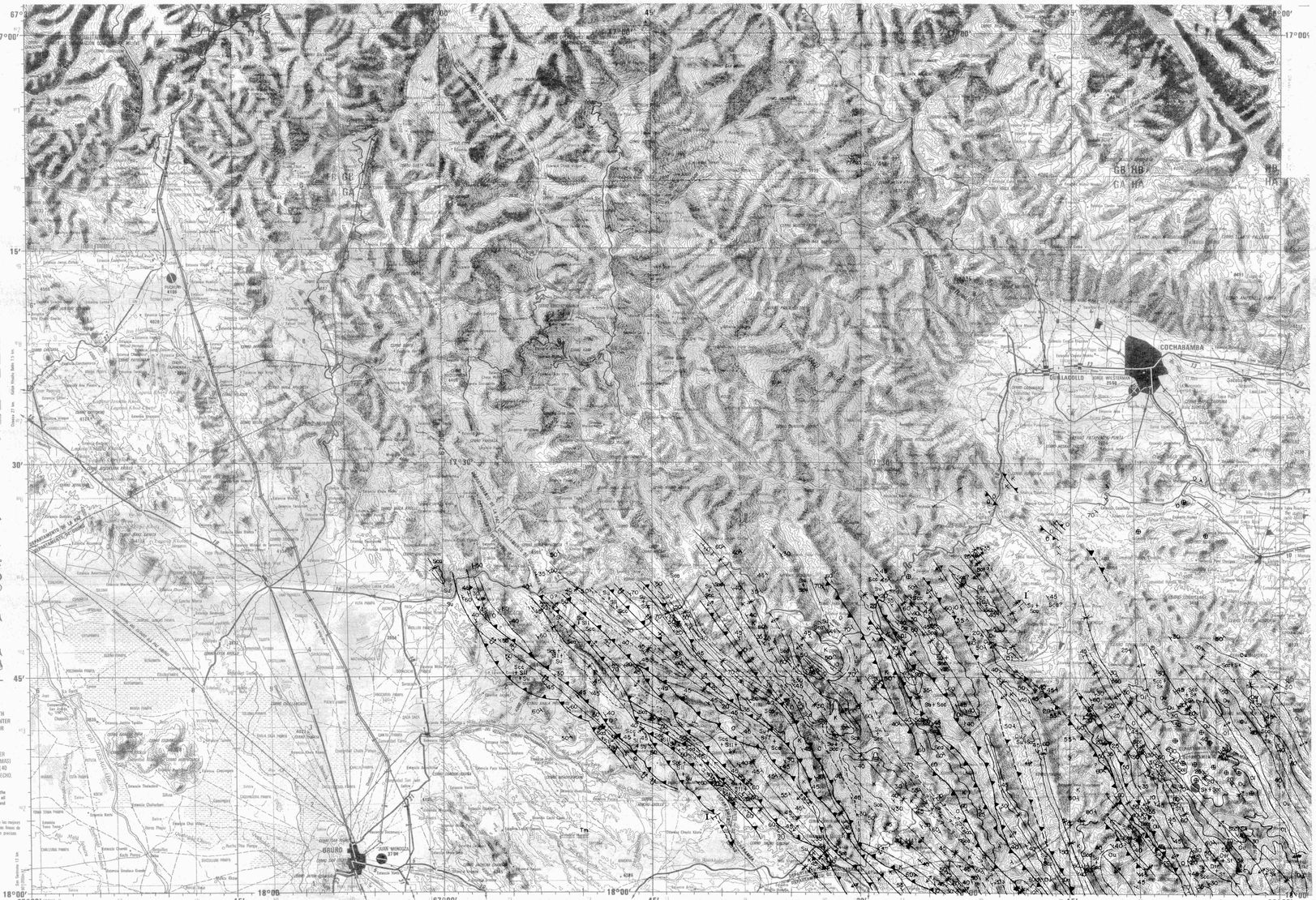

PLATE 1.

GEOLOGIC MAP OF THE COCHABAMBA, BOLIVIA SHEET (SE-19-8)

B. SHEFFELS 1988

QUATERNARY	Qal	QUATERNARY ALLUVIUM	
TERTIARY	Tm	MOROCOCALA IGNIMBRITES	
	T	TERTIARY SEDIMENTARY ROCKS (UNDIFFERENTIATED)	
CRETACEOUS	K	CRETACEOUS SEDIMENTARY ROCKS (UNDIFFERENTIATED)	
DEVONIAN	Dsr + St		SANTA ROSA FORMATION, TARABUCO FORMATION
SILURIAN	Sca	CATAVI FORMATION	
	Su + Sll + Scc	UNCÍA FORMATION, LLALLAGUA FORMATION, CANCANIRI FORMATION	
	Sk + Scc		KIRUSILLAS FORMATION, CANCANIRI FORMATION
ORDOVICIAN	O: Ou, Ol	O-ORDOVICIAN SEDIMENTARY ROCKS (UNDIFFERENTIATED) Ou-UPPER ORDOVICIAN Ol-LOWER ORDOVICIAN	

PALEOZOIC MESOZOIC CENOZOIC

CONTACTS	DEFINITE	APPROXIMATE	UNCERTAIN	CONCEALED
FAULTS	THRUST OR REVERSE (BARBS ON UPPER PLATE)	NORMAL (TICKS ON DOWNTHROWN SIDE)	STRIKE-SLIP	
	DEFINITE	APPROXIMATE	UNCERTAIN	CONCEALED
BEDDING	INCLINED	HORIZONTAL	VERTICAL	OVERTURNED
FOLDS	SYNCLINE, WITH DIRECTION OF PLUNGE		ANTICLINE, WITH DIRECTION OF PLUNGE	
	DEFINITE	APPROXIMATE	UNCERTAIN	CONCEALED
	OVERTURNED SYNCLINE		OVERTURNED ANTICLINE	

AMERICA DEL SUR, 1:250.000 — PUNATA — EDICION 1-I.G.M. — HOJA SE 20-5, SERIE H531

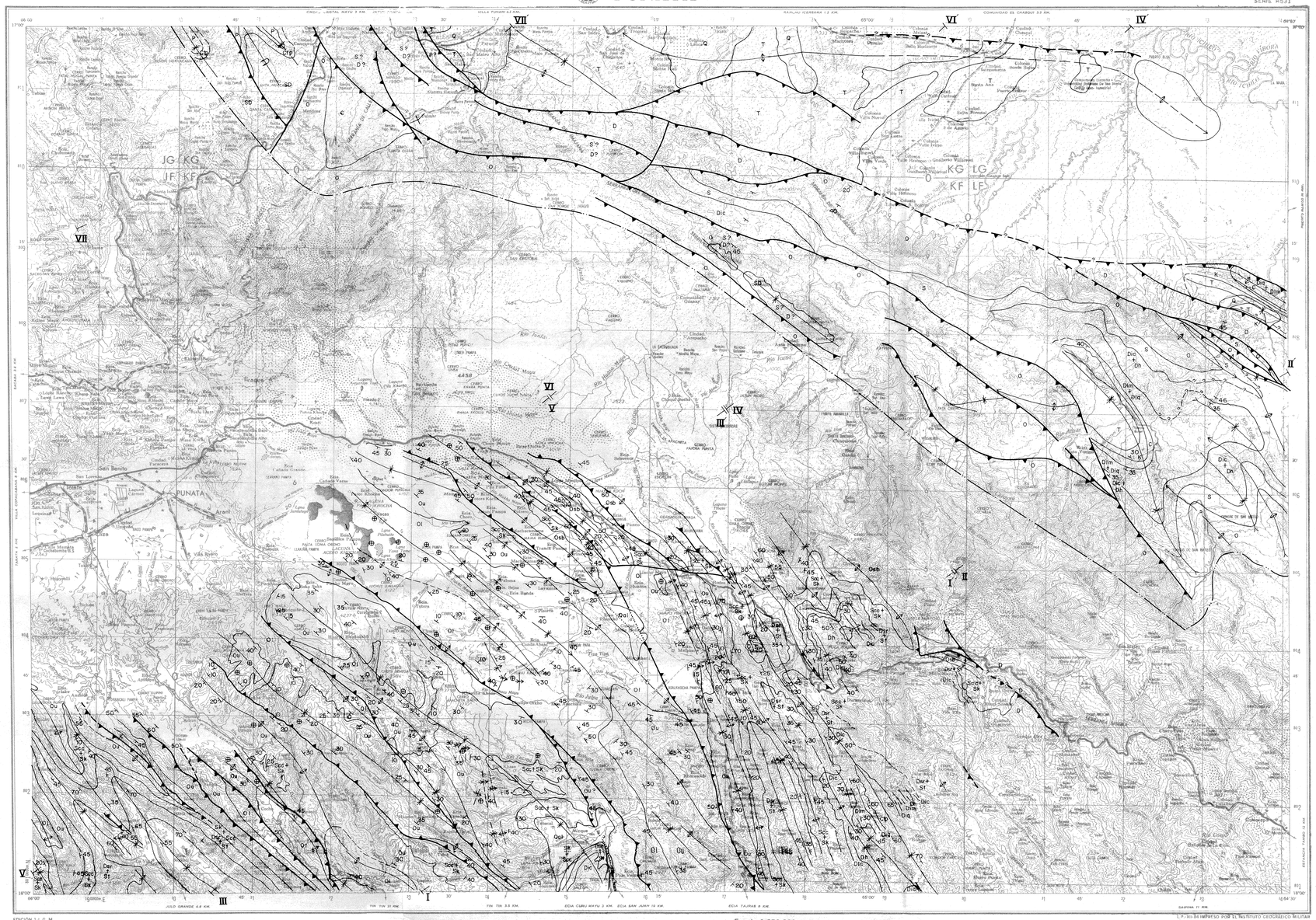
PUNATA
San Benito
Villa Rivero
Río Juntas
Río Chorani Mayu
Río Mojo Mayu
Río Chorani Pampa
Río Chorani Grande
Río Chorani Chico
Río Chorani Quebrada
Río Chorani Punta
Río Chorani Alto
Río Chorani Bajo
Río Chorani

SANTA CRUZ DE LA SIERRA

EDICIÓN 1-I.G.M.

SE 20-6
SERIE H 531

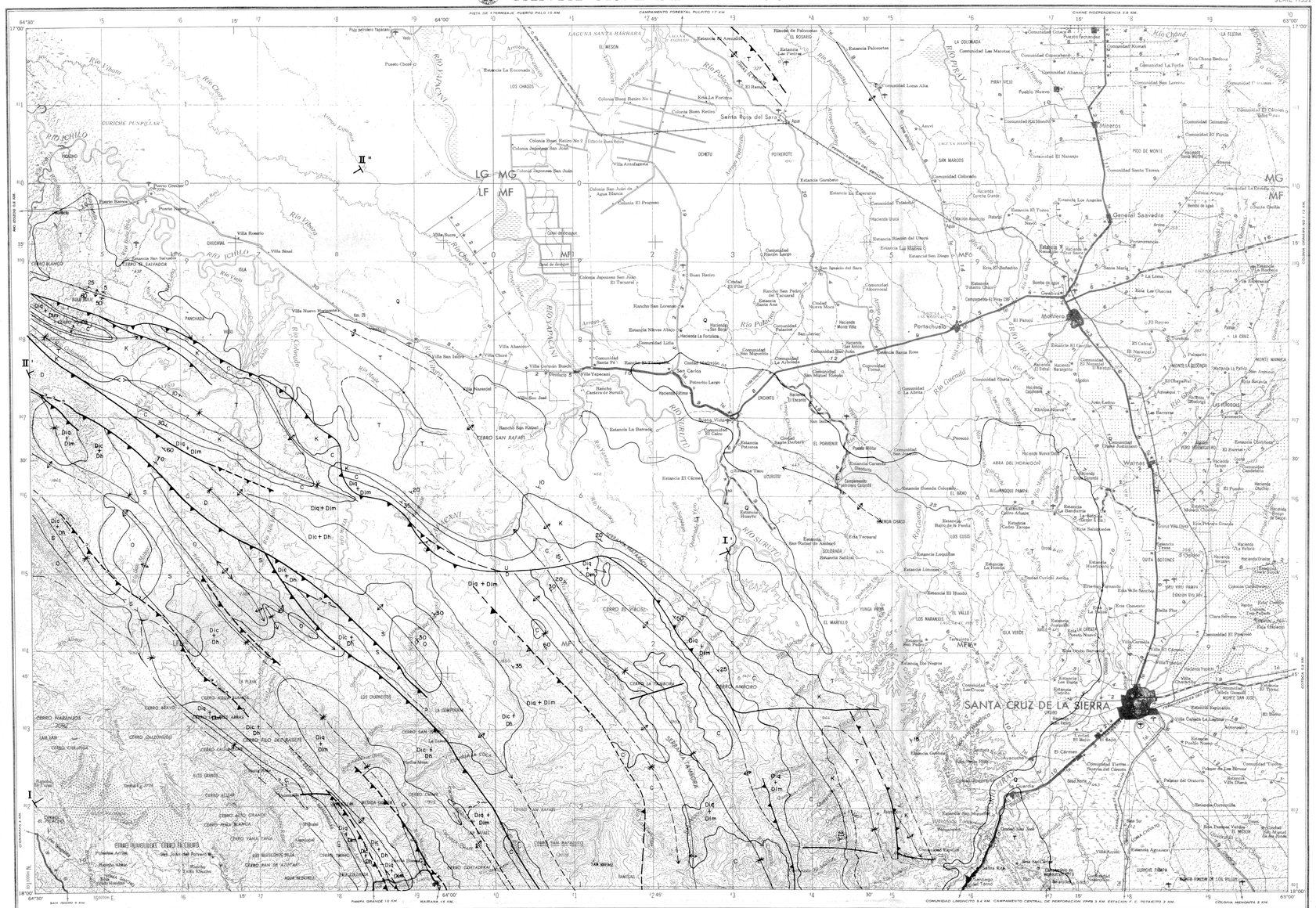
SANTA CRUZ DE LA SIERRA
CAMPAMENTO FORESTAL PULPITO 17 KM.
CHANE INDEPENDENCIA 2.6 KM.
PISTA DE ATERRIZAJE PUERTO PALO 10 KM.
LAGUNA SANTA BARBARA
RIO PIRAY
RIO PIRAI
RIO PIRAY VIEJO
RIO CHAPACO
RIO PARAPETI
RIO PARAGUA
RIO CHAPARE
RIO ICHILO
RIO VIBORA
RIO COLORADO
RIO NEGRO
RIO PALMAR
RIO SURUTU
RIO MAMORE
RIO GUAPAY
RIO GUAYBE
RIO YAPACANI
RIO SAN JULIAN
RIO SAN PEDRO
RIO PIRAY
SERRANIA SANTA BARBARA
SERRANIA SAN RAFAEL
SERRANIA SAN MIGUEL
SERRANIA SAN JULIAN
SERRANIA SAN PEDRO
SERRANIA SAN LORENZO
SERRANIA SAN JOSE
SERRANIA SAN MATEO
SERRANIA SAN ANTONIO
SERRANIA SAN ANDRES
SERRANIA SAN ANTONIO
SERRANIA SAN ANTONIO
SERRANIA SAN ANTONIO

UNCÍA

EDICIÓN 1-I.G.M.

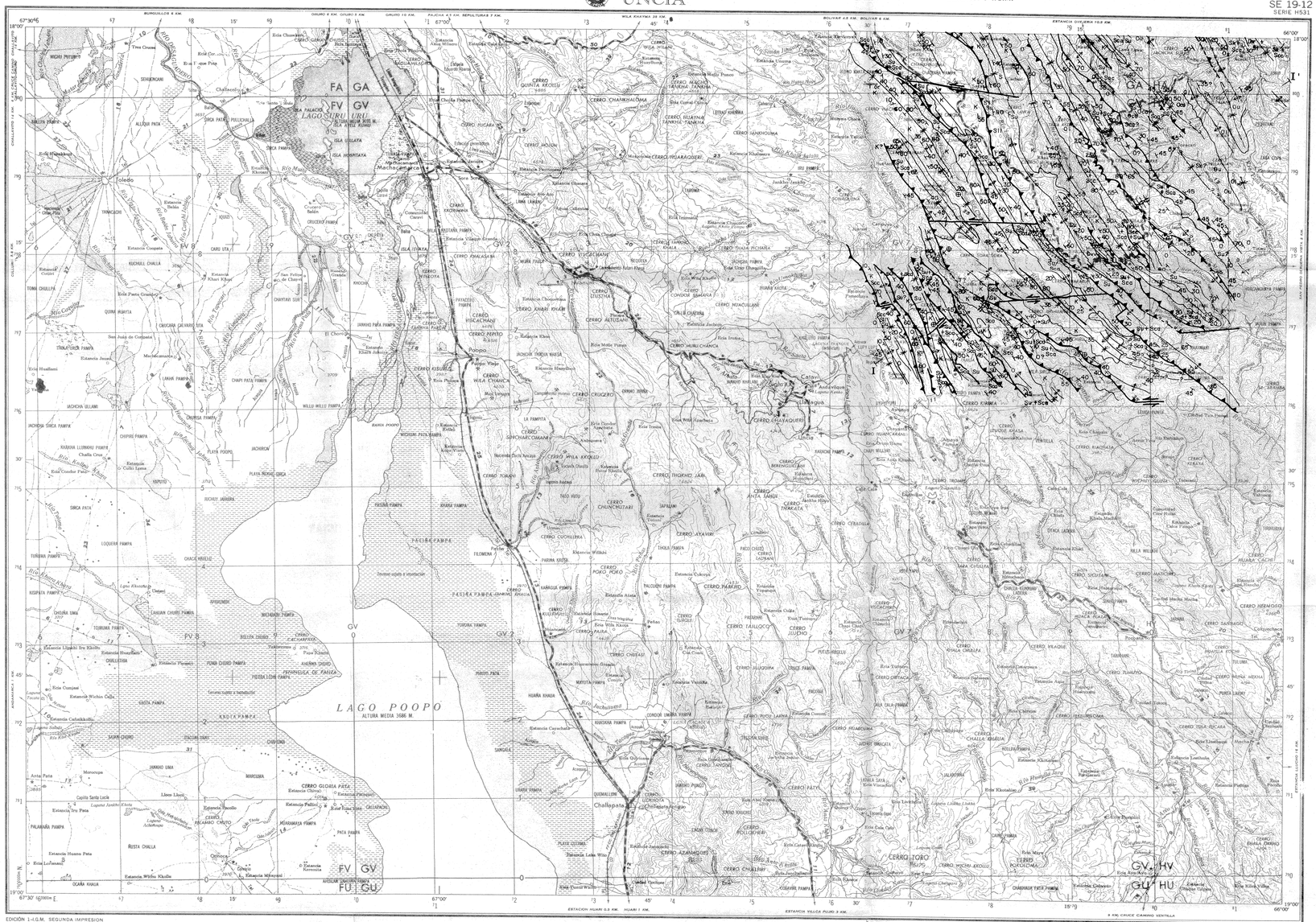
LAGO POOPO
ALTURA MEDIA 3686 M.
Toledo
Challapata
Pampa Aullagas
Río Desaguadero
Río Lacajahuira
Río Antequera
Río Sevaruyo
Río Huanuni
Río Sajama
Río Caracoles
Río Poopó
Río Marquirivi
Río Sabaya
Río Turco
Río Huachacalla
Río Cosapa
Río Challapata
Río Condoriri
Río Huayllamarca
Río Mauri
Río Kasa
Río Kallapas
Río Kkollpa
Río Kkollpa Mayu
Río Kkollpa Jahuira
Río Kkollpa Pampa
Río Kkollpa Pata
Río Kkollpa Pata Pampa
Río Kkollpa Pata Pata
Río Kkollpa Pata Pata Pampa
Río Kkollpa Pata Pata Pata
Río Kkollpa Pata Pata Pata Pampa
Río Kkollpa Pata Pata Pata Pata
Río Kkollpa Pata Pata Pata Pata Pampa
Río Kkollpa Pata Pata Pata Pata Pata
Río Kkollpa Pata Pata Pata Pata Pata Pampa
Río Kkollpa Pata Pata Pata Pata Pata Pata
Río Kkollpa Pata Pata Pata Pata Pata Pata Pampa
Río Kkollpa Pata Pata Pata Pata Pata Pata Pata
Río Kkollpa Pata Pata Pata Pata Pata Pata Pata Pampa
Río Kkollpa Pata Pata Pata Pata Pata Pata Pata Pata
Río Kkollpa Pata Pata Pata Pata Pata Pata Pata Pata Pampa
Río Kkollpa Pata Pata Pata Pata Pata Pata Pata Pata Pata
Río Kkollpa Pata Pata Pata Pata Pata Pata Pata Pata Pata Pampa
Río Kkollpa Pata Pata Pata Pata Pata Pata Pata Pata Pata Pata
Río Kkollpa Pata Pata Pata Pata Pata Pata Pata Pata Pata Pata Pampa
Río Kkollpa Pata Pata Pata Pata Pata Pata Pata Pata Pata Pata Pata
Río Kkollpa Pata Pata Pata Pata Pata Pata Pata Pata Pata Pata Pata Pampa
Río Kkollpa Pata Pata Pata Pata Pata Pata Pata Pata Pata Pata Pata Pata
Río Kkollpa Pata Pata Pata Pata Pata Pata Pata Pata Pata Pata Pata Pata Pampa
Río Kkollpa Pata Pata Pata Pata Pata Pata Pata Pata Pata Pata Pata Pata Pata
Río Kkollpa Pata Pata Pata Pata Pata Pata Pata Pata Pata Pata Pata Pata Pata Pampa
Río Kkollpa Pata Pata Pata Pata Pata Pata Pata Pata Pata Pata Pata Pata Pata Pata
Río Kkollpa Pata Pata Pata Pata Pata Pata Pata Pata Pata Pata Pata Pata Pata Pata Pampa
Río Kkollpa Pata Pata Pata Pata Pata Pata Pata Pata Pata Pata Pata Pata Pata Pata Pata
Río Kkollpa Pata Pata Pata Pata Pata Pata Pata Pata Pata Pata Pata Pata Pata Pata Pata Pampa
Río Kkollpa Pata Pata Pata Pata Pata Pata Pata Pata Pata Pata Pata Pata Pata Pata Pata Pata
Río Kkollpa Pata Pata Pata Pata Pata Pata Pata Pata Pata Pata Pata Pata Pata Pata Pata Pata Pampa
Río Kkollpa Pata Pata Pata Pata Pata Pata Pata Pata Pata Pata Pata Pata Pata Pata Pata Pata Pata
Río Kkollpa Pata Pata Pata Pata Pata Pata Pata Pata Pata Pata Pata Pata Pata Pata Pata Pata Pata Pampa
Río Kkollpa Pata Pata Pata Pata Pata Pata Pata Pata Pata Pata Pata Pata Pata Pata Pata Pata Pata Pata
Río Kkollpa Pata Pata Pata Pata Pata Pata Pata Pata Pata Pata Pata Pata Pata Pata Pata Pata Pata Pata Pampa
Río Kkollpa Pata Pata Pata Pata Pata Pata Pata Pata Pata Pata Pata Pata Pata Pata Pata Pata Pata Pata Pata
Río Kkollpa Pata Pata Pata Pata Pata Pata Pata Pata Pata Pata Pata Pata Pata Pata Pata Pata Pata Pata Pata Pampa
Río Kkollpa Pata Pata Pata Pata Pata Pata Pata Pata Pata Pata Pata Pata Pata Pata Pata Pata Pata Pata Pata Pata
Río Kkollpa Pata Pata Pata Pata Pata Pata Pata Pata Pata Pata Pata Pata Pata Pata Pata Pata Pata Pata Pata Pata Pampa
Río Kkollpa Pata Pata Pata Pata Pata Pata Pata Pata Pata Pata Pata Pata Pata Pata Pata Pata Pata Pata Pata Pata Pata
Río Kkollpa Pata Pata Pata Pata Pata Pata Pata Pata Pata Pata Pata Pata Pata Pata Pata Pata Pata Pata Pata Pata Pata Pampa
Río Kkollpa Pata Pata Pata Pata Pata Pata Pata Pata Pata Pata Pata Pata Pata Pata Pata Pata Pata Pata Pata Pata Pata Pata
Río Kkollpa Pata Pata Pata Pata Pata Pata Pata Pata Pata Pata Pata Pata Pata Pata Pata Pata Pata Pata Pata Pata Pata Pata Pampa
Río Kkollpa Pata Pata Pata Pata Pata Pata Pata Pata Pata Pata Pata Pata Pata Pata Pata Pata Pata Pata Pata Pata Pata Pata Pata
Río Kkollpa Pata Pata Pata Pata Pata Pata Pata Pata Pata Pata Pata Pata Pata Pata Pata Pata Pata Pata Pata Pata Pata Pata Pata Pampa
Río Kkollpa Pata Pata Pata Pata Pata Pata Pata Pata Pata Pata Pata Pata Pata Pata Pata Pata Pata Pata Pata Pata Pata Pata Pata Pata
Río Kkollpa Pata Pata Pata Pata Pata Pata Pata Pata Pata Pata Pata Pata Pata Pata Pata Pata Pata Pata Pata Pata Pata Pata Pata Pata Pampa
Río Kkollpa Pata Pata Pata Pata Pata Pata Pata Pata Pata Pata Pata Pata Pata Pata Pata Pata Pata Pata Pata Pata Pata Pata Pata Pata Pata
Río Kkollpa Pata Pata Pata Pata Pata Pata Pata Pata Pata Pata Pata Pata Pata Pata Pata Pata Pata Pata Pata Pata Pata Pata Pata Pata Pata Pampa
Río Kkollpa Pata Pata Pata Pata Pata Pata Pata Pata Pata Pata Pata Pata Pata Pata Pata Pata Pata Pata Pata Pata Pata Pata Pata Pata Pata Pata
Río Kkollpa Pata Pata Pata Pata Pata Pata Pata Pata Pata Pata Pata Pata Pata Pata Pata Pata Pata Pata Pata Pata Pata Pata Pata Pata Pata Pata Pampa
Río Kkollpa Pata Pata Pata Pata Pata Pata Pata Pata Pata Pata Pata Pata Pata Pata Pata Pata Pata Pata Pata Pata Pata Pata Pata Pata Pata Pata Pata
Río Kkollpa Pata Pata Pata Pata Pata Pata Pata Pata Pata Pata Pata Pata Pata Pata Pata Pata Pata Pata Pata Pata Pata Pata Pata Pata Pata Pata Pata Pampa
Río Kkollpa Pata Pata Pata Pata Pata Pata Pata Pata Pata Pata Pata Pata Pata Pata Pata Pata Pata Pata Pata Pata Pata Pata Pata Pata Pata Pata Pata Pata
Río Kkollpa Pata Pata Pata Pata Pata Pata Pata Pata Pata Pata Pata Pata Pata Pata Pata Pata Pata Pata Pata Pata Pata Pata Pata Pata Pata Pata Pata Pata Pampa
Río Kkollpa Pata Pata Pata Pata Pata Pata Pata Pata Pata Pata Pata Pata Pata Pata Pata Pata Pata Pata Pata Pata Pata Pata Pata Pata Pata Pata Pata Pata Pata
Río Kkollpa Pata Pata Pata Pata Pata Pata Pata Pata Pata Pata Pata Pata Pata Pata Pata Pata Pata Pata Pata Pata Pata Pata Pata Pata Pata Pata Pata Pata Pata Pampa
Río Kkollpa Pata Pata Pata Pata Pata Pata Pata Pata Pata Pata Pata Pata Pata Pata Pata Pata Pata Pata Pata Pata Pata Pata Pata Pata Pata Pata Pata Pata Pata Pata
Río Kkollpa Pata Pata Pata Pata Pata Pata Pata Pata Pata Pata Pata Pata Pata Pata Pata Pata Pata Pata Pata Pata Pata Pata Pata Pata Pata Pata Pata Pata Pata Pata Pampa
Río Kkollpa Pata Pata Pata Pata Pata Pata Pata Pata Pata Pata Pata Pata Pata Pata Pata Pata Pata Pata Pata Pata Pata Pata Pata Pata Pata Pata Pata Pata Pata Pata Pata
Río Kkollpa Pata Pata Pata Pata Pata Pata Pata Pata Pata Pata Pata Pata Pata Pata Pata Pata Pata Pata Pata Pata Pata Pata Pata Pata Pata Pata Pata Pata Pata Pata Pata Pampa
Río Kkollpa Pata Pata Pata Pata Pata Pata Pata Pata Pata Pata Pata Pata Pata Pata Pata Pata Pata Pata Pata Pata Pata Pata Pata Pata Pata Pata Pata Pata Pata Pata Pata Pata
Río Kkollpa Pata Pata Pata Pata Pata Pata Pata Pata Pata Pata Pata Pata Pata Pata Pata Pata Pata Pata Pata Pata Pata Pata Pata Pata Pata Pata Pata Pata Pata Pata Pata Pata Pampa
Río Kkollpa Pata Pata Pata Pata Pata Pata Pata Pata Pata Pata Pata Pata Pata Pata Pata Pata Pata Pata Pata Pata Pata Pata Pata Pata Pata Pata Pata Pata Pata Pata Pata Pata Pata
Río Kkollpa Pata Pata Pata Pata Pata Pata Pata Pata Pata Pata Pata Pata Pata Pata Pata Pata Pata Pata Pata Pata Pata Pata Pata Pata Pata Pata Pata Pata Pata Pata Pata Pata Pata Pampa
Río Kkollpa Pata Pata Pata Pata Pata Pata Pata Pata Pata Pata Pata Pata Pata Pata Pata Pata Pata Pata Pata Pata Pata Pata Pata Pata Pata Pata Pata Pata Pata Pata Pata Pata Pata Pata
Río Kkollpa Pata Pata Pata Pata Pata Pata Pata Pata Pata Pata Pata Pata Pata Pata Pata Pata Pata Pata Pata Pata Pata Pata Pata Pata Pata Pata Pata Pata Pata Pata Pata Pata Pata Pata Pampa
Río Kkollpa Pata Pata Pata Pata Pata Pata Pata Pata Pata Pata Pata Pata Pata Pata Pata Pata Pata Pata Pata Pata Pata Pata Pata Pata Pata Pata Pata Pata Pata Pata Pata Pata Pata Pata Pata
Río Kkollpa Pata Pata Pata Pata Pata Pata Pata Pata Pata Pata Pata Pata Pata Pata Pata Pata Pata Pata Pata Pata Pata Pata Pata Pata Pata Pata Pata Pata Pata Pata Pata Pata Pata Pata Pata Pampa
Río Kkollpa Pata Pata Pata Pata Pata Pata Pata Pata Pata Pata Pata Pata Pata Pata Pata Pata Pata Pata Pata Pata Pata Pata Pata Pata Pata Pata Pata Pata Pata Pata Pata Pata Pata Pata Pata Pata
Río Kkollpa Pata Pata Pata Pata Pata Pata Pata Pata Pata Pata Pata Pata Pata Pata Pata Pata Pata Pata Pata Pata Pata Pata Pata Pata Pata Pata Pata Pata Pata Pata Pata Pata Pata Pata Pata Pata Pampa
Río Kkollpa Pata Pata Pata Pata Pata Pata Pata Pata Pata Pata Pata Pata Pata Pata Pata Pata Pata Pata Pata Pata Pata Pata Pata Pata Pata Pata Pata Pata Pata Pata Pata Pata Pata Pata Pata Pata Pata
Río Kkollpa Pata Pata Pata Pata Pata Pata Pata Pata Pata Pata Pata Pata Pata Pata Pata Pata Pata Pata Pata Pata Pata Pata Pata Pata Pata Pata Pata Pata Pata Pata Pata Pata Pata Pata Pata Pata Pata Pampa
Río Kkollpa Pata Pata Pata Pata Pata Pata Pata Pata Pata Pata Pata Pata Pata Pata Pata Pata Pata Pata Pata Pata Pata Pata Pata Pata Pata Pata Pata Pata Pata Pata Pata Pata Pata Pata Pata Pata Pata Pata
Río Kkollpa Pata Pata Pata Pata Pata Pata Pata Pata Pata Pata Pata Pata Pata Pata Pata Pata Pata Pata Pata Pata Pata Pata Pata Pata Pata Pata Pata Pata Pata Pata Pata Pata Pata Pata Pata Pata Pata Pata Pampa
Río Kkollpa Pata Pata Pata Pata Pata Pata Pata Pata Pata Pata Pata Pata Pata Pata Pata Pata Pata Pata Pata Pata Pata Pata Pata Pata Pata Pata Pata Pata Pata Pata Pata Pata Pata Pata Pata Pata Pata Pata Pata
Río Kkollpa Pata Pata Pata Pata Pata Pata Pata Pata Pata Pata Pata Pata Pata Pata Pata Pata Pata Pata Pata Pata Pata Pata Pata Pata Pata Pata Pata Pata Pata Pata Pata Pata Pata Pata Pata Pata Pata Pata Pata Pampa
Río Kkollpa Pata Pata Pata Pata Pata Pata Pata Pata Pata Pata Pata Pata Pata Pata Pata Pata Pata Pata Pata Pata Pata Pata Pata Pata Pata Pata Pata Pata Pata Pata Pata Pata Pata Pata Pata Pata Pata Pata Pata Pata
Río Kkollpa Pata Pata Pata Pata Pata Pata Pata Pata Pata Pata Pata Pata Pata Pata Pata Pata Pata Pata Pata Pata Pata Pata Pata Pata Pata Pata Pata Pata Pata Pata Pata Pata Pata Pata Pata Pata Pata Pata Pata Pata Pampa
Río Kkollpa Pata Pata Pata Pata Pata Pata Pata Pata Pata Pata Pata Pata Pata Pata Pata Pata Pata Pata Pata Pata Pata Pata Pata Pata Pata Pata Pata Pata Pata Pata Pata Pata Pata Pata Pata Pata Pata Pata Pata Pata Pata
Río Kkollpa Pata Pata Pata Pata Pata Pata Pata Pata Pata Pata Pata Pata Pata Pata Pata Pata Pata Pata Pata Pata Pata Pata Pata Pata Pata Pata Pata Pata Pata Pata Pata Pata Pata Pata Pata Pata Pata Pata Pata Pata Pata Pampa
Río Kkollpa Pata Pata Pata Pata Pata Pata Pata Pata Pata Pata Pata Pata Pata Pata Pata Pata Pata Pata Pata Pata Pata Pata Pata Pata Pata Pata Pata Pata Pata Pata Pata Pata Pata Pata Pata Pata Pata Pata Pata Pata Pata Pata
Río Kkollpa Pata Pata Pata Pata Pata Pata Pata Pata Pata Pata Pata Pata Pata Pata Pata Pata Pata Pata Pata Pata Pata Pata Pata Pata Pata Pata Pata Pata Pata Pata Pata Pata Pata Pata Pata Pata Pata Pata Pata Pata Pata Pata Pampa
Río Kkollpa Pata Pata Pata Pata Pata Pata Pata Pata Pata Pata Pata Pata Pata Pata Pata Pata Pata Pata Pata Pata Pata Pata Pata Pata Pata Pata Pata Pata Pata Pata Pata Pata Pata Pata Pata Pata Pata Pata Pata Pata Pata Pata Pata
Río Kkollpa Pata Pata Pata Pata Pata Pata Pata Pata Pata Pata Pata Pata Pata Pata Pata Pata Pata Pata Pata Pata Pata Pata Pata Pata Pata Pata Pata Pata Pata Pata Pata Pata Pata Pata Pata Pata Pata Pata Pata Pata Pata Pata Pata Pampa
Río Kkollpa Pata Pata Pata Pata Pata Pata Pata Pata Pata Pata Pata Pata Pata Pata Pata Pata Pata Pata Pata Pata Pata Pata Pata Pata Pata Pata Pata Pata Pata Pata Pata Pata Pata Pata Pata Pata Pata Pata Pata Pata Pata Pata Pata Pata
Río Kkollpa Pata Pata Pata Pata Pata Pata Pata Pata Pata Pata Pata Pata Pata Pata Pata Pata Pata Pata Pata Pata Pata Pata Pata Pata Pata Pata Pata Pata Pata Pata Pata Pata Pata Pata Pata Pata Pata Pata Pata Pata Pata Pata Pata Pata Pampa
Río Kkollpa Pata Pata Pata Pata Pata Pata Pata Pata Pata Pata Pata Pata Pata Pata Pata Pata Pata Pata Pata Pata Pata Pata Pata Pata Pata Pata Pata Pata Pata Pata Pata Pata Pata Pata Pata Pata Pata Pata Pata Pata Pata Pata Pata Pata Pata
Río Kkollpa Pata Pata Pata Pata Pata Pata Pata Pata Pata Pata Pata Pata Pata Pata Pata Pata Pata Pata Pata Pata Pata Pata Pata Pata Pata Pata Pata Pata Pata Pata Pata Pata Pata Pata Pata Pata Pata Pata Pata Pata Pata Pata Pata Pata Pata Pampa
Río Kkollpa Pata Pata Pata Pata Pata Pata Pata Pata Pata Pata Pata Pata Pata Pata Pata Pata Pata Pata Pata Pata Pata Pata Pata Pata Pata Pata Pata Pata Pata Pata Pata Pata Pata Pata Pata Pata Pata Pata Pata Pata Pata Pata Pata Pata Pata Pata
Río Kkollpa Pata Pata Pata Pata Pata Pata Pata Pata Pata Pata Pata Pata Pata Pata Pata Pata Pata Pata Pata Pata Pata Pata Pata Pata Pata Pata Pata Pata Pata Pata Pata Pata Pata Pata Pata Pata Pata Pata Pata Pata Pata Pata Pata Pata Pata Pata Pampa
Río Kkollpa Pata Pata Pata Pata Pata Pata Pata Pata Pata Pata Pata Pata Pata Pata Pata Pata Pata Pata Pata Pata Pata Pata Pata Pata Pata Pata Pata Pata Pata Pata Pata Pata Pata Pata Pata Pata Pata Pata Pata Pata Pata Pata Pata Pata Pata Pata Pata
Río Kkollpa Pata Pata Pata Pata Pata Pata Pata Pata Pata Pata Pata Pata Pata Pata Pata Pata Pata Pata Pata Pata Pata Pata Pata Pata Pata Pata Pata Pata Pata Pata Pata Pata Pata Pata Pata Pata Pata Pata Pata Pata Pata Pata Pata Pata Pata Pata Pata Pampa
Río Kkollpa Pata Pata Pata Pata Pata Pata Pata Pata Pata Pata Pata Pata Pata Pata Pata Pata Pata Pata Pata Pata Pata Pata Pata Pata Pata Pata Pata Pata Pata Pata Pata Pata Pata Pata Pata Pata Pata Pata Pata Pata Pata Pata Pata Pata Pata Pata Pata Pata
Río Kkollpa Pata Pata Pata Pata Pata Pata Pata Pata Pata Pata Pata Pata Pata Pata Pata Pata Pata Pata Pata Pata Pata Pata Pata Pata Pata Pata Pata Pata Pata Pata Pata Pata Pata Pata Pata Pata Pata Pata Pata Pata Pata Pata Pata Pata Pata Pata Pata Pata Pampa
Río Kkollpa Pata Pata Pata Pata Pata Pata Pata Pata Pata Pata Pata Pata Pata Pata Pata Pata Pata Pata Pata Pata Pata Pata Pata Pata Pata Pata Pata Pata Pata Pata Pata Pata Pata Pata Pata Pata Pata Pata Pata Pata Pata Pata Pata Pata Pata Pata Pata Pata Pata
Río Kkollpa Pata Pata Pata Pata Pata Pata Pata Pata Pata Pata Pata Pata Pata Pata Pata Pata Pata Pata Pata Pata Pata Pata Pata Pata Pata Pata Pata Pata Pata Pata Pata Pata Pata Pata Pata Pata Pata Pata Pata Pata Pata Pata Pata Pata Pata Pata Pata Pata Pata Pampa
Río Kkollpa Pata Pata Pata Pata Pata Pata Pata Pata Pata Pata Pata Pata Pata Pata Pata Pata Pata Pata Pata Pata Pata Pata Pata Pata Pata Pata Pata Pata Pata Pata Pata Pata Pata Pata Pata Pata Pata Pata Pata Pata Pata Pata Pata Pata Pata Pata Pata Pata Pata Pata
Río Kkollpa Pata Pata Pata Pata Pata Pata Pata Pata Pata Pata Pata Pata Pata Pata Pata Pata Pata Pata Pata Pata Pata Pata Pata Pata Pata Pata Pata Pata Pata Pata Pata Pata Pata Pata Pata Pata Pata Pata Pata Pata Pata Pata Pata Pata Pata Pata Pata Pata Pata Pata Pampa
Río Kkollpa Pata Pata Pata Pata Pata Pata Pata Pata Pata Pata Pata Pata Pata Pata Pata Pata Pata Pata Pata Pata Pata Pata Pata Pata Pata Pata Pata Pata Pata Pata Pata Pata Pata Pata Pata Pata Pata Pata Pata Pata Pata Pata Pata Pata Pata Pata Pata Pata Pata Pata Pata
Río Kkollpa Pata Pata Pata Pata Pata Pata Pata Pata Pata Pata Pata Pata Pata Pata Pata Pata Pata Pata Pata Pata Pata Pata Pata Pata Pata Pata Pata Pata Pata Pata Pata Pata Pata Pata Pata Pata Pata Pata Pata Pata Pata Pata Pata Pata Pata Pata Pata Pata Pata Pata Pata Pampa
Río Kkollpa Pata Pata Pata Pata Pata Pata Pata Pata Pata Pata Pata Pata Pata Pata Pata Pata Pata Pata Pata Pata Pata Pata Pata Pata Pata Pata Pata Pata Pata Pata Pata Pata Pata Pata Pata Pata Pata Pata Pata Pata Pata Pata Pata Pata Pata Pata Pata Pata Pata Pata Pata Pata
Río Kkollpa Pata Pata Pata Pata Pata Pata Pata Pata Pata Pata Pata Pata Pata Pata Pata Pata Pata Pata Pata Pata Pata Pata Pata Pata Pata Pata Pata Pata Pata Pata Pata Pata Pata Pata Pata Pata Pata Pata Pata Pata Pata Pata Pata Pata Pata Pata Pata Pata Pata Pata Pata Pata Pata
Río Kkollpa Pata Pata Pata Pata Pata Pata Pata Pata Pata Pata Pata Pata Pata Pata Pata Pata Pata Pata Pata Pata Pata Pata Pata Pata Pata Pata Pata Pata Pata Pata Pata Pata Pata Pata Pata Pata Pata Pata Pata Pata Pata Pata Pata Pata Pata Pata Pata Pata Pata Pata Pata Pata Pata Pata
Río Kkollpa Pata Pata Pata Pata Pata Pata Pata Pata Pata Pata Pata Pata Pata Pata Pata Pata Pata Pata Pata Pata Pata Pata Pata Pata Pata Pata Pata Pata Pata Pata Pata Pata Pata Pata Pata Pata Pata Pata Pata Pata Pata Pata Pata Pata Pata Pata Pata Pata Pata Pata Pata Pata Pata Pata Pata
Río Kkollpa Pata Pata Pata Pata Pata Pata Pata Pata Pata Pata Pata Pata Pata Pata Pata Pata Pata Pata Pata Pata Pata Pata Pata Pata Pata Pata Pata Pata Pata Pata Pata Pata Pata Pata Pata Pata Pata Pata Pata Pata Pata Pata Pata Pata Pata Pata Pata Pata Pata Pata Pata Pata Pata Pata Pata Pata
Río Kkollpa Pata Pata Pata Pata Pata Pata Pata Pata Pata Pata Pata Pata Pata Pata Pata Pata Pata Pata Pata Pata Pata Pata Pata Pata Pata Pata Pata Pata Pata Pata Pata Pata Pata Pata Pata Pata Pata Pata Pata Pata Pata Pata Pata Pata Pata Pata Pata Pata Pata Pata Pata Pata Pata Pata Pata Pata Pata
Río Kkollpa Pata Pata Pata Pata Pata Pata Pata Pata Pata Pata Pata Pata Pata Pata Pata Pata Pata Pata Pata Pata Pata Pata Pata Pata Pata Pata Pata Pata Pata Pata Pata Pata Pata Pata Pata Pata Pata Pata Pata Pata Pata Pata Pata Pata Pata Pata Pata Pata Pata Pata Pata Pata Pata Pata Pata Pata Pata Pata
Río Kkollpa Pata Pata Pata Pata Pata Pata Pata Pata Pata Pata Pata Pata Pata Pata Pata Pata Pata Pata Pata Pata Pata Pata Pata Pata Pata Pata Pata Pata Pata Pata Pata Pata Pata Pata Pata Pata Pata Pata Pata Pata Pata Pata Pata Pata Pata Pata Pata Pata Pata Pata Pata Pata Pata Pata Pata Pata Pata Pata Pata
Río Kkollpa Pata Pata Pata Pata Pata Pata Pata Pata Pata Pata Pata Pata Pata Pata Pata Pata Pata Pata Pata Pata Pata Pata Pata Pata Pata Pata Pata Pata Pata Pata Pata Pata Pata Pata Pata Pata Pata Pata Pata Pata Pata Pata Pata Pata Pata Pata Pata Pata Pata Pata Pata Pata Pata Pata Pata Pata Pata Pata Pata Pata
Río Kkollpa Pata Pata Pata Pata Pata Pata Pata Pata Pata Pata Pata Pata Pata Pata Pata Pata Pata Pata Pata Pata Pata Pata Pata Pata Pata Pata Pata Pata Pata Pata Pata Pata Pata Pata Pata Pata Pata Pata Pata Pata Pata Pata Pata Pata Pata Pata Pata Pata Pata Pata Pata Pata Pata Pata Pata Pata Pata Pata Pata Pata Pata
Río Kkollpa Pata Pata Pata Pata Pata Pata Pata Pata Pata Pata Pata Pata Pata Pata Pata Pata Pata Pata Pata Pata Pata Pata Pata Pata Pata Pata Pata Pata Pata Pata Pata Pata Pata Pata Pata Pata Pata Pata Pata Pata Pata Pata Pata Pata Pata Pata Pata Pata Pata Pata Pata Pata Pata Pata Pata Pata Pata Pata Pata Pata Pata Pata
Río Kkollpa Pata Pata Pata Pata Pata Pata Pata Pata Pata Pata Pata Pata Pata Pata Pata Pata Pata Pata Pata Pata Pata Pata Pata Pata Pata Pata Pata Pata Pata Pata Pata Pata Pata Pata Pata Pata Pata Pata Pata Pata Pata Pata Pata Pata Pata Pata Pata Pata Pata Pata Pata Pata Pata Pata Pata Pata Pata Pata Pata Pata Pata Pata Pata
Río Kkollpa Pata Pata Pata Pata Pata Pata Pata Pata Pata Pata Pata Pata Pata Pata Pata Pata Pata Pata Pata Pata Pata Pata Pata Pata Pata Pata Pata Pata Pata Pata Pata Pata Pata Pata Pata Pata Pata Pata Pata Pata Pata Pata Pata Pata Pata Pata Pata Pata Pata Pata Pata Pata Pata Pata Pata Pata Pata Pata Pata Pata Pata Pata Pata Pata
Río Kkollpa Pata Pata Pata Pata Pata Pata Pata Pata Pata Pata Pata Pata Pata Pata Pata Pata Pata Pata Pata Pata Pata Pata Pata Pata Pata Pata Pata Pata Pata Pata Pata Pata Pata Pata Pata Pata Pata Pata Pata Pata Pata Pata Pata Pata Pata Pata Pata Pata Pata Pata Pata Pata Pata Pata Pata Pata Pata Pata Pata Pata Pata Pata Pata Pata Pata
Río Kkollpa Pata Pata Pata Pata Pata Pata Pata Pata Pata Pata Pata Pata Pata Pata Pata Pata Pata Pata Pata Pata Pata Pata Pata Pata Pata Pata Pata Pata Pata Pata Pata Pata Pata Pata Pata Pata Pata Pata Pata Pata Pata Pata Pata Pata Pata Pata Pata Pata Pata Pata Pata Pata Pata Pata Pata Pata Pata Pata Pata Pata Pata Pata Pata Pata Pata Pata
Río Kkollpa Pata Pata Pata Pata Pata Pata Pata Pata Pata Pata Pata Pata Pata Pata Pata Pata Pata Pata Pata Pata Pata Pata Pata Pata Pata Pata Pata Pata Pata Pata Pata Pata Pata Pata Pata Pata Pata Pata Pata Pata Pata Pata Pata Pata Pata Pata Pata Pata Pata Pata Pata Pata Pata Pata Pata Pata Pata Pata Pata Pata Pata Pata Pata Pata Pata Pata Pata
Río Kkollpa Pata

AIQUILE

EDICIÓN 1-I.G.M.

SE 20-9
SERIE H531

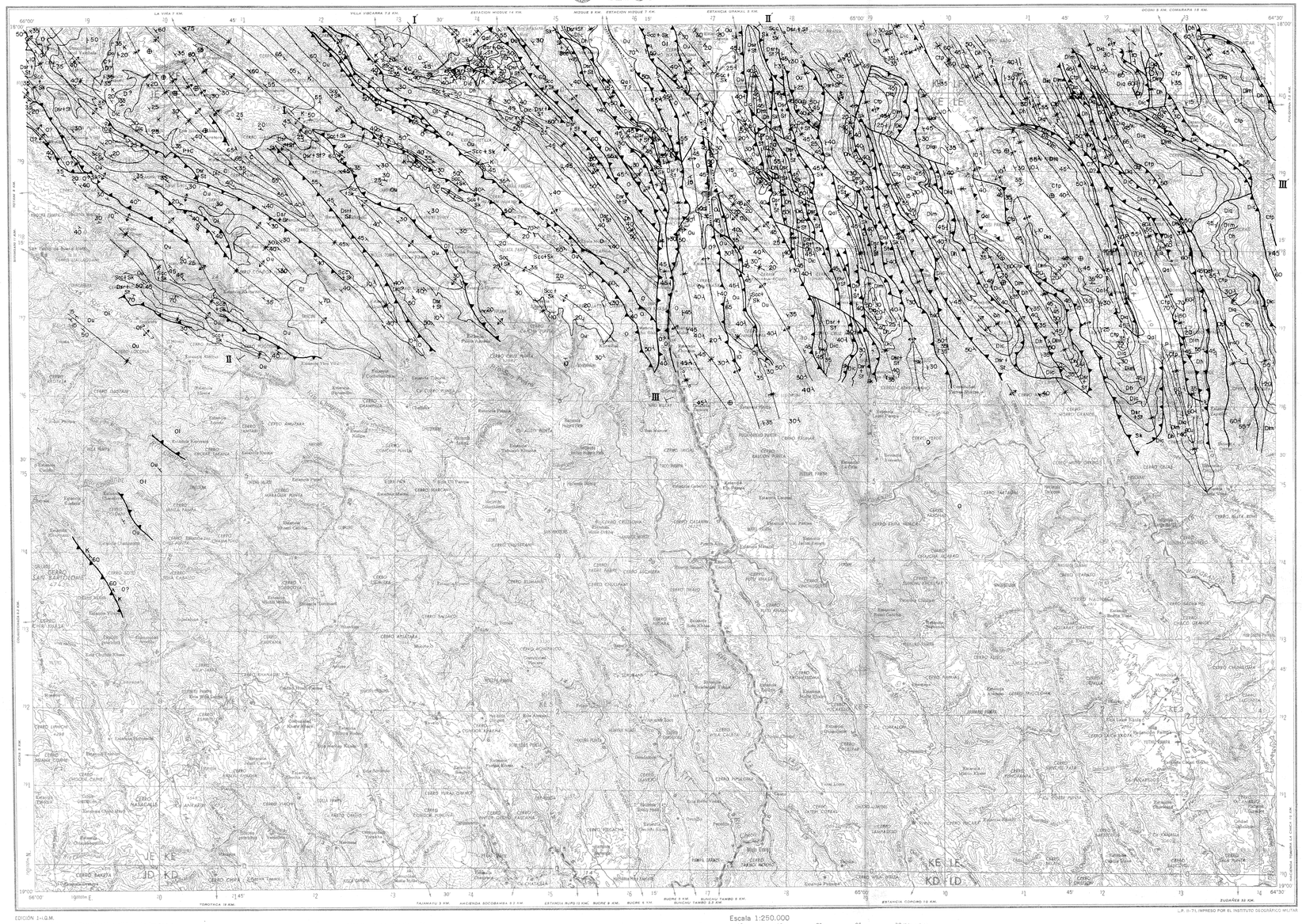

EDICIÓN 1-I.G.M.

Preparado por el Instituto Geográfico Militar (I.G.M.), La Paz-Bolivia, en colaboración con el Servicio Geológico Interamericano (I.A.G.S.). Compilado en 1969 de mapas de buena precisión de la serie Carta Nacional, a escala 1:50.000, que fueron compilados en 1968 por métodos fotogramétricos.

GLOSARIO (QUECHUA)

río	mayu	Cerro	orkho
Quebrada	wayko	Loma	pata
Laguna	khocha	Roca	khaxha
Agua	yaku	Rincón	khuchu
Portezuelo	khata	Hoyo	choko
Arroyo	larkha	Habra	apacheta
Salar	kollpa	Planicie	pampa
Grande	jatun	Casa	huasi
Pequeño	ch'uxu	Camino	ñan
Viento	huayra	Piedra	rumi

SIGNOS CONVENCIONALES

Los números en rojo indican las distancias kilométricas aproximadas entre estrellas
En este mapa se considera que una vía tenga un ancho mínimo de 2,5 metros.

POBLACIONES

Representación en el mapa
Más de 100.000 habitantes — LA PAZ
50.000 a 100.000 " — SANTA CRUZ
10.000 a 50.000 " — TRINIDAD
2.000 a 10.000 " — Aiquile
Menos de 2.000 — Tyrotore
Menos de 40 edificios — Estancia Kasterín

LIMITES

Nacional
Departamental
Provincial

CAMINOS

Transitable todo el año:
Afirmado sólido, dos vías
Revestimiento suelto o ligero, dos vías
Afirmado sólido, una vía
Revestimiento suelto o ligero una vía
Transitable en tiempo bueno o seco:
Revestimiento suelto
Rodera; Vereda

FERROCARRILES

Vía sencilla, trocha normal
Vía sencilla, trocha estrecha

Aeropuerto; Campo de aterrizaje
Puerto fluvial y lacustre
Accidente terrestre importante
Iglesia; Escuela; Mina
Elevaciones de importancia en metros
Punto de control horizontal
Bosque o monte; Matorral
Tholar; Yareta; Superficie rocosa
Hierba tropical; Totoral
Arena; Salar

Escala 1:250.000

5 0 5 10 15 20 25 30 Kilometros
5 0 5 10 15 20 Millas Terrestres

CURVAS DE NIVEL CON INTERVALOS DE 100 METROS

PROYECCIÓN TRANSVERSA DE MERCATOR

LAS LÍNEAS AZULES NUMERADAS INDICAN LA CUADRÍCULA UNIVERSAL TRANSVERSA DE MERCATOR A 10.000 METROS ZONA 20. ESFEROIDE INTERNACIONAL
SE HAN OMITIDO LAS ULTIMAS CUATRO CIFRAS DE LOS NUMEROS CUADRICULARES

LA DECLINACIÓN MAGNÉTICA DE 1971 PARA LA HOJA, VARIA DESDE 3°36' EN DIRECCIÓN AL OESTE PARA EL CENTRO DEL BORDE OESTE, HASTA 1°58' EN DIRECCIÓN AL OESTE, PARA EL CENTRO DEL BORDE ESTE DE LA HOJA. EL CAMBIO DE VARIACIÓN ANUAL ES DE 06'AL OESTE

SE SOLICITA DE LOS LECTORES QUE ENCUENTREN ERRORES O OMISIONES EN ESTE MAPA, MARCAR LAS CORRECCIONES EN EL MISMO Y ENVIARLO AL COMANDANTE DEL INSTITUTO GEOGRÁFICO MILITAR, LA PAZ, BOLIVIA. ESTOS MAPAS SERÁN DEVUELTOS O SUBSTITUIDOS. SI ASÍ SE DESEA

DIAGRAMA PARA LA LOCALIZACIÓN DE LA HOJA SE 20-9

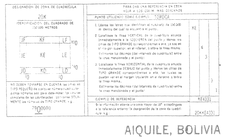

AIQUILE, BOLIVIA

PLATE 5.

GEOLOGIC MAP OF THE AIQUILE, BOLIVIA SHEET (SE-20-9)

B. SHEFFELS 1988

MESOZOIC CENOZOIC

- QUATERNARY — Qal — QUATERNARY ALLUVIUM
- TERTIARY — T — TERTIARY SEDIMENTARY ROCKS (UNDIFFERENTIATED)
- CRETACEOUS — K — CRETACEOUS SEDIMENTARY ROCKS (UNDIFFERENTIATED)

PALEOZOIC

- PERMIAN — P — COPACABANA FORMATION
- CARBONIFEROUS — C — CARBONIFEROUS SEDIMENTARY ROCKS (UNDIFFERENTIATED)
  - Ce — ESCARPMENT FORMATION
  - Ctp — TARIJA/TAIGUATI FORMATIONS, TUPAMBI FORMATION, ITACUA FORMATION
- DEVONIAN
  - Dlq — IQUIRI FORMATION
  - Dlm — LOS MONOS FORMATION
  - Dh — HUAMAMPAMPA FORMATION
  - Dic — ICLA FORMATION
  - Dsr + St — SANTA ROSA FORMATION, TARABUCO FORMATION
- SILURIAN
  - Sk, Scc — KIRUSILLAS FORMATION, CANCANIRI FORMATION
- ORDOVICIAN
  - Ou — UPPER ORDOVICIAN
  - Ol — LOWER ORDOVICIAN

CONTACTS: DEFINITE; APPROXIMATE; UNCERTAIN; CONCEALED

FAULTS: THRUST OR REVERSE (BARBS ON UPPER PLATE); NORMAL (TICKS ON DOWNTHROWN SIDE); STRIKE-SLIP

DEFINITE; APPROXIMATE; UNCERTAIN; CONCEALED

BEDDING: INCLINED; HORIZONTAL; VERTICAL; OVERTURNED

FOLDS: SYNCLINE, WITH DIRECTION OF PLUNGE; ANTICLINE, WITH DIRECTION OF PLUNGE

DEFINITE; APPROXIMATE; UNCERTAIN; CONCEALED

OVERTURNED SYNCLINE; OVERTURNED ANTICLINE

CONFIDENCE DIAGRAM

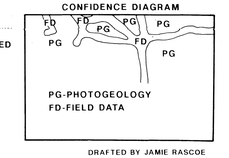

DRAFTED BY JAMIE RASCOE

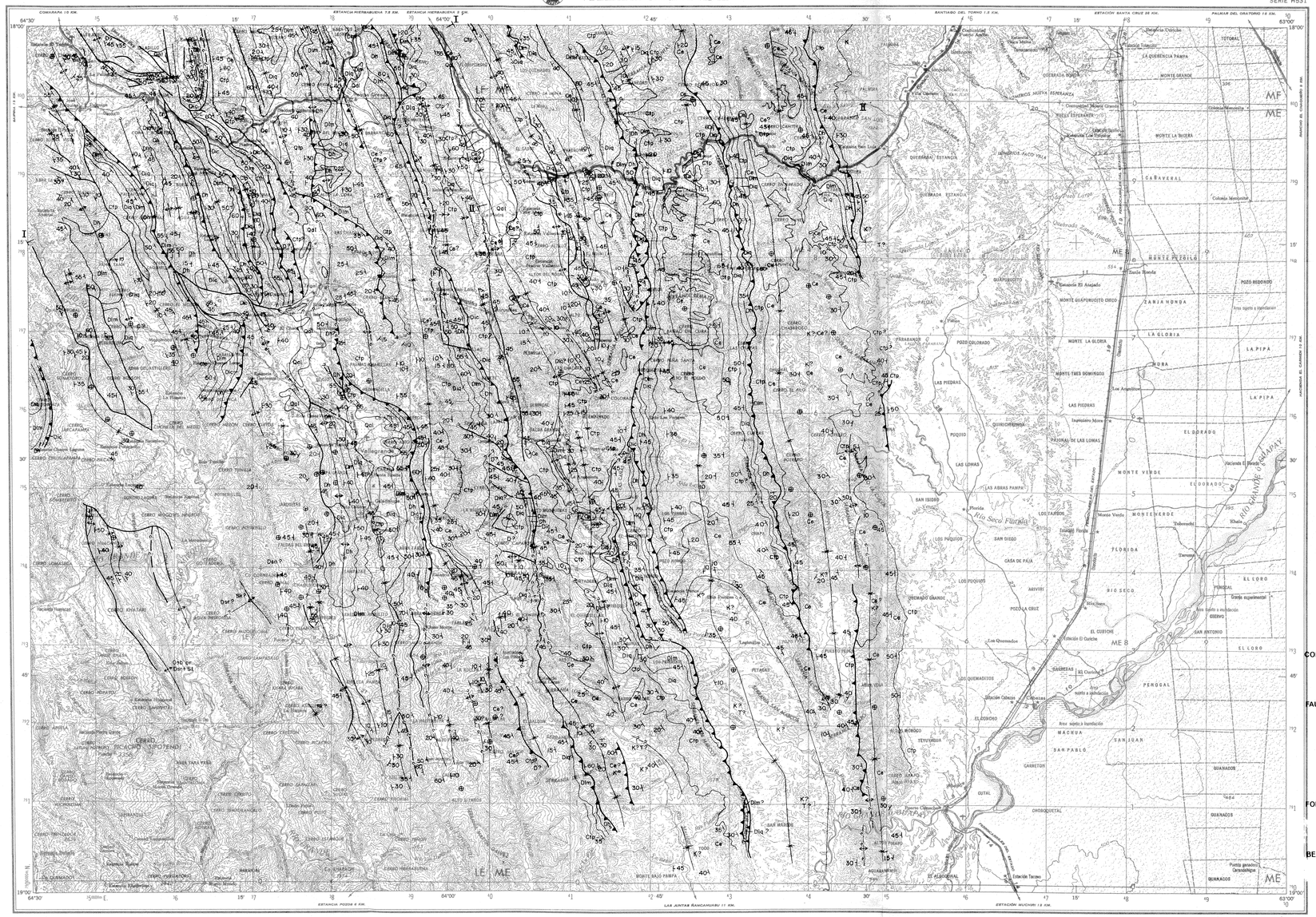
COMARAPA 10 KM.
ESTANCIA HIERBABUENA 7.5 KM.
ESTANCIA HIERBABUENA 2 KM.
SANTIAGO DEL TORNO 1.5 KM.
ESTACIÓN SANTA CRUZ 26 KM.
PALMAR DEL ORATORIO 1.5 KM.
ESTANCIA POZOS 6 KM.
LAS JUNTAS RANCHAHUAYU 11 KM.
ESTACIÓN MUCHURI 13 KM.
LE
ME
MF
ME
ME 8
Río Seco
Río Florida
Río Grande o Guapay
Río Piraí
Río Yapacaní
LA QUERENCIA PAMPA
MONTE GRANDE
MONTE LA BICERA
CARAVERAL
MONTE PUZOLO
MONTE GUAPUNGOTO CHICO
ZANJA HONDA
MONTE LA GLORIA
LA GLORIA
LA PIPA
MONTE TRES DOMINGOS
EL DORADO
MONTE VERDE
ELDORADO
LAS LOMAS
LAS ABRAS PAMPA
SAN ISIDRO
LOS TARDOS
MONTEVERDE
FLORIDA
SAN DIEGO
CASA DE PAJA
LOS PUQUIOS
PUQUIO
LAS PIEDRAS
POZO COLORADO
QUIRICHIPAMPA
PAJONAL DE LAS LOMAS
PRIMERO GRANDE
POZO LA CRUZ
ARIVIRI
RIO SECO
EL CUSIRI
Estación El Cuiche
Los Quemados
GASPERAS
EL CUSICHE
EL CHORRO
MACHUA
SAN JUAN
SAN PABLO
TEYUMAYA
GABRETON
CHORQUETAL
PERUGAL
EL LORO
Granja experimental
SAN ANTONIO
GUANACOS
Estación Cabeza
Estación Tacopaya
Cabeza Mendoza
Cabeza Monteverde
Cabeza Florida
Cabeza Los Tardos
Cabeza Arivivi
Cabeza El Cusiri
Cabeza Machua
Cabeza Gabreton
Cabeza Chorquetal
Cabeza Perugal
Cabeza El Loro
Cabeza Guanacos
Área sujeta a inundación
Área sujeta a inundación
Área sujeta a inundación

PLATE 7. ORURO – SANTA CRUZ TRANSECT

0 20 KM

UNCIA CROSS SECTION
UNCIA MAP SHEET

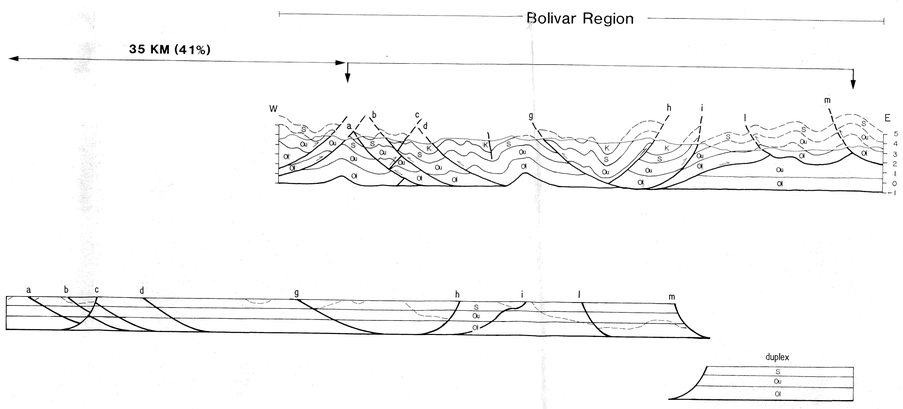

WEST AIQUILE CROSS SECTION
AIQUILE MAP SHEET

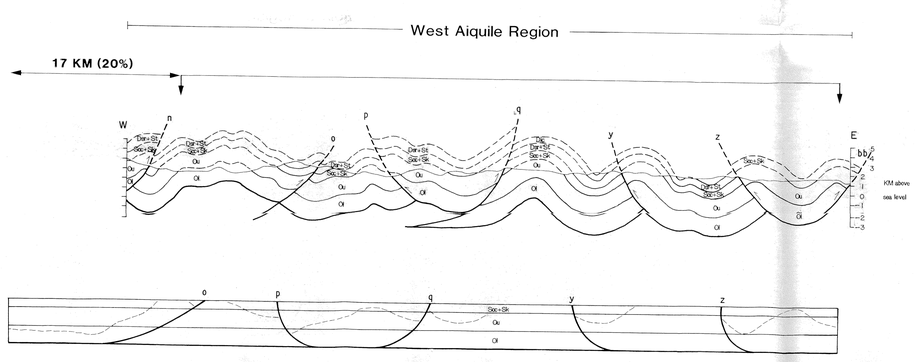

EAST AIQUILE CROSS SECTION
AIQUILE MAP SHEET

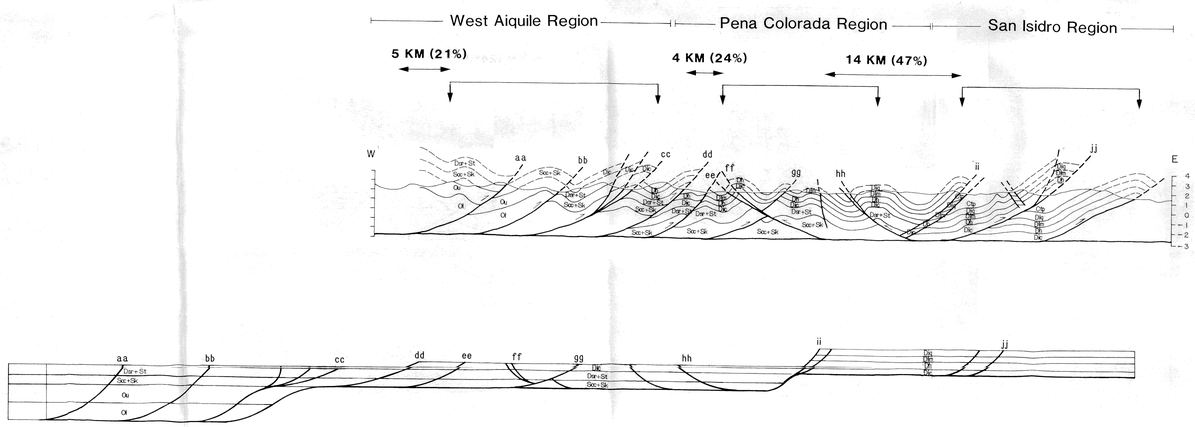

WEST VALLEGRANDE CROSS SECTION
VALLEGRANDE MAP SHEET

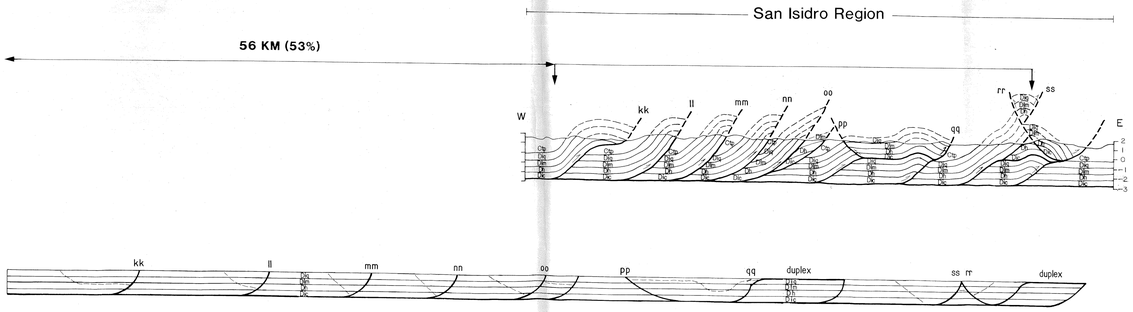

EAST VALLEGRANDE CROSS SECTION
VALLEGRANDE MAP SHEET

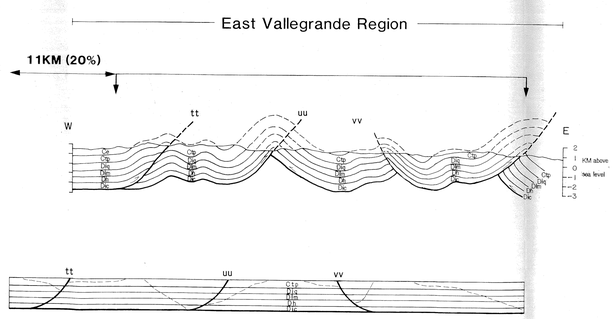

PLATE 8. ORURO – PUNATA – CHAPARE TRANSECTS

0 20 KM

LIMBO CROSS SECTION
PUNATA MAP SHEET

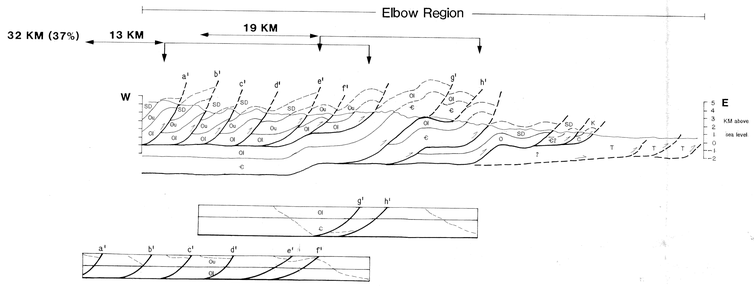

COCHABAMBA CROSS SECTION
COCHABAMBA MAP SHEET

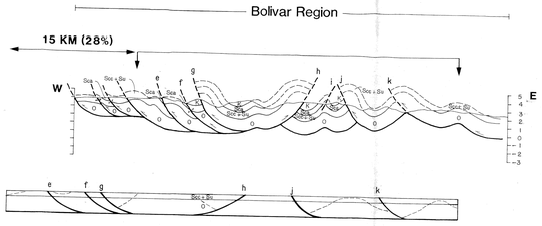

NORTH PUNATA CROSS SECTION
PUNATA MAP SHEET

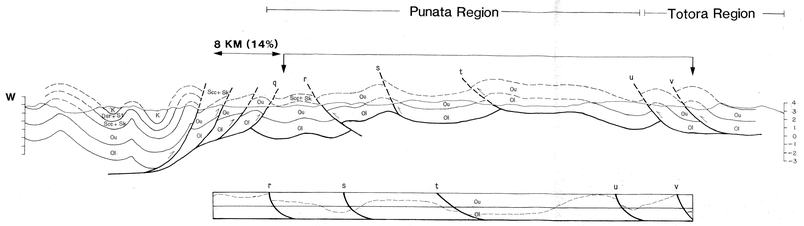

NORTH TOTORA CROSS SECTION
PUNATA MAP SHEET

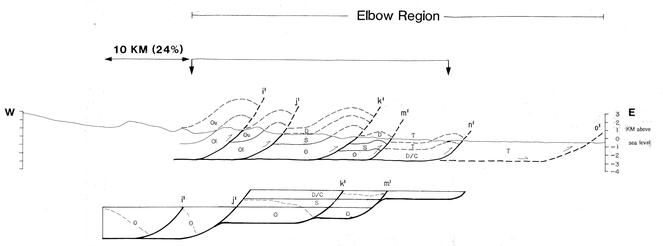

CENTRAL PUNATA CROSS SECTION
AIQUILE AND PUNATA MAP SHEETS

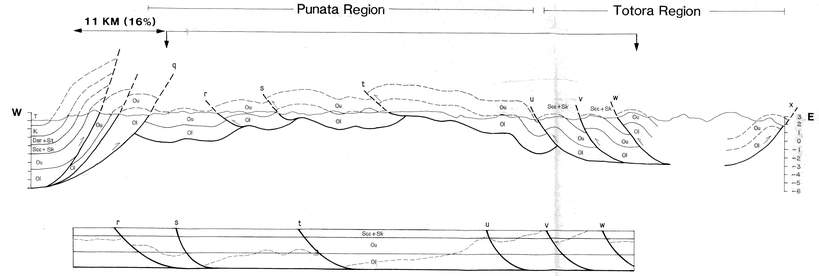

CENTRAL TOTORA CROSS SECTION
PUNATA MAP SHEET

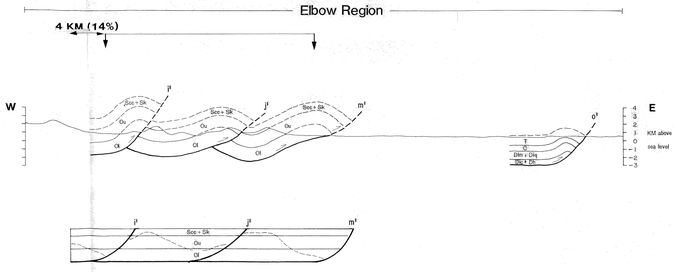

SOUTH PUNATA CROSS SECTION
AIQUILE AND PUNATA MAP SHEETS

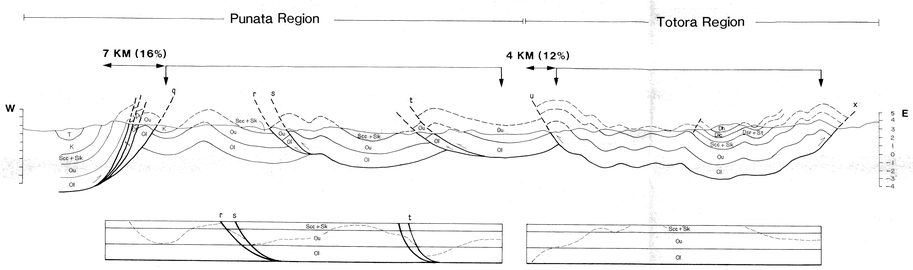

SOUTH TOTORA CROSS SECTION
PUNATA AND SANTA CRUZ DE LA SIERRA MAP SHEETS

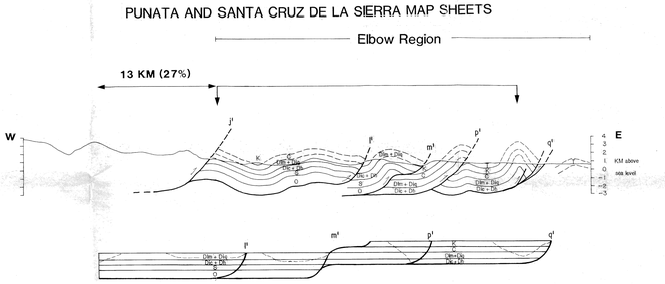
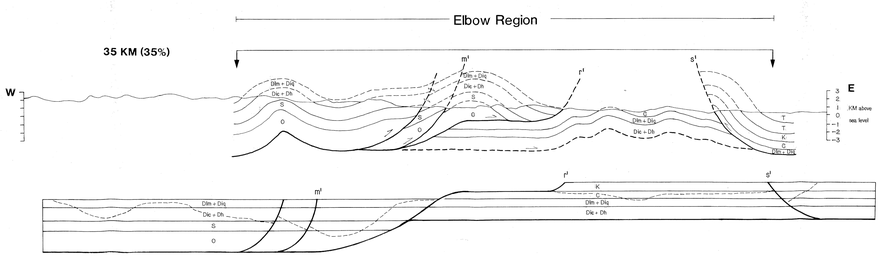
SOUTH SANTA CRUZ CROSS SECTION
SANTA CRUZ DE LA SIERRA MAP SHEET